

Comments from Anonymous Referee #1 and Responses to comments (*italics*) (Section and page numbers refer to the original version submitted)- Paragraphs added or modified and additional references in the revised manuscript are highlighted in yellow for the convenience of the Referee.

The authors of this study were pleased that the Referee was satisfied in the way this paper was written and considered carefully the comments he made.

General comments:

- 1) The suggestion to add one sentence in the beginning stressing why summer is more important to review than any other time of the year.

We fully agree with the Referee, accordingly, a paragraph enumerating the essential factors affecting the EM during summer was added at the beginning of the Introduction chapter.

- 2) The comment made by the Referee on adding an Appendix which will tabulate the abbreviations and notations used.

Since all terms are detailed in the main text, we believe that an Appendix tabulating the abbreviations used in the text is redundant and was therefore not added to the manuscript as suggested by the Referee.

- 3) The suggestion made by the Referee on adding a Table of Content at the beginning of the paper, if allowed by the Journal's style.

We checked this issue with an Editorial representative of Copernicus Publications and received a negative reply while mentioning that a table of contents should not be included according to their house standards.

- 4) The comment made on unifying the notation of the PPB and PPBV units used.

We agree with the Referee. PPBV are the volumetric mixing ratios. The notation was unified and corrected throughout the text as well as in Figs. 14, 19, 20, and 21.

- 5) Comment made by the Referee on the necessity to complete all figure legends and Table headings with a period at the end.

Done.

Minor suggestions:

- 1) Page 14, line 5 missing quotes "hot pot"; Page 15, line 17 "et al."

Done.

- 2) Page 15, line 20: Appropriate reference.

The Referee is right, we apologize for the confusion. The sentence was corrected and the reference of Daskalakis et al., 2015 was omitted.

- 3) Page 15, line 28: inappropriateness to start a sentence with O₃.

We agree with the Referee and rephrased this sentence with "Measurements of O₃"

- 4) Page 15 lines 28-30 and Page 16 lines 1-3: Comment made by the Referee on implying on the summer O₃ maximum observed over the Aegean Sea and Finokalia based on just two sets of measurements (Finokalia and Thessaloniki).

We fully agree that this paragraph was expressed in a rather confusing manner. Inferring on the summer maximum O₃ over the Aegean Sea and Finokalia, Crete was based on several measurements and for rather long periods: 1) An O₃ analyzer installed in a vessel traveling routinely from Heraklion, Crete to Thessaloniki, Greece, from Aug. to Nov. 2000, 2) From the regional monitoring station of Finokalia, Crete from Sept.1997 to Sept. 1999 (Kouvarakis et al. 2000) and 3) From a site nearby Thessaloniki (40^o 32' N, 23^o 50' E) from Mar. 2000 to Jan. 2001. The text was corrected accordingly.

Ref: Kouvarakis, G., K. Tsigaridis, M. Kanakidou, and N. Mihalopoulos, Temporal variations of surface regional background ozone over Crete Island in southeast Mediterranean, J. Geophys. Res., 105, 4399 – 4407, 2000.

- 5) Page 16, line 11: put a comma after ppbv.

Done.

- 6) Page line 21-22: pollutants concentrations OR pollutant concentrations?

The right term is "air pollutant concentrations". This term was applied throughout the text.

- 7) Page 29 line 8: omit coma.

Done.

- 8) Page 30 line 17: Starting a sentence with CH₄ does not seem appropriate.

*We tend to agree with the Referee, and started this paragraph as follows:
“Methane (CH₄) is the most abundant hydrocarbon in the atmosphere....”*

**Comments from Anonymous Referee #3 and Responses to comments (italics)
(Section and page numbers refer to the original version submitted)- Paragraphs
added or modified and additional references in the revised manuscript are
highlighted in yellow for the convenience of the Referee.**

First, we would like to thank the Referee for his valuable and insightful comments which improved much this review study. Following are our detailed responses to each of the comment posted:

- 1) Section 2.1, page 4, line 15:

The authors state that dry north Etesian winds are generated by the Persian Trough. It is actually generated by the east–west pressure gradient manifested by large scale circulation features, low pressures over eastern Mediterranean/Middle East as an extension of the PT and the high pressure over central and southeastern Europe.

We agree with the Referee, the text was corrected accordingly and referred to Tyrlis and Lelieveld, 2013.

- 2) Section 2.1, page 4, lines 16-21:

The discussion for the eastern Mediterranean subsidence during summertime needs elaboration in connection to the discussion in page 5 (lines 16-19) based on the paper of Rodwell and Hoskins. The current consensus view recognizes the importance of the interaction with the mid-latitude westerlies of an equatorially trapped Rossby wave to its west induced by the South Asian monsoon heating as well as an enhancement of the descent due to diabatic radiative cooling under clear sky conditions (Rodwell and Hoskins 1996, 2001; Tyrlis et al. 2012).

We would like to thank the reviewer for this important comment. A full paragraph was added to the revised manuscript so as to explain better the

summer thermodynamic and dynamic conditions and the important role of the South Asian monsoon on summer subsidence over the EM.

3) Section 2.1, page 4, line 25:

The discussion for the eastward progression of the subtropical high needs clarification. Which subtropical high do the authors mean? During summer, the Azores High moves westward toward Bermuda (when it is known as the Bermuda high). Furthermore, a number of studies point out the differences between the acticylonic center over central and southeastern Europe causing the Etesians and the Azores permanent Anticyclone (Prezerakos, 1984; Tyrllis and Lelieveld, 2013; Anagnostopoulou et al., 2014). The acticylonic center over central and southeastern Europe causing the Etesians is related primarily with anticyclonic vorticity advection from Northwestern Africa and secondly with diabatic cooling under clear skies.

We agree with the Referee as regarded to the anticyclonic centers formed over the Balkans. A paragraph was added to the revised manuscript explaining why such centers cannot be considered as extensions of the Azores. A description of the dynamic conditions for their development is given.

4) Section 2.2, page 6, line 11:

The authors state "Since this turbulent layer is mainly governed by synoptic-scale circulation patterns ..." What exactly do the authors mean? Please clarify. Is this a general comment or a comment associated with the specific cited study of Dayan et al., 1988?

In order to better explain the role of the synoptic scale circulation on shaping the structure and depth of the atmospheric mixed layer, a short paragraph and references (Businger and Charnock, 1983; Holt and Raman, 1990; Sinclair et al., 2010) supporting such a statement was added to the text.

5) and 6): Sections 2.2:

There is extensive description of the link between synoptic patterns and the structure of the mixing layer in Israel within this session. As a reader, I am rather confused and I do not really see the scope of such extended description of this link for a specific region in the frame of an overview paper for the regional baseline atmospheric pollution concentrations over Eastern Mediterranean. The majority of the discussed articles refer to studies at the coast of Israel which leads to an unbalanced discussion for Eastern Mediterranean boundary layer. There are a number of boundary layer studies from other coastal regions in Eastern Mediterranean and their links to atmospheric pollution (e.g. Melas and Enger, 1993; Kallos et al., 1993; Svensson, 1996; Kostopoulos and Helmis, 2014; Tombrou et al., 2015).

We do agree with the Referee as regarded to the rather unbalanced description of the MLD in the EM by reviewing studies representing mostly the coast of Israel. Consequently, this whole section was rewritten while referring to other boundary layer studies from other coastal regions in the EM basin such as the Greek Peninsula Crete and Cyprus. (Kassomenos et al. 1995, Svensson 1996, Leventidu et al. 2013, Tombrou et al. 2015, Zbinden et al., 2016),

- 7) The connection of the Sections 2.2, 2.3 and 2.4 with the discussion of the manuscript in later sections is fragile. The Sections 2.2, 2.3 and 2.4 could be merged into one broader in scope section for the role of the atmospheric boundary layer for atmospheric pollution over Eastern Mediterranean and make a stronger link with the core part of the review paper which is the atmospheric pollution concentration distribution during summer.

We adopted the suggestion made by the Referee and merged sections 2.2, 2.3 and 2.4 into one broader section entitled: "Atmospheric dispersion conditions over the EM". This new section describes the spatio-temporal distribution of the MLD and points on the differences observed in these characteristics among several sites within the EM basin. We believe that this modification indeed reinforces the link between both essential components of this review, the atmospheric processes and the issuing tropospheric pollutant concentrations.

- 8) Section 2.5: This section in its current form provides basically information from a single study for a receptor site at Israel. It does not provide an overview over Eastern Mediterranean. I am not sure what the added value of this Section is in its current form.

We do believe that the chemical composition of an air mass is inevitably related to its origins and pathways. Therefore, we think that such a section dealing with air mass origins is necessary. However, we fully agree that one sole study representing the flow climatology during summer over the EM is not sufficient. Accordingly, a paragraph was added to this section by describing the essential results that were obtained from other similar flow climatology studies conducted over Greece (Katsoulis 1999) and Turkey (Kubilay (1996) and compared them to the one performed over the central coast of Israel.

- 9) Page 13, lines 17-19:

The authors state that "in general, mineral dust does not affect the EM during summer". This is a rather strong statement. Consider that there a number of observational and modeling studies indicating a contribution of 25-30 % of dust aerosols on the total aerosol optical depth during summer

over land and sea in Eastern Mediterranean (Gerasopoulos et al., 2011; Georgoulas et al., 2016; Tsikerdekis et al., 2017; Marinou et al., 2017).

We admit that our statement as regarded to the partial contribution of mineralogical dust to the EM during summer was expressed in a rather too strong and liberal manner. Actually, besides the references given by the Referee on this issue, we ourselves were involved in such studies, e.g., Erel et al., 2007; Kalderon-Asael et al., 2009; Erel et al., 2013. The decision to limit ourselves only to the contribution of gaseous pollutants was derived from our awareness of the numerous studies published on the subject, in order not to create an overwhelming article. The relevant paragraph in the original manuscript has been moved to the Introduction and modified accordingly.

Ref:

Erel, Y., B. Kalderon-Asael, U. Dayan, and A. Sandler (2007): European Pollution Imported by Cooler Air Masses to the Eastern Mediterranean during the Summer Environ. Sci. Technol. 41, 5198-5203.

Kalderon-Asael, B., Y. Erel, A. Sandler and U. Dayan (2009): Mineralogical and chemical characterization of suspended atmospheric particles over the East Mediterranean based on synoptic-scale circulation patterns. Atmospheric Environment, doi: 10.1016/j.atmosenv.2009.03.057.

Erel, Y., O. Tirosh, N. Kessler, U. Dayan, S. Belkin, M. Stein, A. Sandler, and J.J. Schauer (2013): Atmospheric particulate matter (PM) in the Middle East: Toxicity, transboundary transport, and influence of synoptic conditions, in P. Censi et al. (eds.), Medical Geochemistry: Geological Materials and Health, DOI 10.1007/978-94-007-4372-4__3, © Springer Science C Business Media Dordrecht 2013.

10) Page 15, lines 7-14:

This is not exactly the finding of the study by Tyrllis and Lelieveld (2013). The various components observed over the Eastern Mediterranean that include the Etesians, subsidence, tropopause folds, stratospheric intrusions, and the summer ozone pool are dynamically interwoven manifestations of the influences induced by the South Asian monsoon and the midlatitudes. Tropopause folds and the subsidence are the key components yielding high ozone concentrations in the middle and lower free troposphere over the region (see e.g. the recent publications on the topic by Tyrllis et al., 2014 and Akritidis et al., 2016).

On the key components yielding high ozone concentrations in the middle and lower free troposphere over the region: We would like to thank the Referee for this constructive comment while driving our attention to further

references enabling us to give a better description of the referenced interlaced dynamical processes yielding to the concentration measured and simulated. Accordingly, a full paragraph was added while referring to Tyrllis and Lelieveld, 2013 and Tyrllis et al., 2014).

11) Page 18, lines 19-20:

"... controlled by the strength of Azores High and the PT". See my comment 3. There are a number of studies showing the differences between the anticyclonic center over central and southeastern Europe causing the Etesians and the Azores High.

The text was corrected as regarded to the anticyclonic centers formed over the Balkans which generate the Etesians rather than the Azores High.

12) Section 3.2:

The majority of the discussed articles refer to studies at the coast of Israel which leads to an unbalanced discussion for Eastern Mediterranean sulfate aerosols. Consider that there are some other earlier and recent studies for sulfate aerosols, SO₂ and their transport over Eastern Mediterranean during summer (e.g. Mihalopoulos et al., 1997; Kouvarakis and Mihalopoulos; Zerefos et al., 2000; Kubilay et al., 2002; Karnieli et al., 2009; Georgoulas et al., 2009; 2016).

We agree that the survey on EM sulfate aerosols could be further broadened for a better-balanced presentation of this issue. Consequently, we revised and used the references offered by the Referee and others in order to enrich the discussion of this section.

13) 14) and 15) Section 3.3:

The discussion of the NO_y species is fragmented, with lack of coherency and it does not provide a thorough overview over the Eastern Mediterranean regional baseline. In the beginning, there is some reference to baseline observational studies, then there is a sudden shift to a more extensive discussion of NO_y and NO_x species at urban sites at Israel and in the end, there is a short discussion of satellite studies of tropospheric NO₂ columnar densities.

Page 24, line 14: It is written that " NO_y, the total reactive nitrogen (NO + NO₂ + HNO₃) ...". The NO_y includes also PAN along with HNO₄, N₂O₅, NO₃ and other PAN homologues (PANs) and organic nitrates (Emmons et al., 1997). Page 24, line 23: It is written that NO of 20 pptv were observed at Finokalia. This is rather low and not typical for Finokalia station. For example, Kouvarakis et al., (2002) reports that NO concentrations ranged between the detection limit of 50 pptv (most of the time) and 100 pptv and NO_x' between 0.1 and 4 ppbv. Also, Gerasopoulos et al (2006) reports average day-time

values of NO up to 80 pptv and respective NO_z values up to 1.6 ppbv. See also related articles for NO_y measurements at Eastern Mediterranean from the MINOS campaign (Traub et al., 2003; Heland et al., 2003).

We agree on the constructive comments made by the Referee. Consequently, the whole Section 3.3 was restructured. We referred to some more studies related to NO_y measurements over Greece and Turkey along the references that were given by the Referee plus some others (Lammel and Cape, 1996; Amaroso et al., 2008; Im et al., 2008; and Ozden et al., 2008). Our referring to these additional studies, lead to a more balanced discussion reflecting better the whole EM region. Moreover, some parts of this section giving too many specific details of Israeli studies were significantly shortened. We do believe that this section in its reconstructed version gives a much more complete overview of the NO_y baseline levels as observed over the EM during summer.

16) Section 3.4:

The section focuses on CO sources and pathways but I think it is essential to give in the beginning also an overview of the CO baseline levels at Eastern Mediterranean based on observational studies. Furthermore, the discussion is not balanced e.g. from page 27 (line 8) to page 29 (line 29) there is extending discussion on the results of a single article (Drori et al., 2012).

As suggested by the Referee, we added a full paragraph to this section surveying several observational studies to get an insight of the CO baseline levels as reported from few EM countries (i.e., Greece (Riga-Karandinos and Saitanis, 2005), Lebanon (Saliba et al. 2006) and the Gaza strip, Palestine (Elbayoumi et al. (2014)). Furthermore, for a better balancing of this section, we reduced slightly the discussion on CO sources and pathways based mainly on the results of Drori et al. (2012) paper.

17) Section 3.5:

Methane is a long-lived species in contrast to all other species discussed earlier. I think the authors should make a distinction in the discussion of the short-lived pollutants versus the long-lived pollutants.

Discussing Methane as a long-lived species: A full paragraph was added to this section in which the long lifetime nature of Methane in contrast to other trace gases was demonstrated by few studies dealing with its possible association to low frequency atmospheric circulation patterns (i.e., ENSO and NAO). Moreover, the differing lifetimes of the pollutants surveyed in this study and their issuing implications was mentioned in the Introduction section.

Atmospheric pollution over the eastern Mediterranean during summer – A review

Uri Dayan¹, Philippe Ricaud², Régina Zbinden² and François Dulac³

¹Department of Geography, The Hebrew University of Jerusalem, Jerusalem, 91905, Israel

²CNRM, Météo-France, CNRS UMR3589, Toulouse, France

³Laboratoire des Sciences du Climat et de l'Environnement (IPSL-LSCE), CEA-CNRS-UVSQ, Univ. Paris-Saclay, Gif-sur-Yvette, France

Correspondence to: Uri Dayan (msudayan@mcc.huji.ac.il)

Abstract. The eastern Mediterranean (EM) is one of the regions in the world where elevated concentrations of primary and secondary gaseous air pollutants have been reported frequently, mainly in summer. This review discusses published studies of the atmospheric dispersion and transport conditions characterizing this region during the summer, followed by a description of some essential studies dealing with the corresponding concentrations of air pollutants such as ozone, carbon monoxide, total reactive nitrogen, methane and sulfate aerosols observed there.

The interlaced relationship between the downward motion of the subsiding air aloft induced by global circulation systems affecting the EM and the depth of the Persian Trough, a low-pressure trough that extends from the Asian monsoon at the surface controlling the spatio-temporal distribution of the mixed boundary layer during summer is discussed. The strength of the wind flow within the mixed layer and its depth affect much the amount of pollutants transported and determine the potential of the atmosphere to disperse contaminants off their origins in the EM. The reduced mixed layer and the accompanying weak westerlies, characterizing the summer in this region, lead to reduced ventilation rates, preventing an effective dilution of the contaminants. Several studies pointing at specific local (e.g. ventilation rates) and regional peculiarities (long-range transport) enhancing the building up of air pollutant concentrations are presented.

Tropospheric ozone (O_3) concentrations observed in the summer over the EM are among the highest over the northern hemisphere. The three essential processes controlling its formation (i.e., long-range transport of polluted air masses, dynamic subsidence at mid-tropospheric levels, and stratosphere-to-troposphere exchange) are reviewed. Airborne campaigns and satellite-borne initiatives have indicated that the concentration values of reactive nitrogen identified as precursors in the formation of ~~ozone~~ O_3 over the EM were found to be 2 to 10 times higher than in the hemispheric background troposphere. Several factors favor sulfate particulate abundance over the EM. Models, aircraft measurements, and satellite derived data, have clearly shown that sulfate has a maximum during spring and summer over the EM. The carbon monoxide (CO) seasonal cycle, as obtained from global background monitoring sites in the EM is mostly controlled by the tropospheric concentration of the hydroxyl radical (OH), and therefore demonstrates high concentrations over winter months and the lowest during summer when photochemistry is active. Modeling studies have shown that the diurnal variations in CO concentration during the summer result from long-range CO transport from European anthropogenic sources, contributing 60 to 80% of the boundary-layer CO over the EM. The values retrieved from satellite data enable us to derive the spatial distribution of methane (CH_4), identifying August as the month with the highest levels over the EM. The outcomes of a recent extensive examination of the distribution of methane over the tropospheric Mediterranean Basin, as part of the Chemical and Aerosol Mediterranean Experiment (ChArMEx) program, using model simulations and satellite measurements is coherent with other previous studies. Moreover, this methane study provides some insights on the role of the Asian monsoon anticyclone in controlling the variability of CH_4 pollutant within mid-to-upper tropospheric levels above the EM in summer.

1 Introduction

The relationship between atmospheric air pollutant concentrations and large-scale atmospheric circulation systems have been examined over the past decades (e.g., Davis and Kalkstein, 1990; Dayan et al., 2008). This strong relationship and its issuing dispersion condition at several scales, and climatically related variables such

as air pollutants, is presented in this work as part of the Chemistry-Aerosol Mediterranean Experiment (ChArMEx; <http://charmex.lsce.ipsl.fr>).

However, a first major drawback in attributing air pollutant concentrations to variations in large-scale atmospheric circulation arises from the fact that changes in removal processes and upwind emissions are not necessarily concurrent with variations in circulation. Some efforts were undertaken, mainly through coupled ~~climate~~-chemistry-climate models to treat and analyze at the same time, the changes in general circulation and atmospheric chemistry (Hein et al., 2001; Dastoor and Larocque, 2004). Moreover, secondary pollutants such as tropospheric ozone (O₃) result basically from photochemical reactions among precursors and, as such, are controlled by air mass characteristics such as temperature and humidity, and cloud cover/solar radiation. Accordingly, changes in trace gases concentrations are modified with respect to exposure of the differing air masses driven by ~~by exposure to differing air masses as governed by~~ changes in atmospheric circulation.

A second substantial shortcoming in trying to associate changes in pollutant concentration to variation in circulation patterns is their different life span and distribution. For example, durable greenhouse gases (GHG) such as methane (CH₄) and carbon dioxide (CO₂) are characterized by long life times of years as compared to nitrogen oxides and aerosols, which are most relevant for short spatial and temporal scales (Andreae, 2001; Voulgarakis et al., 2010). Radiative forcing of aerosols is of much higher spatial variability than GHG forcings due to the relatively short aerosol lifetime (daily-weekly scale) compared to that of GHG (monthly-yearly scale).

Both natural and man-made factors converge over the EM favoring the accumulation of pollutant concentration during summer. This region is in the crossroad of both large-scale convective motions: Hadley and Walker cells leading to subsidence. This process results in a reduced mixing depth, which inhibits an efficient dispersion of the pollutants. Moreover, the EM is a hotspot of high solar radiation driving the photochemistry of the atmosphere. In addition, the summer prevailing westerlies at shallow tropospheric layers favor the transport of ~~pollutant-enriched~~ rich air masses from central and eastern Europe to the eastern Mediterranean (EM). Based on the above key factors, this review focuses explicitly on summertime. Lelieveld et al. (2002) studied air pollutant transport over the EM in summer-time. They report

that the synoptic flow is controlled by the strong east-west pressure difference between the Azores high and the Asian monsoon low, with additional influence in the upper troposphere from the Tibetan anticyclone. This yields a contrasted situation in the tropospheric column with European influence in the lowermost troposphere, a much longer-range transport from Asia and North America at mid-tropospheric levels, and a major impact from Asia in the upper troposphere and lower stratosphere.

Desert dust is abundant over the EM, transported from two major source regions: the North African Sahara and the Arabian deserts. However, in general and predominantly, mineral dust affect the EM during all seasons except summer~~the winter and the transition seasons in spring and fall~~ (e.g., Dayan et al., 1991; Moulin et al., 1998; Sciare et al., 2003). reason why ~~and~~ mineral dust is not in the scope of this study which is focused on summer conditions.

In this review, –we first describe the atmospheric dynamic conditions favoring the building up of tropospheric air pollutant concentrations. Secondly, we propose a synthesis of the essential studies on air pollutant concentrations including ~~ozone~~ (O_3), sulfate ~~aerosols~~ (SO_4) aerosols, total reactive nitrogen (NO_y), carbon monoxide (CO), and ~~methane~~ (CH_4). The sources of the data reported include in-situ observations, balloon-sounding, aircraft and space-borne observations as well as model data, which results, in terms of dynamics, are mostly updated over 1948-2016 on availability.

2 Summer atmospheric dynamic conditions favoring the building up of tropospheric pollutants concentrations

Different spatial and temporal scales of motion affect pollutant transport and dispersion: the microscale, mesoscale, synoptic scale, and macro-, or global scale. At the scale of a few months, the planetary boundary layer is relatively well mixed. However, on shorter timescales and near the Earth's surface (where pollutants are emitted), transport and dispersion are often limited by atmospheric conditions. In this section, we will focus on the global and synoptic scale processes that favor a potential accumulation of pollutants in the EM troposphere.

2.1 Global and synoptic scales inducing subsiding conditions over the aastern eastern Mediterranean

In general, the atmospheric conditions over the EM are persistent during the summer and subject to two essential processes. The first is the cool advection at shallow tropospheric layers caused by the strong, dry north Etesian winds generated by the east–west pressure gradient manifested by large scale circulation features, low pressures over the EM as an extension of the Persian Trough (PT) and the high pressure over central and southeastern Europe- (Tyrlis and Lelieveld, 2013)–. This surface low pressure trough extends from the Asian monsoon through the Persian Gulf and further, along southern Turkey to the Aegean Sea (Figs. 1 and 2). The second is the dynamic subsidence generated by several global-scale processes: the African Monsoon as part of the subtropical descending branch of the Hadley cell (Fig. 3 left), the Asian Monsoon as part of the Walker cell (Fig. 3 right) and subsidence caused by the negative relative vorticity characterizing this region, during summer, as explained further on.

Rodwell and Hoskins (1996) used a hydrostatic primitive equation model initialized by a six-year June to August climatology derived from the European Center for Medium Range Weather Forecasts (ECMWF) analyses to investigate the monsoon desert mechanism enhancing summertime descent in the Mediterranean subtropics. They argued that the subsidence center in the eastern-MediterraneanEM is governed by the Asian monsoon rather than by the Hadley circulation and explained it by diabatic heating in the Asian monsoon region that induces a Rossby wave to its west, which generates air masses descent. This adiabatic descent balances the horizontal advection on the southern flank of the mid-latitude westerlies. Among the summertime descent regions, the strongest is located over the EM. Initiation of the descent over the EM coincides with the northward movement of heating during the onset of the monsoon. The anticyclonic center over north-west Africa and the monsoon result in an adiabatic warming that reduces the specific humidity and consequently enhances further the descent due to diabatic radiative cooling under cloudless sky conditions. Moreover, trajectory calculations performed by Rodwell and Hoskins (1996) revealed that the bulk of the sinking air masses originate from mid-latitude regions rather than over the intense monsoon convection areas over northern India. This is consistent with Tyrlis et al. (2013) who analyzed the thermodynamic state over the EM and calculated the temperature changes caused by horizontal advection by using ECMWF forecasts for diabatic heating over this region. They

found that subsidence at mid and lower levels is primarily driven by the midlatitude westerly flow. Furthermore, Tyrllis et al. (2013) pointed at the steep slopes of the isentropes in the free troposphere caused by the westward migration of the mid and upper level warming of the atmosphere away from the diabatic heating sources, which further enhances subsidence over the EM.

However, subsidence is neither restricted to mid-tropospheric levels nor solely associated to the descending branch of these both general circulation cells. In summer, at higher atmospheric layers, air masses converge and subside over the EM as contributed by –an anticyclonic curvature caused by ~~anticyclonic~~ anticyclonic centers formed over the Balkans. Such centers cannot be considered as extensions of the Azores high since they exhibit typical warm-core high structures from the surface up to mid-tropospheric levels (Anagnostopoulou et al., 2014); Tyrllis and Lelieveld (2013) point at wave disturbances originating over the North Atlantic that activate intense ridges over the Balkans. These ridges are further amplified by anticyclonic vorticity advection from northwestern Africa and in tandem with diabatic cooling under clear skies form such centers over central and southeastern Europe. The second dynamic factor inducing subsidence is an anticyclonic wind shear as related to the position of the Subtropical Jet. Under these circumstances, the southeastern part of the EM is exposed to the southern flank of the jet and therefore prone to negative shear vorticity. Although shear vorticity is an order of magnitude smaller than planetary vorticity, nearby jet streak makes this relative vorticity component significant due to the strong change in wind speeds across the jet. Contribution of both components enhances negative vorticity resulting in a total long-term mean negative vorticity of -1 to ~~-3~~ $-3 \cdot 10^{-5} \text{ s}^{-1}$ at 200 hPa (~12 km above sea level; a.s.l.) featuring the summer season over the EM (Fig. 4).

The contribution of the above-mentioned dynamic subsidence generated by all processes results in positive Omega values, defined as the Lagrangian rate of change in pressure with time, indicating a downward air motion over the whole EM with its highest core of maximum subsidence over Crete as depicted over mid-tropospheric levels (500 hPa geopotential height) (Fig. 5).

Following the subsidence caused by the large-scale downward motion, the warming and drying up is manifested by the delimiting sharp decrease in relative humidity over the EM Basin (Fig. 6).

Based on National Centers for Environmental Prediction/National Center for Atmospheric Research (NCEP/NCAR) reanalysis for 2000–2012, Lensky and Dayan (2015) have recently shown that the coincidence of negative vorticity advection aloft accompanied by cold horizontal advection, at lower tropospheric levels, featuring the EM during PT synoptic conditions drives the wind flow out of the thermal wind balance inducing a vertical downward motion (Figs. 2 and 7).

Ziv et al. (2004) found that the cool advection associated to the PT (Fig. 2) and the subsidence related to both descending branches of the African and Asian Monsoons monsoons (Fig. 3) are interrelated and tend to balance each other. They suggest that this compensation mechanism explains the reduced day to day temperature variations over the eastern part of the basinEM in summer (Fig. 8).

However, this monotonic regime is interrupted by the occurrence of hot day events resulting from an expansion of the Subtropical High from North Africa towards the EM, which are prone for elevated concentration of air pollutants. Harpaz et al. (2014) found that such episodes are confined to the lower 4 km and controlled by the intensity of the negative temperature advection rather than by the prevailing subsidence.

2.2 Atmospheric dispersion ~~conditions~~ overconditions over the eastern Mediterranean

The vertical velocity involved in the mixing process within the turbulent layer near the surface and specifically its depth are important parameters in determining air pollutant concentrations at shallow tropospheric levels (Zhang and Rao, 1999). The changes in the mixing layer depth (MLD, i.e. the height of the convective atmospheric boundary layer marked by the base of a thermal inversion) is governed by several factors: surface heating (Holtslag and Van Ulden, 1983), horizontal advection determined by the intensity of the sea breeze in coastal areas (McElroy and Smith, 1991; Lensky and Dayan, 2012), local terrain over the continent (Kalthoff et al., 1998), and the strength of the subsiding atmospheric air mass capping the mixed

layer, defined by the temperature profile within this stable layer and synoptic scale vertical motion (Dayan et al., 1988). **Beside these factors, the MLD is controlled also by thermal advection associated with synoptic weather systems and therefore, develops under strong forcing by synoptic scale circulations (Businger and Charnock, 1983; Holt and Raman, 1990; Sinclair et al., 2010).** ~~Consequently, both~~ Consequently, both the surface synoptic systems and their associated upper tropospheric conditions should be taken into consideration for understanding the behavior of the MLD over the EM basin and its adjacent coastal region.

Within the EM, ~~numerous—studies~~ numerous studies on the relationship between synoptic circulation and the structure of the MLD over the continental EM were conducted in Israel, the southeastern part of the basin. In particular, several studies were undertaken to characterize the spatial and temporal behavior of the MLD (Neumann, 1952; Halevy and Steinberger, 1974; Rindsberger, 1974, 1976; Dayan et al., 1988; Glaser et al., 1993; Lieman and Alpert, 1993; Dayan et al., 1996; Dayan and Rodnizki, 1999; Dayan et al., 2002; Ziv et al., 2004) using sounding measurements at the Israel Meteorological Service permanent site in Beit-Dagan (31.99°N, 34.82°E, 39 m a.s.l.), 8 km southeast of Tel Aviv and at other sporadic sounding sites.

The atmospheric noon-time mixed layer during the summer over the EM region is featured by a persistent elevated inversion base formed by a clear boundary line separating two differing air masses, a cool and humid mass above ground capped by a much warmer and subsiding dry air. The MLD is controlled by the interlaced relationship between the downward motion of the subsiding air aloft and the depth of the PT at the surface (Fig. 9).

Due to the existing correlation between the MLD featuring the PT and air pollution episodes over the EM evidenced in previous studies (Dayan and Graber 1981; Dayan et al., 1988; Koch and Dayan, 1992), this barometric system was classified into three essential types (Fig. 10) defined by the surface-pressure difference between Nicosia (35.16°N, 33.36°E, 149 m a.s.l.) in Cyprus and Cairo (30.1°N, 31.4°E, 75 m a.s.l.) in Egypt, and the temperature at 850-hPa in Beit-Dagan (Israel): Moderate PT, Shallow PT, and Deep PT (for details see Dayan et al., 2002).

Analyses of upper air measurements carried out regularly at Beit-Dagan, in the central coastal plain of Israel, point at significant differences of the MLD for the several

modes of the PT. The overall summer mean noon time mixing depth values for 1981-1984 is 764 ± 320 m (Dayan et al., 1988). A classification [with respect to the along-the](#) modes defined above resulted in mean and standard deviation values of 428 ± 144 m and 1010 ± 214 m for the shallow and deep PT modes respectively (Koch and Dayan, 1992). The spatial distribution of the mixing depth is rather homogeneous under deep PT conditions over the central coastal plain of Israel as compared to the shallow mode where its value is kept almost uniform above sea-level while penetrating inland. Due to the important implication of this behavior on the building up concentration of air pollutants, the lateral variance of the mixing depth was tested for part of the upper air measurements performed at 4 sites concurrently during the 1981-1984 campaign (Dayan et al., 1988). These sites on a west-east transect were: Nizanim (31.7°N , 34.63°E , 10 m a.s.l.) on the southern coastal shore of Israel; Beit-Dagan (31.99°N , 34.82°E , 39 m a.s.l.) on the coastal plain; Ruchama (31.5°N , 34.7°E , 210 m a.s.l.) ~20 km inland in the northern Negev Desert; and Jerusalem (31.77°N , 35.21°E , 786 m a.s.l.). The average thickness of the mixed layer when moving from the coast inland is reduced by 350 m while reaching Jerusalem (Fig. 11). The longitudinal variance of the MLD North-South vertical cross section on 21 summer noon-time upper air measurements performed simultaneously at 3 sites ~60 km apart along the Israeli coast revealed that the MLD decreases gradually from north to south (Dayan et al., 1988). This finding is explained by the greater distance of the southern sites from the cyclonic core of the PT (which persists in summer to the northeast of Israel) as well as the decreased distance from the anticyclonic center of the North African subtropical high (which persists during all seasons to the southwest of Israel). This lateral and longitudinal variance indicates that the most reduced summer MLDs are expected over the southeastern coast of the EM.

Most of the boundary layer studies from other coastal regions in the EM were conducted over the Greek Peninsula and the Aegean Sea. Kassomenos et al. (1995) analyzed the seasonal distribution of the MLD over the greater Athens area as obtained from the upper-air station of the Greek Meteorological Service at the Hellinicon airport for the period 1974-1990. They point at a noticeable annual variability in the afternoon MLD with maximum values (~800–1100 m a.s.l.) being observed by the end of July. They explain these high values observed during summer and the elevated inversion formed by the higher incoming solar radiation

characterizing this season, which is efficiently converted into sensible heat flux, favoring the development of a deep mixing layer and the horizontal transport of warm air masses. Nevertheless, few summer days with stably stratified atmosphere and very low MLDs (~300 m a.s.l.) inducing high surface pollution levels in Athens's basin (Greece) were identified as well. This is consistent with Svensson (1996) who analyzed such a summer day over the Athens's basin by applying a three-dimensional coupled mesoscale meteorological and photochemical model. Tombrou et al. (2015) mapped the MLD as part of the Aegean – GAME (Aegean Pollution Gaseous and Aerosol airborne Measurements) ~~during~~for two summer days under Etesian flow conditions over the Aegean Sea. The thermal profiles they analyzed demonstrate a well inflated MLD of 700 to 1000 m a.s.l. during noon-time over Crete as compared to the shallow marine boundary layer (~400-500 m a.s.l.) observed over both the east and west Aegean marine regions.

Characterizing the structure of the MLD spatial variation offshore over the EM basin is of importance for getting a better insight on the processes, which control the dispersion of contaminants over the sea. Few investigators (Gamo et al. (1982) and Kuwagata et al. (1990) for Japan; Stunder and Sethuraman (1985) for the United States; Gryning (1985) for Denmark) have analyzed the spatial variations of the atmospheric mixing layer in coastal areas. Similar studies as related to the EM Basin are quite limited and deal also mainly on the conditions not directly located over the open sea but rather at sites distant from the coastline.

In a 2006-2011 study based on a remote sensing tool, the ECMWF model and radiosonde observations launched at Thessaloniki's airport (Greece, 40.6°N, 22.9°E, 10 m a.s.l.) ~1 km from the coastline, Leventidu et al. (2013) found the MLD seasonal cycles peak with a summer maximum of 1400, 1800, and 2100 m a.s.l. in June, July and August, respectively.

Much earlier in the unique study of this type we are aware of, Dayan et al. (1996) have evaluated the spatial and seasonal distribution of the MLD over the whole Mediterranean Basin. Based on ~65000 air measurements from 45 radiosonde stations within and surrounding the basin from spring 1986 through winter 1988, the MLD was derived from the potential temperature gradient measured within the boundary layer and the capping stable layer above it. As expected, the summer values prove to

be generally higher over land and minimum over the most eastern and western limits of the Mediterranean Basin (Fig. 12). They concluded that the distance from the coastline and topography are the main factors influencing the spatial distribution of the MLD. The steep gradient in MLD values observed as moving onshore is consistent with the elevated summer values in Thessaloniki (Greece) reported by Leventidu et al. (2013).

Moreover, Dayan et al. (1996) found that the most striking temporal effect on MLD distribution over the basin is caused by synoptic weather systems and the intensity of the sea-breeze along the coast. The diminishing of the MLD over the Mediterranean Basin as moving from its center eastwards toward the EM coast they have observed is consistent with the unique series of measurements of the temperature profiles performed during the summer of 1987 near Ashdod Harbor (31.82°N, 34.65°E), some 40 km south of Tel-Aviv (Israel) at 2 to 22 km from shore using a tethered balloon where prominent inversion bases of 350 to 600 m a.s.l. were observed (Barkan and Feliks, 1993). Moreover, such limited MLD values over the sea were obtained in the airborne Gradient in Longitude of Atmospheric constituents above the Mediterranean basin (GLAM) campaign in August 2014 (Zbinden et al., 2016): the MLD over the sea measured in the period 6-10 August 2014 was approx. 800 m a.s.l. over Crete diminishing to about 400–500 m a.s.l. over Cyprus.

The diurnal behavior of the ~~MLD is~~ MLD is assessed in the Israeli coastal ~~plain~~ plain based ~~based~~ plain based on routine radiosonde ascents that are, unfortunately, of coarse temporal resolution. The hourly maximum MLD is between 23:00 UTC and 05:00 UTC for all seasons and decreases gradually toward its minimal value at 18:00 UTC ([Dayan and Rodnizki, 1999](#))~~Ref. missing~~.

However, since this cycle is governed mainly by synoptic weather systems, and the strength of the sea-breeze, this behavior would be more significant for the summer. During this season, the variation of the mixed-layer height due to diurnal variations of solar radiation and local terrain effects is not obstructed by large-scale variations caused by frequent transitions between different synoptic configurations, as featured by other seasons. Consequently, MLD variation is most evident during the summer, mainly controlled by the daily sea-breeze cycle and heat fluxes that are most intensive then. The layer minimal depth along the coast, of 760 m. a.s.l., is usually observed

during late afternoon hours when heat fluxes dissipate rapidly and the wind speed of the cool sea breeze reaches its minimal rate. This process results in a decrease of the marine turbulent boundary layer depth (Dayan and Rodnizki, 1999). These MLDs are less developed as compared to the mean MLDs of 850 m. a.s.l. observed over the Athens basin by Kassomenos et al. (1995).

Assessing ~~The~~the atmospheric dispersion conditions is commonly derived from the ventilation rates calculation. This term is the MLD multiplied by the mean wind speed in the mixed layer, representing the potential of the atmosphere to dilute and transport contaminants away from a source region. Matvev et al. (2002) have calculated over 1948-1999 the mean and standard deviation of the mixing depth, wind speed and long-term range of ventilation rates at the Israel Meteorological Service sounding site in Beit-Dagan (Israel) for the summer. A criterion usually adopted is that if the ventilation coefficient is less than $6000 \text{ m}^2 \text{ s}^{-1}$ the site has limited ventilation (Dobbins, 1979; Pielke and Stocker, 1991).

Their results (Table 1) clearly show that the monthly long-term mean ventilation rates of $\sim 4500 \text{ m}^2 \text{ s}^{-1}$ characterizing the EM coastal zone during summer are reduced and therefore inhibit an efficient dispersion of pollutants as compared to the summer mean values of $\sim 7000 \text{ m}^2 \text{ s}^{-1}$ obtained by Kassomenos et al. (1995) over the greater Athens area.

2.3 Air mass origins over the eastern Mediterranean

The chemical composition of an air mass is inevitably related to its origin and pathway. Consequently, these both terms are indispensable in explaining its composition (Fleming et al., 2012). Studies of the long-range transport (LRT) of pollution by trajectory models help us interpreting and better defining the movement and removal processes affecting atmospheric concentrations. Although changes in wind direction are observed on a diurnal and seasonal basis depending on the synoptic conditions affecting the region, the prevailing wind flows over the EM are from the west towards the east. Therefore, air pollutants emitted from upwind sources to the west of the EM will reach the EM and will be added to those emitted locally. Indeed, numerous observational and modeling studies have confirmed that the EM is affected by the long-range transport of air pollutants originating from Europe (e.g., Dayan,

1986; Luria et al., 1996; Wanger et al., 2000; Erel et al., 2002, 2007 and 2013, Matvev et al., 2002; Rudich et al., 2008; Drori et al., 2012).

To get an insight on the LRT over the EM, the Air Resources Laboratory's trajectory model (GAMBIT- Gridded Atmospheric Multi-Level Backward Isobaric Trajectories; Harris, 1982) was applied over 1978-1982 (Dayan, 1986). The duration of each trajectory was chosen as 5-days backward in time enabling the tracing of air masses originating from Europe, the Mediterranean Basin (MB), North Africa and the Near East close to the EM central coast of Israel (Fig. 13).

The 850-hPa level (~1500 m a.s.l.) was chosen as the most representative of the transport layer. This level is selected as the intermediary level between the surface wind regime and the regime of upper winds relatively free from local surface effects. Trajectory direction was divided into five distinctive geographical classes as shown in Figure 13. Respective occurrences and seasonal distributions can be summarized as follows:

- 1) Long fetch of maritime air masses from northwest Europe crossing the Mediterranean Sea, accounting for 36%, was the most frequent on average and fell evenly throughout the whole year;
- 2) Northeast continental flow that originated in eastern Europe, accounting for 30%, was the most frequent during the summer season;
- 3) Southeast flow from the Arabian Peninsula, accounting for 5%, was infrequent, occurring mainly during the autumn;
- 4a) Southwest flow along the North African coast, accounting for 11%, was the most frequent during late winter and spring; and
- 4b) South-southwest flow from inland North Africa was accounting for 7%, with a late winter and spring maximum.

Therefore, 1) and 2) trajectory types are indeed predominant with a summer maximum occurrence (>66%) over the EM coastal zone.

The 5-years (1983-87) flow climatology study of back trajectories at Aliartos, Greece (38.22°N, 23.00°E) revealed that about 40% of the 850-hPa back trajectories arriving

to this site during summer, originate from northwest and north sectors (Katsoulis, 1999), which is consistent with the flow patterns reported by Kubilay (1996) for Mersin, Turkey. Katsoulis (1999) suggested that these predominant flow directions point at northeastern Europe and northwestern Asia as potential source regions.

These studies show that the main flow direction to the EM observed during summer lies between west and north wind sectors. This implies that the most probable source areas reaching and affecting the northern and eastern parts of this basin are the industrialized countries of eastern and central Europe located upwind to this part of the basin.

3. Summer atmospheric air pollutant concentrations

The EM is one of the regions in the world where elevated concentrations of primary and secondary gaseous air pollutants have been reported frequently. This region is influenced not only by local atmospheric dispersion conditions but also by the ability of the atmosphere to inherit a significant proportion of pollutants from European sources.

After reviewing the atmospheric dispersion and transport conditions characterizing the EM during the summer, a summary of the essential results published over the last decade dealing with trace gases and anthropogenic sulfate aerosol concentrations over this region is presented. These studies demonstrate how the above described global and synoptic scale processes control the extent of trans-boundary transport of air pollutants and chemical composition and concentrations over the EM.

3.1 Processes controlling O₃ formation

Most tropospheric O₃ formation occurs when nitrogen oxides (NO_x), ~~carbon monoxide~~ (CO) and volatile organic compounds (VOCs) react in the atmosphere in the presence of sunlight. Due to cloud free conditions, high incoming solar radiation characterizes the EM during summer (Lelieveld et al., 2002), which enhances the building-up of O₃ concentrations.

Numerous researchers have identified the EM as a “hot spot” of summertime tropospheric ozone (e.g., Stohl et al., 2001; Roelofs et al., 2003; Zbinden et al., 2013; Zanis et al., 2014; Doche et al., 2014; Safieddine et al., 2014).

Zbinden et al. (2013) derived the climatological profiles and column contents of tropospheric O₃ from the Measurements of Ozone by Airbus Aircraft program (MOZAIC) over the mid-northern latitudes (24°N to 50°N) over the 1994-2009 period. Among the 11 most visited sites by the MOZAIC aircrafts, is the EM cluster, which comprises 702 profile data from the two airports of Cairo (31.39°E, 30.10°N, [in Egypt](#)), and Tel-Aviv, (34.89°E, 32.00°N, [in Israel](#)), from which monthly means were derived. The O₃ volume mixing ratio obtained were converted to Dobson units (DU) and validated against coincident ozonesonde profiles. Considering all sites, the EM reaches the largest tropospheric O₃ column concentration of 43.2 DU in July [that is related to an extreme summer maximum within 1-5km](#), in agreement with [the results derived from the space-borne Ozone Monitoring Instrument \(OMI\) and Microwave Limb Sounder \(MLS\) the summer extreme found](#) by Ziemke et al. (2011), pointing at the favorable photochemical conditions characterizing this region.

Zanis et al. (2014) identified a summertime pool with high O₃ concentrations in the mid-troposphere over the EM over the 1998-2009 period as derived from the ERA-Interim reanalysis O₃ data, the Tropospheric Emission Spectrometer (TES) satellite O₃ data, and simulations with the EMAC (ECHAM5–MESSy) atmospheric chemistry–climate model. They indicated that the high O₃ pool over the mid-troposphere is controlled by the downward transport from the upper-troposphere and lower-stratosphere over this part of the MB, which is characterized by large-scale subsidence. This subsidence is regulated by the Asian Monsoon as described in Section 2.1. Furthermore, Zanis et al. (2014) based on previous case studies (e.g., Galani et al., 2003; Akritidis et al., 2010) and climatological studies (e.g., Sprenger and Wernli, 2003; James et al., 2003) and their own results deduced that the mechanism leading to high tropospheric O₃ over the EM consists of two essential consecutive phases. In a first stage, an enrichment in stratospheric O₃ occurs into the upper-troposphere via a stratosphere-to-troposphere transport process. In the second stage, these ~~ozone~~[O₃](#)-rich air masses are transported downward by the strong summertime subsidence characterizing this region.

Doche et al. (2014) analyzed tropospheric O₃ concentrations for the 2007-2012 period as observed over the MB by the space-borne Infrared Atmospheric Sounding Interferometer (IASI). They identified an abrupt west–east O₃ gradient in the lower troposphere over the Mediterranean Basin with the highest concentrations observed over its eastern part. These concentrations were observed at mid-tropospheric layers (3 km) caused by subsiding ozoneO₃-rich air masses from the upper-troposphere, typifying summer. A clear and consistent seasonal variability emerges from their measurements, showing a maximum of the 3-km partial column O₃ concentration in July (Fig. 14). This is consistent with the study of Tyrlis and Lelieveld (2013) who found that the key dynamic driving factors yielding to high O₃ concentrations in late July and early August, in mid and lower free troposphere, are maximum tropopause folding activity, i.e., stratospheric air intruding into the troposphere and the subsidence over the EM, featuring Etesian outbreaks, which are temporally well correlated with the Indian monsoon. This tropopause folding is manifested by a slightly lower tropopause in mid and lower free troposphere observed during such outbreaks over the latitude of the Aegean forming a narrow “transport corridor” of positive Potential Vorticity anomalies. Tyrlis and Lelieveld (2013) argue that such frequent subsidence of high Potential Vorticity illustrates the important role of stratospheric intrusions in the summer dynamic conditions over the EM. Furthermore, a climatology of tropopause folds over this region based on the ERA-Interim data spanning the period 1979–2012 identified the Anatolian plateau as hot spot of fold development that occurs ~25% of the time during July and August, and a seasonal evolution linked with the South Asian Monsoon-monsoon (Tyrlis et al., 2014). The contribution of tropopause folds in the summertime pool of tropospheric ozone-O₃ over the EM was confirmed by Akritidis et al (2016) as simulated with the EMAC atmospheric chemistry model.

Based on IASI measurements and the Weather Research and Forecasting Model with Chemistry (WRF-Chem), Safieddine et al. (2014) have shown that the air column of the first 2 km above ground is enriched by anthropogenic O₃. Above 4 km, O₃ is mostly originating from outside the Mediterranean Basin by LRT process or generated through stratosphere-to-troposphere exchange characterizing the eastern part of the MBEM during the summer.

Air masses from surrounding regions in the EM atmosphere have a great impact on surface O₃ concentrations. In a recent study, Myriokefalitakis et al. (2016) have investigated the contribution of LRT on O₃ and CO budget in the EM basin, using a global chemistry transport model (CTM), the TM4-ECPL, driven by ECMWF Interim re-analysis project (ERA-Interim) meteorology. They found that about 8% of surface O₃ concentrations are affected by local anthropogenic emissions, whereas subsiding air masses from the free-troposphere and horizontal transport from surrounding regions provide about 38% and 51% of O₃ sources, respectively, into the EM mixed layer depth. Although elevated O₃ concentrations over the EM during the summer are mainly attributed to LRT of polluted air masses originating from Europe and lingering over the Mediterranean Basin, its enhancement as a secondary pollutant is also caused by its precursors emitted along the coasts of the EM. Consequently, several studies dealing with O₃ concentrations measured over coastal sites surrounding the EM and its inland penetration are presented.

Measurements of O₃ were performed at several sites in Crete and Greece and for rather long periods: over the northern coast of Crete, at Finokalia (35.50°N, 26.10°E) 70 km northeast of Heraklion, from September 1997 to September 1999 (Kouvarakis et al. 2000); from a rural area (40.53°N, 23.83°E) close to Thessaloniki in the north of Greece from March 2000 to January 2001 and from an O₃ analyzer installed in a vessel traveling routinely from Heraklion, Crete to Thessaloniki, Greece, from Aug. to Nov. 2000. Based on these measurements, Kouvarakis et al. (2002) pointed out the existence of a well-defined seasonal cycle in boundary layer O₃, with a summer maximum both above the Aegean Sea and at Finokalia. They indicated that LRT is the main factor accounting for the elevated O₃ levels above the EM. This finding is consistent with the 1997–2004 surface O₃ time series at Finokalia (Crete) of Gerasopoulos et al. (2005) who investigated the mechanisms that control O₃ levels and its variability. They identified transport from the European continent as the main mechanism controlling the O₃ levels in the EM, especially during summer when O₃ reaches a July maximum of 58 ±10 ppbv. Moreover, on a larger regional scale, Kourtidis et al. (2002) used ozonesonde ascents, lidar observations, ship cruises, and aircraft flights, to show that south and southwestern synoptic flows associated with Saharan dust events result in lower O₃ above the planetary boundary layer by 20–35 ppbv, as compared to northerly flows, which transport air from continental Europe.

Based on sixteen years of O₃ concentrations measured at the EMEP Agia Marina Xyliatou rural background station in Cyprus and 3 other remote marine sites, over the western, central and eastern parts of the island, Kleanthous et al. (2014) have shown that local precursors contribute to only about 6% (~3 ppbv) of the observed O₃. However, elevated concentrations of this secondary pollutant occurring in summer are attributed to LRT of air masses mainly originating from northerly and westerly directions. The summer average annual maximum of 54.3 ±4.7 ppbv was observed to be related to the transport of polluted air masses from [the Middle East, Near Asia, East and Central Europe](#) toward Cyprus.

Despite the prevailing synoptic meteorological conditions featuring the EM in summer, the differing pathways of the LRT of polluted air masses can affect differently the buildup of pollutants concentrations. To investigate such changes, Wanger et al. (2000) performed a comprehensive study that included 150 hours of instrumented aircraft monitoring flights comparing two events of air mass transport (September 1993 and June 1994) representing two distinct types of LRT. This airborne study comprised flight paths performed approximately 70 km offshore parallel to the Israeli coastline and 180 km in length with Tel-Aviv in the center.

These flights were performed during midday under westerly wind flow conditions ~~and~~ at an altitude of 300 m a.s.l. (well within the atmospheric mixed layer). While both wind flow conditions were nearly similar through the measurement periods and along the 180-km flight path, the air mass sampled in September 1993 was much “cleaner” than the one sampled in June 1994. The ~~averaged O₃ concentrations~~ of ~~O₃~~ ~~averaged~~ ~~for~~ the first campaign was 39 ±7 ppbv, against 48 ±9 ppbv in the second period. Therefore, Wanger et al. (2000) model simulation showed that the pollution sources in southern Europe and the Balkans did not affect the EM coasts in September 1993, contrarily to the synoptic conditions and simulation results for the June 1994 period where the winds over the EM tended to be northwesterly and thus forcing the polluted air masses toward the coasts of the EM.

The summer synoptic and dynamic conditions prevailing over the EM supply the essential ingredients for the building up of O₃ concentrations. Based on the similar climatic conditions between the Los Angeles Basin ([USA](#)) and the EM, Dayan and Koch (1996) proposed a theoretical description of the cyclic mechanism in summer,

leading to fumigation (i.e., a downward dispersion of an enriched O₃ cloud toward the ground) further inland from the EM coast. Under the deep mode of the PT, stronger westerly winds, acting as a weak cold front (Fig. 15, panel A1), penetrate far inland, undercutting the mixed layer polluted by O₃ from the previous day (Fig. 15, panel A2). In this way, part of the mixed layer containing O₃ is pushed upward and isolated from the ground. If the pressure gradient weakens on the following day, the western flow weakens (Fig. 15, panel B1). The cooling effect of the cool and moist marine air is consequently reduced and the convective boundary layer inflates rapidly. When the top of the mixed layer reaches the elevated O₃ cloud, the latter is penetrated by convective currents (Fig. 15, panel B2) and parts of the cloud are entrained toward the ground in this fumigating process.

Elevated O₃ concentrations (>117 ppbv) were measured at inland rural sites of central Israel during the 1988-1991 early summer months (Peleg et al., 1994). Based on air mass back-trajectory analyses, these elevated O₃ mixing ratios were found only in case of air masses overpassing Tel Aviv metropolitan area. Furthermore, the very low ratio of SO₂/NO_x ([sulfur dioxide, SO₂](#)) clearly indicates that O₃ precursors such as ~~nitrogen oxides (NO_x, the sum of NO and NO₂), carbon monoxide (CO), and volatile organic compounds (VOC)~~ originate mainly from fossil-fuel combustion from mobile sources (Nirel and Dayan, 2001). These pollutants are subjected to chemical and photochemical transformations in the presence of solar radiation and atmospheric free radicals to form O₃.

Over central Israel, the main source for these precursors emitted along the Israeli coastline is transportation (Peleg et al., 1994). Since O₃ and other secondary pollutants formation takes several hours, significant transport and mixing occur simultaneously with the chemical reactions (Seinfeld, 1989; Kley, 1997). Thus, increasing urban and commercial activity along the highly populated Israeli coastal region, together with expanding transportation activity in the Gaza region, was found to strongly deteriorate inland air quality and, specifically, to cause increasingly elevated inland O₃ levels. Model results showed that traffic emissions during the morning rush hour from the Tel Aviv metropolitan area contribute about 60% to the observed O₃ concentrations (Ranmar et al., 2002). Moreover, their study showed the summer season features a shallow mixed layer and weak zonal flow, leading to poor ventilation rates, which restrict O₃ dispersion efficiency. These poor ventilation rates

result in the slow transport of O₃ precursors, enabling their photochemical transformation under intense solar radiation during their travel inland from the EM coast.

However, elevated O₃ concentrations are not limited to the summer over the EM. Dayan and Levy (2002) found 103 “high-ozone days” where O₃ is >80 ppbv for at least 2 hours based on 24 Israeli sites over 1997-1999. From their O₃ temporal analyses, they concluded that the highest values are more frequent during the transitional (spring and autumn) seasons (65% of 103 days) than during the summer season (35%).

Based on the recent remote sensing tools in conjunction with meteorological observations and models, we conclude on the three essential processes that control the O₃ concentration during summer at various tropospheric levels over the EM: 1/ in the shallow troposphere, the horizontal transport of O₃-enriched air masses from eastern continental Europe to the region controlled by the anticyclonic center over central and southeastern Europe and the PT causing the Etesians; 2/ the dynamic subsidence at mid-tropospheric levels; and 3/ the stratosphere-to-troposphere exchange in the upper troposphere. At the surface of the EM coast, during transitional seasons, high O₃ episodes are associated with hot and dry air masses originating east of Israel, where O₃ precursor emissions are negligible, demonstrating that high O₃ levels are more dependent on air mass characteristics than on upwind precursor emissions.

3.2 Particulate sulfate (SO₄) abundance

Globally, the two main particulate sulfate (SO₄) precursors are sulfur dioxide (SO₂) from anthropogenic sources and volcanoes, and dimethyl sulfide (DMS) from biogenic sources, especially marine plankton. In the EM atmosphere, particulate sulfate-SO₄ contributes more than 50% to the submicron aerosol mass (Bardouki et al., 2003a, b; Sciare et al., 2005). A first attempt to quantify the biogenic contribution caused by the oxidation of marine DMS as possible source to particulate sulfate-SO₄ observed over the EM coastal region, was carried out by Ganor et al. (2000). They used an instrumented aircraft during August 1995 to sample DMS and methane sulphonic acid (MSA) offshore and over land of Israel. Being exclusively produced by oxidation of DMS, MSA was used as tracer. Ganor et al. (2000) found this source as a rather limited contributor: between 6 and 22% of the non-sea-salt SO₄ (nss-SO₄)

measured during summer was attributed to marine biogenic production. Evidently, several other factors favor particulate ~~sulfate-SO₄~~ abundance over the EM. The homogeneous conversion of gaseous SO₂ to particulate ~~sulfate-SO₄~~ is rather slow, i.e., about 1–3% per hour (Meagher et al., 1981). Wet deposition chiefly governs the atmospheric lifetime of ~~sulfate-SO₄~~, estimated to be up to 6 days on a global average (Chin et al., 2000). Due to rainless conditions and associated wet deposition in summer, and the slow dry deposition velocity of ~~sulfate-SO₄~~ aerosol (~0.01–0.4 cm s⁻¹), ~~sulfate-SO₄~~ aerosols account for 50–90% of the total sulfur (S) in transported air masses toward the EM (Matvey et al., 2002). Two additional factors favor late spring and summer particulate ~~sulfate-SO₄~~ regional abundance. First is the intense radiant energy emitted by the sun under clear sky conditions that leads to an efficient oxidation of SO₂ to SO₄ via hydroxyl radical (OH) as the predominant oxidant during daytime (Mihalopoulos et al., 2007). Second is the prevailing summertime westerly winds that transport ~~sulfate-SO₄~~-rich air masses from sources over central Europe before significant removal occurs. A pioneering study to measure particulate ~~sulfate-SO₄~~ in the background atmosphere of the EM was carried out by Mihalopoulos et al (1997) in Finokalia-, Greece. They reported a mean ~~sulfate-SO₄~~ aerosol concentration of 188 neq m⁻³ (~9-μg m⁻³) with a minor marine contribution of about 5% resulting in a concentration of 178 neq m⁻³ (~8.5 μg m⁻³) for ~~nss~~for nss-SO₄. These summer concentrations, about 10% higher than those observed in Thessaloniki (Tsidouridou and Samara, 1993), were associated with transport from eastern and central Europe. This is consistent with Sciare et al. (2003) who measured particulate nss-SO₄ during a one-month experiment in summer 2000 at a background site on Crete. They found a high average concentration of 6 μg m⁻³ (~62 nmole m⁻³) for air masses originating from Turkey and Central Europe. Identical results were obtained by Koulouri (2008) who measured similar nss-SO₄ concentrations during the period July 2004–July 2006.

Another source of ~~sulfate-SO₄~~ aerosols is ship emissions, which contribute substantially to atmospheric pollution over the summertime Mediterranean region. Based on a regional atmospheric-chemistry model and a radiation model, Marmer and Langmann (2005) found that the summer mean ~~sulfate-SO₄~~ aerosol column burden over the Mediterranean is 7.8 mg m⁻², 54% originating from ship emissions.

Concentrations of ~~sulfate~~SO₄-rich air masses have been measured intermittently at various downwind ground sites in Israel, the easternmost Mediterranean region, from an instrumented aircraft for a 10-year period between 1984 and 1993 by Luria et al. (1996). They found that the concentration of particulate ~~sulfate~~SO₄ observed during the summer was relatively high compared to other world locations, ~~exceeding~~. ~~The highest values~~ occasionally ~~exceed~~ 500 nmole m⁻³ ~~as compared to~~. ~~Note W~~wintertime levels ~~that~~ were in the range of 50-100 nmole m⁻³. ~~From airborne observations In their airborne study~~, Wanger et al. (2000) measured an averaged SO₄ concentration of 38 ±7 nmole m⁻³ in their first series of measurement between 5 and 9 September 1993, and up to 108 ±63 nmole m⁻³ between 15 and 21 June, 1994. The annual average, calculated in Luria et al. (1996), is 100 ±15 nmole m⁻³, which is twice as high as predicted for the region by a global model and as high as reported for some of the most polluted regions in the USA. They pointed to several indicators suggesting that the origin of the particulate ~~sulfate~~SO₄ over the EM region is not from local sources but the result of LRT. The indicators include the lack of correlation between SO₄ and primary pollutants, the high SO₄ to total ~~sulfur~~S values, the origin of the air mass back trajectories and the fact that similar levels were observed during concurrent periods at different sites. Throughout their study, a higher concentration of SO₄ was found during the afternoon hours, especially during the summer and at the inland locations. **However, aerosol chemical analyses from a two-stage aerosol sampler from a receptor site in Sde-Boker (31.13°N, 34.88°E, 400 m a.s.l.) in southern Israel, point at a significant decline of 24% of these elevated nss-SO₄ mean concentrations for the summer months (July and August) from ~3 μg m⁻³ in 1994 to ~2.3 μg m⁻³ for 2004. This decline is attributed to the decrease of ~~sulfur~~S emissions in central and eastern Europe over the past 3 decades. Indeed, the majority (60%) of the calculated air mass back trajectories related to extreme events (during which the fine fraction ~~sulfur~~S concentration at Sde-Boker exceeded a threshold of 3 μg m⁻³) originated from Russia, Ukraine and northern Black Sea region (Karnieli et al., 2009).**

The effect of land and sea breeze (~~LSB~~) on coastal meteorology in general and the interaction between ~~land and sea breeze~~ LSB and air pollutants in particular plays an important role in determining many aspects of coastal environments around the world. A meteorological phenomenon that is often associated with the ~~land and sea breeze~~ LSB is air mass recirculation in coastal regions (Miller et al., 2003; Levy et al., 2008).

Sulfate particles measured along the central coast of Israel in mid-August 1987 and mid-August 1995 and identified by lesser microprobe analysis have shown that the concentration during land breeze were 6-10 times higher ($34.6\text{--}64.1 \mu\text{g m}^{-3}$) as compared to sea breeze conditions ($4.3\text{--}7.1 \mu\text{g m}^{-3}$) (Ganor et al., 1998).

In another attempt to quantify the sulfur-S flux arriving at Israel's western coast from Europe and the Israeli pollution contribution to the air masses leaving its eastern borders towards Jordan, Matvev et al. (2002) conducted 14 research flights at an altitude of approximately 300 m above ground level, measuring sulfur-dioxide SO_2 and particulate sulfates SO_4 during the summer and autumn seasons. Two different legs were performed for each research flight: the first over the Mediterranean Sea, west of the Israeli coast and the second along the Jordan Valley. Their results have shown that the influx of sulfur (S) reaching the Israeli coast from Europe varied in the range of $1\text{--}30 \text{ mg S h}^{-1}$, depending on the measuring season. The SO_4 level in the incoming LRT air masses was at least 50% of the total sulfur-S content. The contribution of the local pollutant sources to the outgoing easterly fluxes also strongly varied with the season. The Israeli sources contributed an average of 25 mg S h^{-1} to the total pollution flux during the early and late summer as compared to only approximately 9 mg S h^{-1} during the autumn period. The synoptic analysis indicates that conditions during the summer in Israel favor the accumulation of pollution species above the Mediterranean Basin from upwind European sources. This season is characterized by weak zonal flow within a shallow mixed layer that lead to poor ventilation rates, limiting an efficient dispersion of these pollutants during their transport eastward. Under these summer conditions, in-flux local contribution and the total out-flux of these pollutants are elevated as opposed to other seasons. To illustrate, during autumn, the EM is usually subjected to weak easterly winds, interrupted at times by strong westerly wind flows inducing higher ventilation rates. Such autumnal meteorological conditions and the lack of major emitting sources eastwards of Israel result in lower sulfur-S budgets to and from Israel.

An estimate of the yearly flux showed that approximately 0.06 Tg S arrived at the Israeli coast from the west (Matvev et al., 2002). This is approximately 15% of the pollution leaving Europe towards the EM. The outgoing flux towards Jordan contributed by local sources was calculated to be 0.13 Tg S per year, i.e. almost all the sulfur-S air pollution emitted in Israel. The results of the flux rates for the sulfur-S

compounds over Israel are summarized in Table 2 for the different research flights and field campaigns. These latter results show for the early summer time that the uppermost fluxes from the west were ~~for the early summer time~~, averaging 0.19 Tg y^{-1} . During this season, the levels doubled the averages for late summer (0.085 Tg y^{-1}) and were over five times the average levels measured for the autumn (0.035 Tg y^{-1}). The wide range in fluxes derived is explained by the varying distance from the polluted coastline.

The Aerosol Optical Depth (AOD), the vertical integral over an atmospheric column of the incident light scattered and absorbed by aerosols, is often used to estimate the aerosol loading in the atmosphere. Particulate SO_4 are among the numerous aerosol types. Nabat et al. (2013) compared AOD from several model data to satellite derived data for the period 2003-2010 over the Mediterranean region. They found that the AOD seasonal cycle obtained from the Monitoring Atmospheric Composition and Climate (MACC) reanalysis model, which includes Moderate-Resolution Imaging Spectroradiometer (MODIS) AOD assimilation at 550 nm resembles much the satellite-derived AOD variability and have the best spatio-temporal correlation compared to Aerosol RObotic NETwork (AERONET) stations. Based on these models and satellite derived data, Nabat et al. (2013) have clearly shown that particulate ~~sulfate~~ SO_4 , ~~as one of the aerosol types~~, has a maximum during spring and summer over the ~~eastern MBEM~~ (Fig. 16). Matvev et al. (2002) performed airborne measurements along a 150-km line west of the Israeli coast. They derived an annual flux of the order of 0.06 Tg yr^{-1} of (dry) ~~sulfur~~S across the corresponding surface. Given the observed ratio of ~~sulfate~~ SO_4 to total ~~sulfur~~S of 40-90% in the region (Matvev et al., 2002; Sciare et al., 2003), the annual flux of SO_4 based on field measurements is $0.024\text{-}0.054 \text{ Tg y}^{-1}$. Rudich et al. (2008) used satellite data to estimate the pollution transport toward the EM. MODIS Terra- and Aqua-derived estimates of the annual ~~sulfate~~ SO_4 flux along the same transect are 0.038 and 0.040 Tg y^{-1} , respectively, in the middle of the range obtained from field observations.

Rudich et al. (2008) also found that MODIS-based estimates (from Terra and Aqua satellites) of the ~~sulfate~~ SO_4 flux agree reasonably well with the Goddard Chemistry Aerosol Radiation and Transport (GOCART) model simulations of anthropogenic ~~sulfate~~ SO_4 , as shown in Figure 17 for seasonal averages. Compared to Terra, The annual SO_4 flux from the GOCART model is 0.181 Tg y^{-1} , about 18% higher than the

~~MODIS/Terra estimate of 0.153 Tg y⁻¹. Similar comparison on a seasonal basis the GOCART exhibits that GOCART model over estimates are s the winter (by ~85%) and spring (by ~30%) fluxes about 85% and 30% higher in winter and spring, respectively, but 10-25% whilst lower estimates the summer and autumn fluxes by 10-25% lower in summer and autumn than the MODIS based estimates. The annual sulfate SO₄ flux from the GOCART model is 0.181 Tg y⁻¹, about 18% larger than the MODIS estimate of 0.153 Tg y⁻¹. If we consider the comparison between the GOCART model and MODIS/Aqua GOCART, the model annual flux is 0.201 Tg y⁻¹, about 25% higher than the MODIS/Aqua estimate of 0.159 Tg y⁻¹. On a seasonal basis, their estimates simulations are in excellent agreement with MODIS/Aqua estimates in summer and fall, but about 50% higher in the MODIS/Aqua winter and spring estimates. The GOCART simulated annual flux of 0.201 Tg y⁻¹ is about 25% higher than the MODIS/Aqua estimate of 0.159 Tg y⁻¹. Based on the comparison of the two instruments, the model results, and the consistency with the aircraft measurements, they concluded suggested that both MODIS instruments can be used for estimating the flux of pollution based on their daily AOD retrievals.~~

3.3 Local formation and long-range transport of total reactive nitrogen (NO_y)

Total reactive nitrogen (NO_y) is a collective term for oxidized forms of nitrogen in the atmosphere such as nitric oxide (NO), nitrogen dioxide (NO₂), nitric acid (HNO₃), nitrous acid (HNO₂), nitrate (NO₃), nitrogen pentoxide (2N₂O₅), peroxy nitric acid (HNO₃, HNO₄), PAN (peroxyacetyl nitrate (PAN), and other organic nitrates (Emmons et al., 1997). Research studies measuring inorganic reactive nitrogen compounds over marine areas in general, and more specifically over the EM basin are scarce (Lawrence and Crutzen, 1999; Corbett et al., 1999; Veceras et al., 2008). Measurements of NO₂, HNO₃ and HNO₂ undertaken with instrumentation on board a research vessel in the Aegean Sea between 25 to 29 July 2000 revealed typical NO₂ concentrations of 4–6 ppbv with a broad maximum of 20–30 ppbv. The level of NO₂ was relatively high during the night and low during the day due to enhanced photochemical activity, vertical mixing and the daily wind characteristics. Extreme NO₂ concentration were caused by up slope wind bringing air from marine traffic emissions trapped within the marine atmospheric boundary layer. The concentration of both, nitric and nitrous acids, in ambient air of the Aegean Sea was low, below 50 pptv. Večeřa et al. (2008) explained these results by the lack of

precursors for these acids (Cohen et al., 2000), the high solar irradiation leading to HNO_3 dissociation, and the reaction of ~~nitric acid~~ HNO_3 with sodium chloride aerosol.

NO_y , -identified as precursors in the O_3 formation, was measured by Wanger et al. (2000) for two summer airborne campaigns over the EM at an altitude of about 300 m (well within the MLD) using a high-sensitivity NO-NO_y analyzer (TEII 42 S, chemiluminescence method, ± 0.1 ppbv sensitivity). In the first campaign of September 1993, characterized by cleaner air mass conditions, an average NO_y concentration of 1.0 ± 0.6 ppbv was measured as compared to 3.9 ± 1.8 ppbv sampled during the June 1994 campaign.

The Mediterranean Intensive Oxidant Study (MINOS) campaign, performed in the summer of 2001, allowed Lelieveld et al. (2002) to examine the air pollution conditions at shallow and mid-tropospheric levels over the EM Basin. During this experiment, elevated concentrations, typically 0.1 to 0.2 ppbv, of NO in the upper troposphere and only about 20 pptv within the MLD were observed at the Finokalia station. However, the value measured within the MLD at Finokalia was rather low and not typical for this site. From fall 1998 to summer 2000, a Thermo Environmental Model 42C high-sensitivity chemiluminescence NO_x analyzer with a detection limit of 50 pptv was operated at Finokalia in parallel with the O_3 analyzer to monitor NO and NO_x (Kouvarakis et al., 2002). During the whole examined period, NO concentrations ranged between ~~the detection limit of~~ 50 pptv (most of the time) and 100 pptv, and NO_x' ($\text{NO}_x' = \text{NO} + \text{NO}_2 + \text{PAN}$) between 0.1 and 4 ppbv. Kouvarakis et al. (2002) interpreted the very low NO/NO_x' ratio obtained as pointing at the influence of the Finokalia station by aged air masses. Furthermore, they argued that the similar diurnal amplitude of O_3 above the Aegean Sea and at Finokalia during summer, indicates that the regime of NO_x above the Aegean is similar to that observed at Finokalia.

The observed diurnal evolution at Finokalia of NO and NO_z' - the later expressing mainly the sum of NO_2 , NO , ~~peroxyacetyl nitrate (PAN)~~-like compounds, organic nitrates and ~~nitric acid~~ HNO_3 - were used as tracers of pollution by Gerasopoulos et al. (2006) to analyze the diurnal variability of O_3 over the EM. The diurnal cycles of these two tracers based on 3.5 year of measurements point at a maximum value of ~ 70 pptv for NO and up to ~ 1.55 ppbv for NO_z' . These maxima were observed 1-2 h after the minimal O_3 concentration measured at about 06:30 UTC.

Ambient concentrations of NO, NO₂ and NO_x have been also reported over the northwestern parts of Turkey. An NO₂ concentration of 8.5 ±4.8 ppbv was obtained for the summer of 2005 by collecting weekly average data in a sampling site of the city Eskişehir, located 230 km to the west to the capital of Turkey by use of passive samplers (Ozden et al., 2008). Im et al (2008) studied O₃ pollution and its relationship with nitrogen-oxide (NO_x) species based on hourly concentration levels of ozone O₃, nitrogen-oxide NO, and hydrocarbon measured between 2001 and 2005 in Kadıköy, an urban district in the Anatolian side of İstanbul. The mean and standard deviation for the summer (June-August) NO, NO₂ and NO_x concentrations reported for this 5-year period were 14.4 ±6.2, 22.75 ±2.7, and 37.7 ±14.3 ppbv respectively. Moreover, they suggested that the very strong correlation they found between NO and NO_x, implies that the NO_x species are mainly from local sources.

Traub et al (2003) analyzed several trace gas concentrations measured along flight tracks of the Deutsches Zentrum für Luft- und Raumfahrt (DLR) Falcon aircraft over the eastern and central Mediterranean Sea during MINOS in August 2001. In order to inquire into the role of long-range transport (LRT) of pollutants of-in the air masses into above the Mediterranean area and to determine their source regions, 5-day backward trajectories were computed and initialized along the Falcon flight tracks. They found that all trajectories with source regions in eastern Europe were associated with higher mean concentrations than those from westerly directions. Traub et al (2003) hey measured a mean NO and NO_y concentration of 0.05 ±0.02 ppbv for NO and 1.4 ±0.4 ppbv respectively for the computed trajectories within the MLD originating from eastern Europe as compared to 1.4 ±0.4 ppbv 0.04±0.01 and 1.1±0.5 ppbv respectively for trajectories originating from western Europe. NO_x for about 74% of the computed trajectories within the MLD, trajectories originating from eastern Europe.

Increasing urban and commercial activity along the highly populated Israeli coastal region, together with expanding transportation activity has yielded few ground-based measurements studies in order to quantify the impact of local urban versus regional and foreign sources on the concentrations of the nitrogen-oxide NO_x species, which vary in their atmospheric fate.

Results of half-hourly NO_x concentrations recorded from 9 monitoring stations from 2002 to 2005 in the Haifa Bay, Israel, resulted in a typical mean mixing ratio of 25 ppbv (Yuval et al., 2007) and a typical background value below 0.5 ppbv for the summer over the EM (Alpert-Siman Tov et al., 1997). This background value was further evidenced by Dayan et al. (2011) who analyzed NO_x concentrations during the Day of Atonement. In this day, all traffic and most of the industrial activities cease in the Jewish populated parts of the country, which provides a unique opportunity to test the relative contribution of pollution sources within urban centers versus regional and foreign sources.

In a study aimed at analyzing the sources and sinks of ~~nitrous acid~~ HONO in urban areas, and their seasonal dependency, Amaroso et al. (2008) carried out measurements of HONO, NO_x, O₃, and SO₂ during autumn and summer in Ashdod (31°49'N, 34°40'E, 10 m a.m.s.l.) (south of Tel Aviv, Israel), a typical coastal Mediterranean urban area. The 15-day July campaign consisted of 5-min averaged 4320 measurements, of HONO, NO and NO₂. HONO analyses were performed with a liquid coil scrubbing/UV-vis instrument (see Amaroso et al., 2008). NO and NO₂ measurements were performed by a thermos Model 42C NO-NO_x analyzer. The mean concentration obtained for this campaign was 1.4 ±2.0, 6.0 ±8.8 and 14.8 ±7.3 ppbv for HONO, NO, and NO₂, respectively. The HONO mixing ratios obtained clearly point at the typical diurnal cycle with nighttime maxima and daytime minima (Lammel and Cape, 1996).

Ranmar et al. (2002) addressed the dynamics of transboundary air pollution, where transportation emissions (such as NO_x and VOC) originating from Israeli major coastal sources impact the onshore mixing layer. Analysis of NO_y data (here, the sum of all nitrogen oxide species, excluding N₂O) collected from 1 June to 30 September for the years 1999 and 2000 at a monitoring station located in metropolitan Tel Aviv, yielded an average of 24.5 ±15.1 ppbv. They noted the higher initial NO_y levels during the morning rush hour emissions that were subjected to a noticeable bleaching by the late morning sea breeze in comparison to inland locations, which leveled off at relatively higher midday concentrations. Ranmar et al. (2002) argued that this may indicate, in the absence of any alternative NO_y source, that the early morning NO_x produced by transportation sources in Tel Aviv is transported inland, providing additional NO_y to the regions along its path.

Beside cruises of research vessels, airborne campaigns, and ground truth measurements, satellite-borne initiatives have been undertaken to get a better insight on the reactive nitrogen concentrations over the EM. Marmer et al. (2009) used ~~the Ozone Monitoring Instrument (OMI) instrument~~ (Boersma et al., 2007) as an observation tool to measure atmospheric NO₂ column concentrations in order to validate ship emission inventories over the Mediterranean Basin. Figure 18 shows the average OMI NO₂ tropospheric columns (gridded to 0.125°×0.125°) over the Mediterranean Sea for June-August 2006. The most prominent feature here is the elevated NO₂ monthly mean. Under cloud free conditions, typical values ranged from 1.2 to 2.0 10¹⁵ molecules cm⁻² over the northeastern African coast, the EM coast, the southern coast of Turkey and the whole Aegean Sea, as compared to over 6 10¹⁵ molecules cm⁻² for European inland congested regions. Based on OMI NO₂ tropospheric columns and the Goddard Earth Observing System GEOS-Chem chemistry transport (GEOS-Chem) model, Vinken et al. (2014) attributed the elevated NO₂ columns regions over the Mediterranean to NO₂ emissions along ship tracks.

3.4 Carbon Monoxide sources and pathways

~~Carbon monoxide~~CO (CO) has a global-average lifetime of about two months in the troposphere and its molecular weight is close to that of air. This molecule is considered as an excellent tracer for pollution sources and pollution pathways through the troposphere. In addition to production by chemical oxidation in the atmosphere, CO is emitted by biomass burning, man-made sources, vegetation, and ocean. The CO seasonal cycle is mainly governed by the concentration of ~~the hydroxyl radical (OH)~~ in the troposphere (Novelli et al., 1992) and is expected to be the lowest in the summer when photochemistry is active and the highest during late winter or spring.

An assessment of CO baseline concentration levels at the surface over the EM is ~~presented~~ presented based on few observational studies that have been conducted for this pollutant. As part of a comparative air quality study, CO was analyzed at ~~two typical Mediterranean coastal sites in Greece, Patras (38.25°N, 21.74°E) and Volos (39.36°N, 22.94°E)~~, two Mediterranean Greek coastal urban sites (Riga-Karandinos and Saitanis, 2005). They observed an annual average hourly mean concentration of 1.14 ppm over 1995-2003 at Volos as compared to 0.95 ppm at

Patras over 2001-2003. The diurnal pattern at both sites during summer showed that vehicle-induced emissions contribute significantly to CO levels with peak concentrations of 1.14 and 0.96 ppm measured at 09:00 UTC at Volos and Patras, respectively. Over the EM coast, hourly average CO measurements conducted by Saliba et al. (2006) in the city of Beirut (33.89°N, 35.50°E), Lebanon, point at an average monthly CO concentration during summer of 1.05 ppm, similar to the concentrations observed in Volos and Patras, Greece (Riga-Karandinos and Saitanis, 2005).

CO concentrations were measured by Elbayoumi et al. (2014) from the fall of 2011 through mid-2012 in the Gaza strip, in the southeastern coast of the EM as part of an exposure study to assess the effect of seasonal variation on the mean daily indoor-outdoor ratio at 12 schools located over the northern, central and southern strip of Gaza. They observed a six-hour average daily outdoor CO concentrations of 0.96 ±0.91 ppm for all the schools. They further reported that the outdoor CO concentration spanned from 0.10 ppm to 2.46 ppm with a mean of 0.88 ppm for urban sites and from 0.10 to 2.71 ppm with a mean of 1.02 ppm for overpopulated sites along the Gaza strip.

Due to the key role CO plays in atmospheric chemistry, several chemistry-transport modeling studies were devoted to this subject. CO was measured and used as a tracer in such a model (Lelieveld and Dentener, 2000) during the summer 2001 MINOS campaign (Lelieveld et al., 2002). The model diagnosed CO from anthropogenic sources in different parts of Europe, North America, and Asia. Trajectory calculations in the lower troposphere identified western and eastern Europe as the main source emissions. Consequently, model simulations were performed for August 2001 over Sardinia (40°N, 8°E) in the western Mediterranean (WM) and over Crete (35°N, 25°E). Considering the negligible impact of local pollution sources, the high CO levels observed over Crete, in excess of 150 ppbv, were surprising. The model results indicated that regions surrounding the Mediterranean such as southern Italy, Greece, Serbia, Macedonia, the Middle East, and North Africa contribute relatively little to the CO pollution, typically about 20%. Furthermore, Lelieveld et al. (2002) found that the EM is affected by CO polluted air emitted from eastern Europe, Poland, the Ukraine, and Russia. This pollution flow, east of the Carpathian Mountains, is channeled over the Black Sea and the Aegean Sea, and contributes 60 to 80% of the boundary-layer

CO over the EM. Their model results are consistent with aircraft measurements, showing that the entire Mediterranean lower troposphere is polluted.

In the free [EM](#) troposphere, where westerly winds predominate, they revealed a quite different situation as compared to concentrations measured within the MLD. The mid-tropospheric CO measurements were ~75-80 ppbv. From their model tracer analysis, the largest contribution over the Mediterranean is found originating from Asia (40 to 50%). The CO typical lifetime (~2 months) enables air mass to circumnavigate the globe, which results in a low variability of its concentrations. Lelieveld et al. (2002) found that contributions by pollution from western and eastern Europe to mid-tropospheric CO were only about 10%.

Drori et al. (2012) conducted a study to locate the various CO sources converging from Europe, North Africa and the Middle East and quantify their respective contributions to the EM. Background CO concentrations are monitored regularly over the southern part of Israel in Sde-Boker ([Weizmann Institute of Science – WIS WIS Station Negev Desert: 31.13°N, 34.88°E, 400 m](#)) as part of the [National Oceanic and Atmospheric Administration \(NOAA\)](#) Earth System Research Laboratory Global Monitoring Division (ESRL/GMD), which aims at representing the EM. While comparing the seasonal cycle of Sde-Boker to other European ESRL/GMD background sites (see Table 3), one essential feature is eminent from their results represented in Figure 19: CO concentrations are high over winter months, decreasing abruptly during April and increasing again from November. A second maximum is observed during August compared to July and September (Drori et al., 2012).

To get an insight on the spatial distribution of CO concentrations over the EM, the Version 4 [Measurement of Pollution in the Troposphere \(MOPITT\)](#) level-2 CO retrievals (Deeter et al., 2010) were employed by Drori et al. (2012) using a priori information for MOPITT V4 CO retrievals based on [the Model for Ozone and Related chemical Tracers \(MOZART-4\)](#) chemistry-transport ~~model~~ [simulation](#) climatology (Emmons et al., 2010). The averaging kernel profile obtained for ~~a retrieval~~ [a retrieval](#) near Sde-Boker ESRL/GMD station shows that, during the day, the 900 hPa retrieval sharply peaks at the same level, indicating that there is a good sensitivity to lower tropospheric concentration. The anomalous high concentration observed at the WIS ESRL/GMD Sde-Boker station, and calculated by

the MOZART-4 model during August (Fig. 19), might be limited to lower levels, and therefore averaging over several layers might hide this signal. Furthermore, Drori et al. (2012) compared the in-situ measurements at Sde-Boker and CO retrieved from MOPITT to MOZART-4 model results. CO sources included direct emissions and secondary production from hydrocarbons oxidation, while CO sinks included a reaction with OH and dry deposition. The seasonal cycle of surface CO at Sde-Boker simulated by MOZART and averaged for five consecutive years shows a similar pattern ~~exhibiting CO concentration reaching~~ exhibiting CO concentration reaching a maximum in February and a second peak in mid-summer months (i.e., July and August) that surpasses those of the early summer (i.e., May–June) (Fig. 19).

To attribute the CO sources affecting the EM, Drori et al. (2012) partitioned these sources using a tagging method into five types: anthropogenic, biogenic, fire, chemical production, and ocean. The total CO concentration and specific contributions 2006–2007 times-series of MOZART at the surface at 30° N and 33.75° E are shown in Figure 20 where ocean sources contributions are not shown (~~Ocean is negligible (not shown)~~). Both biogenic (green line) and biomass burning sources (red line) have a minor contribution. Biogenic sources are characterized by a distinct seasonal cycle with high contribution over winter and low daily variability. Biomass burning has no defined seasonal signature and contributes on an episodic event basis. CO from chemical production (orange) contributes substantially (50–80 ppbv) with a defined seasonal cycle: low during winter and autumn and high during summer featured by a low daily variability. Anthropogenic sources were found to be the main contributor to the total CO (purple, 50–180 ppbv). As expected, their seasonal cycle is featured by winter elevated concentrations decreasing during spring, slightly increasing during summer and decreasing again during autumn. The daily variability is high and similar to the total CO daily variability. Comparing the daily variability of the various sources, Drori et al. (2012) concluded that anthropogenic sources mainly govern total CO daily variability over the EM.

To further attribute the CO surface daily variation, Drori et al. (2012) tagged the anthropogenic sources for the three northern continents, i.e., North America, Europe, and Asia. Figure 21 shows the results of these anthropogenic sources attribution to the CO surface. European anthropogenic sources contribute substantially (10–80 ppbv) to local CO concentrations with the greatest daily variability all year round. Asian and

North American sources are in the same order of magnitude (10–25 ppbv) with low daily variability during most of the year, and very small variability during summer. Obviously, daily summer CO variations in the EM are mainly caused by European anthropogenic sources. The seasonal cycle of the European contribution is very similar to the seasonal cycle of total CO, featured by a high concentration in winter, spring, and autumn and a lower summer concentration. The contribution of European emissions to CO surface concentrations is comparable to that from EM local emissions.

Drori et al. (2012) found, however, that local and European emission contributions to local CO concentrations are generally negatively correlated, meaning that either local or European sources are dominant, except during summer, when both sources affect simultaneously the local CO concentration. A possible explanation for the positive summer correlation might be explained by the short range of air mass transport caused by the dominant summer synoptic system, i.e., the Persian troughPT in its weak mode recirculating local and European emissions, and by the fact that summer chemical production is a major CO source over the EM.

Another recent modeling study focused on CO concentrations was conducted by Myriokefalitakis et al. (2016). They compared and validated model results against in-situ observations at the surface, in the mixed layer and in the free troposphere (between 850 hPa and the tropopause) in the countryside and remote atmosphere over Europe for 2008. This study analyzes the total CO budget and the partial contribution of regional anthropogenic, biogenic and biomass burning CO emissions in the EM. The budget calculated for 2008 in the EM mixed layer, using a basic simulation relying on anthropogenic emissions and meteorology, points at a load of 0.6 Tg of CO, a chemical production of 10 Tg yr⁻¹, primary emissions in the region of 8 Tg yr⁻¹ and a dry deposition flux of 3 Tg yr⁻¹. Moreover, Myriokefalitakis et al. (2016) found that subsidence from higher atmospheric layers typifying the EM summer is an important CO source (12 Tg yr⁻¹) in the EM free troposphere. At the surface, anthropogenic local emissions in the EM were found to contribute by 18% to surface CO levels on an annual average. Over Cairo, out of the total surface CO concentration, roughly 32% are contributed by anthropogenic sources. These EM CO concentration results are consistent with previous modelling studies (e.g., Kanakidou et al., 2011; Drori et al., 2012; Im and Kanakidou, 2012).

3.5 Methane concentrations

Methane (CH_4) is the most abundant hydrocarbon in the atmosphere with concentration originating ~~from natural~~ from natural and anthropogenic sources. It is also the most contributor to affecting greenhouse gas GHG after water vapor and CO_2 due to its high global warming potential relying on as contributed by its infrared absorption and long atmospheric lifetime of ~8 years (Lelieveld et al., 1998), which allows its mixing throughout the atmosphere. CH_4 emissions are primarily caused by microbiological decay of organic matter under depletion of dissolved oxygen in wetlands, followed by decomposition of solid waste and enteric fermentation from domestic livestock. As for the geologic sources, a total geological CH_4 flux of $53 \pm 11 \text{ Tg yr}^{-1}$ was suggested, which accounts for 7–10% of the total global CH_4 budget (Etiope et al., 2008). The geological formations contributing to CH_4 over the greater area of the EM (25-50°N, 5°-55°E) are mud volcanoes with essential hot spots located over eastern Romania, the Black Sea, central and eastern Azerbaijan, and the Caspian Sea.

In contrast to trace gases of short lifetimes such as NO_x and NO_y , the long lifetime of CH_4 over the EM may lead to interannual fluctuations of concentrations caused by circumglobal phenomena such as low frequency global circulation patterns, i.e., El Niño-Southern Oscillation (ENSO) and North Atlantic Oscillation (NAO), or changes in global temperature. Langenfelds et al. (2002) point at major biomass burning events linked to ENSO dry periods, which increased the growth rate of CH_4 over other parts of the world. Artuso et al. (2007) compared the global average temperature anomaly to the growth rate of CH_4 in Lampedusa (35.5°N, 12.6°E) Italy for the period 1995-2005. The 0.71 positive correlation they found reflects the strong relationship between these two factors. Over the EM, the NAO may possibly affect the concentration evolution through changes in the circulation (e.g., weakening of the northwesterly flow). However, so far, no association was found between the NAO index trend and the CH_4 concentration growth over this part of the basin. The only study analyzing directly a possible association between the NAO index and CH_4 concentration growth carried out by Chamard et al. (2003) in Lampedusa have not found any relationship between ~~these~~ these two factors.

Satellite ability to monitor the concentration of trace gases in the atmosphere is important for completing the picture as regarded to their budget. Among the space-borne measurements of trace gases, the SCIAMACHY (Scanning Imaging Absorption Spectrometer for Atmospheric Cartography (SCIAMACHY) instrument was proven as a feasible tool to detect CH₄ concentrations (Bovensmann et al., 1999). Measurements of column-average volume mixing ratios of CH₄ were retrieved on a global basis (Frankenberg et al., 2005).

Georgoulias et al. (2011) used data from the SCIAMACHY instrument on board the European environmental satellite (ENVISAT). SCIAMACHY's spectral near-infrared nadir measurements are sensitive to CH₄ and CO₂ concentration changes at all atmospheric altitudes, including the one in the mixed layer MLD where the signal emitted from the surface source is the largest. Annual, seasonal and monthly spatial distribution of CH₄ were displayed for 2003 and 2004 based on the analysis of Weighting Function Modified Differential Optical Absorption Spectroscopy (WFM-DOAS) version 1.0 (Schneising et al., 2009) dry air column-averaged mole fractions, denoted as XCH₄ (ppbv). The reflectivity of water surfaces is very low, therefore Georgoulias et al. (2011) mapped presented the concentration of CH₄ if results over the EM Basin discarding the Mediterranean sea over land only by depicting the concentration of CH₄ along the coasts of the EM Basin. To reduce the noise inserted by the single pixel retrieval error and the temporal and spatial sparsity of the data, the data were averaged on 1° × 1° monthly mean grids. Annual, summer and August spatial distributions for 2003 are displayed on Fig. 22 top, mid and bottom panel, respectively. Those maps illustrate an eminent seasonal variation with a summer maximum in XCH₄ levels observed in both consecutive years (2004 not shown). The northeastern African coast exhibits the highest XCH₄ values, with a hot spot over the Nile's delta in Egypt in summer and August. The lowest XCH₄ levels along the Arabian Peninsula, the Zagros Mountain and eastern Anatolia mountain barrier coincide spatially with high altitude areas. To examine to what extent the warm period affects the annual, seasonal, and latitudinal patterns, Georgoulias et al. (2011) further proceeded to a monthly analysis. They observed an increase in XCH₄ levels during the summer season, August being the month with the highest levels of 1775-1780 ± 24 ppbv for both 2003 and 2004. The highest values are concentrated in the northeastern part of the area primarily in July-August. From July to September,

there is a shift of high XCH₄ levels from higher to lower latitudes. Despite the abundance of mud volcanoes over the Greater Area of the ~~eastern Mediterranean~~EM region, Georgoulias et al. (2011) ruled out the possibility that the CH₄ total columns from SCIAMACHY (2003-2004) measured over these EM regions were attributed to volcano eruptions.

Ricaud et al. (2014) presented a thorough analysis of atmospheric CH₄ distributions over the Mediterranean Basin in the troposphere, as part of the Chemical and Aerosol Mediterranean Experiment (ChArMEx) program, using both satellite measurements and model simulations. For this sake, they analyzed space-borne measurements from (i) the Thermal And Near infrared Sensor for carbon Observations-Fourier Transform Spectrometer (TANSO-FTS) instrument on the Greenhouse gases Observing SATellite (GOSAT) satellite, (ii) the Atmospheric InfraRed Spectrometer (AIRS) on the AURA platform and (iii) the Infrared Atmospheric Sounder Interferometer (IASI) instrument aboard the MetOp-A platform. These space-borne tools were used in conjunction with the results obtained from three global models: the chemical transport model (CTM) MOCAGE (Teyssedre et al., 2007), and the two chemical climate models (CCMs) CNRM-AOCCM (Michou et al., 2011) and LMDz-OR-INCA (Hourdin et al., 2006). The sensitivity of those space-borne sensors is mainly located in the upper tropospheric layers peaking around 300 hPa with an envelope as defined by the half-width at half-maximum of the averaging kernels (see Figure 23) from 400 to 200 hPa. Consequently, the comparisons between measurements and model outputs of CH₄ is mainly concentrated on the layer around 300 hPa for AIRS and GOSAT, or considering the total column for IASI.

In summer, the horizontal distribution of CH₄ in the upper troposphere shows a clear longitudinal gradient between the East and the West of the Mediterranean Basin, both in the space-borne measurements and in the model calculations (Figure 24). There is a maximum of CH₄ in the eastern MB compared to the western MB, both considering the upper tropospheric layer and the total column information. The difference between the East and the West of the MB has been calculated within all the datasets and the seasonal variations has been investigated (Figure 25). This clearly shows that the East-West difference peaks in summer, mainly in August.

The ~~long-range transport~~LRT conditions in the upper troposphere differ over both parts of the Mediterranean Basin. In the western part, whatever the season considered, air masses are basically coming from the west. However, in the EM, apart from the westerlies influence, air masses are also originating from northern Africa and the Arabic Peninsula (Ziv et al., 2004; Liu et al., 2009), and even farther away, from Asia.

To further examine the origin of air masses reaching the eastern MB, a six-day back-trajectory from the point at 33°N, 35°E located in the EM (red filled circle in Fig. 26) was calculated, considering vertical movement, using the British Atmospheric Data Centre (BADC) trajectory service (<http://badc.nerc.ac.uk/community/trajectory/>) every 12_h in July-August over 2001-2010. The position of the gravity center of all trajectories (i.e. the maximum in the probability density function) is displayed every 24 h in Figure 26 at 850 (red stars), 700 (orange), 500 (green), 300 (blue) and 200 hPa (yellow). For this purpose, data from ECMWF archive (2.5 degree/pressure levels) were used in the calculation.

Based on these studies focused on the EM, Ricaud et al. (2014) proposed a scheme displaying the transport mechanism (Fig. 27) representing the several stages process: (1) capturing of lower tropospheric pollutants, including CH₄, in the Asian monsoon; (2) pollutants ascent to the upper troposphere by the Asian monsoon ; (3) accumulation of pollutants within the Asian monsoon in the upper troposphere; (4) long-range transport and large-scale repartition of pollutants in the upper troposphere from the Asian ~~Monsoon~~monsoon Anticyclone-anticyclone(AMA) to the Middle East and North Africa; (5) ~~s~~Subsiding air masses yielding to the build-up of pollutants at mid-tropospheric layers above the EM.

4. Conclusions and perspectives

This review demonstrates the significant progress made in understanding the atmospheric pollution over the MB. Measurements from space-borne and aircraft instruments and outputs from chemistry-climate models and chemistry transport models clearly revealed that the general atmospheric dynamic summer conditions characterizing the ~~eastern-MB~~EM basin differ much from the western ones. The impact of the different meteorological regimes together with the seasonal variabilities of the emissions of various atmospheric pollutants result in a longitudinal

concentration gradient between the eastern and the western ~~MBs~~Mediterranean Basins.

Several new campaigns have been recently organized to give more insights in the understanding of the processes occurring in the western and eastern parts of this basin in the framework of the ChArMEx program. The TRANsport and Air Quality (TRAQA) campaign (Attié et al., 2014; Di Biagio et al., 2015; Sič et al., 2016) held in summer 2012 was dedicated to the export/import of pollutants from the French continent to the Mediterranean Sea by means of balloon and airborne measurements. The Aerosol Direct Radiative Impact in the Mediterranean (ADRIMED) campaign investigated aerosols of various origins and their optical properties over the western basin in summer 2013 (Mallet et al., 2016). The Secondary Aerosol Formation in the Mediterranean (SAFMED) campaigns focused on the organic reactive gases and aerosol over the northwestern basin and southeastern France in summer 2013 and 2014 (Di Biagio et al., 2015). Finally, the Gradient in Longitude of Atmospheric constituents above the Mediterranean basin (GLAM) campaign (Ricaud et al., 2017) held in August 2014 was dedicated to the study of the gradient of chemical constituents (pollutants and ~~greenhouse-gases~~GHGs) from Toulouse (France) to Larnaca (Cyprus) and the impact of the ~~AMA~~Asian monsoon anticyclone on the EM pollutant levels.

Surface background stations in the ~~eastern MBEM~~ (e.g., Crete, Greece and Larnaca, Cyprus) and in the western Mediterranean Basin (e.g., Menorca, Spain and Lampedusa, Italy) deployed even more instruments to obtain a wide variety of atmospheric parameters (meteorology, chemistry, dynamics, radiation, etc.). These campaigns were organized in close relationship with modelling studies (forecasts, and re-analyses) and space-borne observations. New airborne campaigns are under analysis, e.g. Oxydation Mechanism Observation (OMO) in summer 2015, or in project (Radiative Impact of the Arabian Sea pollutants, greenhouse gases and aerosols on the eastern MEditerranean climate in Summer (RIMES)) in summer ~~2018~~2019) in order to quantify the export of the Asian pollutants to the EM basin and its impact on the chemical constituents loading.

Concurrently to these intensive experiments, new sites have been instrumented. In early 2015, the Agia Marina Xyliatou EMEP rural background air quality station sited

at 532 m in altitude in the center of Cyprus (35.03°N, 33.05°E), and operated since October 1996 (Kleanthous et al., 2014), has been augmented with a package of atmospheric chemistry and physics monitoring instruments thanks to the Cyprus Institute and French laboratories, in order to initiate an enhanced atmospheric chemistry observation period of several years in the easternmost [Mediterranean Basin](#). Unmanned aircraft vehicles are also deployed on a regular basis to document the lower troposphere above the station and the German [Leibniz Institute for Tropospheric Research \(TROPOS\)](#) institute has deployed a full set of aerosol-cloud-water vapor remote sensing instrument for almost a year in October 2016. This unprecedented experimental effort is expected to bring information on the variability of new compounds and processes with a focus on VOCs and secondary and carbonaceous aerosols and their origins, and on interactions between aerosols and the water vapor cycle in this region.

[Acknowledgments](#)

References

Akritidis, D., Zanis, P., Pytharoulis, I., Mavraklis, A., and Karacostas, Th.: A deep stratospheric intrusion event down to the earth's surface of the megacity of Athens, *Meteorol. Atmos. Phys.*, 109, 9–18, doi:10.1007/s00703-010-0096-6, 2010.

Akritidis, D., Pozzer, A., Zanis, P., Tyrlis, E., Škerlak, B., Sprenger, M., and Lelieveld, J.: On the role of tropopause folds in summertime tropospheric ozone over the eastern Mediterranean and the Middle East, *Atmos. Chem. Phys.*, 16, 14025–14039, doi:10.5194/acp-16-14025-2016, 2016.

Alper-Siman Tov, D., Peleg, M., Matveev, V., Mahrer, Y., Seter, I., and Luria, M.: Recirculation of polluted air masses over the east Mediterranean coast, *Atmos. Environ.*, 31, 1441-1448, doi:10.1016/S1352-2310(96)00321-4, 1997.

Amaroso, A., Beine, H.J., Esposito, G., Perrino, C., Catrambone, M., and Allegrini, I.: Seasonal differences in atmospheric nitrous acid near Mediterranean urban

areas, *Water Air Soil Pollut.*, 188, 81–92, doi:10.1007/s11270-007-9526-6, 2008.

Anagnostopoulou, C., Zanis, P., Kratagkou, E., Tegoulas, I., and Tolika, K.: Recent past and future patterns of the Etesian winds based on regional scale climate model simulations, *Clim Dyn.*, 42, 1819–1836, doi:10.1007/s00382-013-1936-0, 2014.

Andreae, M. O.: The dark side of aerosols, *Nature*, 409, 671–672, doi:10.1038/35055640, 2001.

Angevine, W. M., Hare, J. E., Fairall, C. W., Wolfe, D. E., Hill, R. J., Brewer, W. A., and White, A. B.: Structure and formation of the highly stable marine boundary layer over the Gulf of Maine, *J. Geophys. Res.*, 111, D23S22, doi:10.1029/2006JD007465, 2006.

Artuso, F., Chamard, P., Piacentino, S., di Sarra, A., Meloni, D., Monteleone, F., Sferlazzo, D.M., and Thiery, F.: Atmospheric methane in the Mediterranean: Analysis of measurements at the island of Lampedusa during 1995–2005, *Atmos. Environ.*, 41, 3877–3888, doi:10.1016/j.atmosenv.2007.01.024, 2007.

Attié, J. L., Ravetta, F., Durand, P., El Amraoui, L., Di Biaggio, C., Dulac, F., Sicard, M., Renard, J.B., Fleury, L., Bourdon, A., Verdier, N., and the TRAQA/ChArMEx Team: Transport of Pollution and Air Quality experiment over the Mediterranean basin (TRAQA/ChArMEx campaign), *Geophys. Res. Abstr.*, 16, EGU2014-12125, 2014, EGU General Assembly 2014.

Bardouki, H., Berresheim, H., Vrekoussis, M., Sciare, J., Kouvarakis, G., Oikonomou, K., Schneider, J., and Mihalopoulos, N.: Gaseous (DMS, MSA, SO₂, H₂SO₄, and DMSO) and particulate (sulfate and methanesulfonate) sulfur species over the northeastern coast of Crete, *Atmos. Chem. Phys.*, 3, 1871–1886, doi:10.5194/acp-3-1871-2003, 2003a.

Bardouki, H., Liakakou, H., Economou, C., Smolik, J., Zdimal, V., Eleftheriadis, K., Lazaridis, M., and Mihalopoulos, N.: Chemical composition of size resolved atmospheric aerosols in the eastern Mediterranean during summer and winter, *Atmos. Environ.*, 37, 195–208, doi:10.1016/S1352-2310(02)00859-2, 2003b.

Berman, S., Ku, Y. J., and Rao, S. T.: Spatial and Temporal Variation in the Mixing Depth over the Northeastern United States during the Summer of 1995, *J. Appl. Meteorol.*, 38, 1661-1673, doi:10.1175/1520-450(1999)038<1661:SATVIT>2.0.CO;2 1999.

Boersma, K. F., Eskes, H. J., and Brinksma, E. J.: Error analysis for tropospheric NO₂ retrieval from space, *J. Geophys. Res.*, 109, D04311, doi:10.1029/2003JD003962, 2004.

Bovensmann, H., Burrows, J. P., Buchwitz, M., Frerick, J., Noel, S., Rozanov, V. V., Chance, K. V., and Goede, A.P.H.: SCIAMACHY: mission objectives and measurement modes, *J. Atmos. Sci.*, 56, 127–150, doi:10.1175/1520-0469(1999)056<0127:SMOAMM>2.0.CO;2, 1999.

Businger, J.A., Charnock, H.: Boundary layer structure in relation to larger-scale flow: some remarks on the JASIN observations, *Phil. Trans. Roy. Soc. Lond. A*, 308, 1503, 445–449, 1983.

Chamard, P., Thierry, F., di Sarra, A., Ciattaglia, L., De Silvestri, L., Grigioni, P., Monteleone, F., and Piacentino, S.: Interannual variability of atmospheric CO₂ in the Mediterranean: measurements at the island of Lampedusa, *Tellus*, 55B, 83-93, doi:10.1034/j.1600-0889.2003.00048.x, 2003.

Chin, M., Rood, R. B., Lin, S. J., Muller, J. F., and Thompson, A. M.: Atmospheric sulfur cycle simulated in the global model GOCART: Model description and global properties, *J. Geophys. Res.*, 105, 24,671–24,687, doi:10.1029/2000JD900384, 2000.

Cohen, R. C., Perkins, K. K., Koch, L. C., Stimpfle, R. M., Wennberg, P. O., Hanisco, T. F., Lanzendorf, J.E., Bonne, G. P., Voss, P. B., Salawitch, R. J., Del Negro, L. A., Wilson, J. C., McElroy, C.T., and Bui, T. P.: Quantitative constraints on the atmospheric chemistry of nitrogen oxides: An analysis along chemical coordinates, *J. Geophys. Res.*, 105, 24283–24304, doi:10.1029/2000JD900290, 2000.

- Corbett, J. J., Fischbeck, P. S., and Panis, S. N.: Global nitrogen and sulfur inventories for ocean-going ships, *J. Geophys. Res.*, 104, 3457–3470, doi:10.1029/1998JD100040, 1999.
- Dastoor, A. P., and Larocque, Y.: Global circulation of atmospheric mercury: a modeling study, *Atmos. Environ.*, 38, 147-161, doi:10.1016/j.atmosenv.2003.08.037, 2004.
- Davis, R. E., and Kalkstein, L. S.: Using a spatial synoptic classification to assess changes in atmospheric pollution concentrations, *Phys. Geogr.*, 11, 320-342, 1990.
- Dayan, U. 1986: Climatology of back trajectories from Israel based on synoptic analysis. *J. Climatol. Appl. Meteorol.*, 25, 591-595, doi:10.1175/1520-0450(1986)025<0591:COBTFI>2.0.CO;2, 1986.
- Dayan, U., and Graber, M.: Analysis of synoptic conditions in the eastern Mediterranean that led to elevated air pollution concentration in Israel, in *Developments in Arid Zone Ecology and Environmental Quality*, Shuval, H. I. (Ed.), Balaban International Science Services, PA, 383–391, 1981.
- Dayan U., and Koch, J.: Ozone concentration profiles in the Los Angeles Basin - A possible similarity in the build-up mechanism of inland surface ozone in Israel, *J. Appl. Meteorol.*, 35, 1085-1090, doi:10.1175/1520-0450(1996)035<1085:OCPITL>2.0.CO;2, 1996.
- Dayan, U., and Levy, I.: Relationship between synoptic-scale atmospheric circulation and ozone concentrations over Israel, *J. Geophys. Res.*, 107, D24, 4813, doi:2002JD002147, 2002.
- Dayan U., and Rodnizki, J.: The temporal behavior of the atmospheric boundary layer in Israel, *J. Appl. Meteorol.*, 38, 830-836, doi:10.1175/1520-0450(1999)038<0830:TTBOTA>2.0.CO;2., 1999.
- Dayan, U., Shenhav, R., and Graber, M.: The spatial and temporal behavior of the mixed layer in Israel, *J. Appl. Meteorol.*, 27, 1382–1394, doi:10.1175/1520-0450(1988)027<1382:TSATBO>2.0.CO;2, 1988.

[Dayan, U., Heffter, J., Miller, J., and Gutman, G.: Dust intrusion events into the Mediterranean Basin. *J. Appl. Meteorol.*, 30, 1185-1199, doi:10.1175/1520-0450\(1991\)030<1185: DIEITM>2.0.CO;2, 1991.](#)

Dayan, U., Heffter, J., and Miller, J.: Seasonal distribution of the boundary layer depths over the Mediterranean Basin, in Guerzoni, S., and Chester, R. (Eds.), *The Impact of Desert Dust Across the Mediterranean*, 103-112, Kluwer, Dordrecht, 1996.

Dayan, U., Lifshitz-Goldreich, B., and Pick, K.: Spatial and structural variation of the atmospheric boundary layer during summer in Israel—Profiler and rawinsonde measurements, *J. Appl. Meteorol.*, 41, 447-457, doi:10.1175/1520-0450(2002)041<0447:SASVOT>2.0.CO;2., 2002.

Dayan, U., Ziv, B., Shoob, T., and Enzel, Y.: Suspended dust over southeastern Mediterranean and its relation to atmospheric circulations, *Int. J. Climatol.*, 28, 915-924, doi:10.1002/joc.1587, 2008.

Dayan, U., Erel, Y., Shpund, J., Kordova, L., Wanger, A., and Schauer, J. J.: The impact of local sources and meteorological factors on nitrogen oxide and particulate matter concentrations: A case study of the Day of Atonement in Israel, *Atmos. Environ.*, 45, 3325-3332, doi:10.1016/j.atmosenv.2011.02.017, 2011.

Deeter, M. N., Edwards, D. P., Gille, J. C., Emmons, L. K., Francis, G., Ho, S.-P., Mao, D., Masters, D., Worden, H., Drummond, J.R., and Novelli, P. C.: The MOPITT Version 4 CO Product: Algorithm enhancements, validation, and long-term stability, *J. Geophys. Res.*, 115, D07306, doi:10.1029/2009JD013005, 2010.

Di Biagio, C., Doppler, L., Gaimoz, C., Grand, N., Ancellet, G., Raut, J.-C., Beekmann, M., Borbon, A., Sartelet, K., Attié, J.-L., Ravetta, F., and Formenti, P.: Continental pollution in the western Mediterranean basin: vertical profiles of aerosol and trace gases measured over the sea during TRAQA 2012 and SAFMED 2013, *Atmos. Chem. Phys.*, 15, 9611-9630, doi:10.5194/acp-15-9611-2015, 2015.

Dobbins, R.A.: Atmospheric Motion and Air Pollution. Wiley, p. 323, 1979.

Doche, C., Dufour, G., Foret, G., Eremenko, M., Cuesta, J., Beekmann, M., and Kalabokas, P.: Summertime tropospheric-ozone variability over the Mediterranean basin observed with IASI, *Atmos. Chem. Phys.*, 14, 10589–10600, doi:10.5194/acp-14-10589-2014, 2014.

Drori, R., Dayan, U., Edwards, D. P., Emmons, L. K., and Erlick, C.: Attributing and quantifying carbon monoxide sources affecting the Eastern Mediterranean: A combined satellite, modelling, and synoptic analysis study, *Atmos. Chem. Phys.* 12, 1067-1082, doi:10.5194/acp-12-1067-2012, 2012.

Elbayoumi, M., Ramli, N. A., Faizah, N., and Al-Madhoun, W.: The effect of seasonal variation on indoor and outdoor carbon monoxide concentrations in Eastern Mediterranean climate, *Atmos. Poll. Res.*, 5, 315-324, doi:10.5094/APR.2014.037, 2014.

Emmons, L. K., Carroll, M.A., Hauglustaine, D.A., Brasseur, G.P., Atherton, C., Penner, J., Sillman, S., Levy II, H., Rohrer, F., Wauben, W.M.F., Van Velthoven, P.F.J., Wang, Y., Jacob, D., Bakwin, P., Dickerson, R., Doddridge, B., Gerbig, C., Honrath, R., Hubler, G., Jaffe, D., Kondo, Y., Munger, J.W., Torres, A., and Voltz-Thomas, A.: Climatologies of NO_x and NO_y: A comparison of data and models, *Atmos. Environ.*, 31, 1851-1904, doi:10.1016/S1352-2310(96)00334-2, 1997.

Emmons, L. K., Walters, S., Hess, P. G., Lamarque, J.-F., Pfister, G. G., Fillmore, D., Granier, C., Guenther, A., Kinnison, D., Laepple, T., Orlando, J., Tie, X., Tyndall, G., Wiedinmyer, C., Baughcum, S. L., and Kloster, S.: Description and evaluation of the Model for Ozone and Related Chemical Tracers, version 4 (MOZART-4), *Geosci. Model Dev.*, 3, 43–67, doi:10.5194/gmd-3-43-2010, 2010.

Erel, Y., Axelrod, T., Veron, A., Mahrer, Y., and Dayan, U.: Trans-boundary atmospheric lead pollution, *Environ. Sci. Technol.*, 36, 3230-3233, doi:10.1021/es020530q, 2002.

Erel, Y., Kalderon-Asael, B., Dayan, U., and Sandler, A.: European pollution imported by cooler air masses to the eastern Mediterranean during the summer, *Environ. Sci. Technol.*, 41, 5198-5203, doi:10.1021/es062247n, 2007.

Erel, Y., Tirosh, O., Kessler, N., Dayan, U., Belkin, S., Stein, M., Sandler, A., and Schauer, J. J.: Atmospheric particulate matter (PM) in the Middle East: Toxicity, transboundary transport, and influence of synoptic conditions, in Censi, P., Darrah, T., and Erel, Y. (Eds.), *Medical Geochemistry: Geological Materials and Health*, doi:10.1007/978-94-007-4372-43, Springer, Dordrecht, 2013.

Etiopie, G., Lassey, K.R., Lusman, K., and Oschi, B.: Re-appraisal of the fossil methane budget and related emission from geologic sources, *Geophys. Res. Lett.*, 35, L09307, doi:10.1029/2008GL033623, 2008.

Fleming, Z. L., Monks, P.S., and Manning, A.J.: Review: Untangling the influence of air-mass history in interpreting observed atmospheric composition, *Atmos. Res.*, 104-105, 1-39, <https://doi.org/10.1016/j.atmosres.2011.09.009>, 2012.

Frankenberg, C., Meirink, J.F., van Weele, M., Platt, U., and Wagner, T.: Assessing Methane emissions from global space-borne observations, *Science*, 308, 5724, 1010-1014, doi:10.1126/science.1106644, 2005.

Galani, E., Balis, D., Zanis, P., Zerefos, C., Papayannis, A., Wernli, H., and Gerasopoulos, E.: Observations of stratosphere-troposphere transport events over the eastern Mediterranean using a ground-based lidar system, *J. Geophys. Res.*, 108, 8527, doi:10.1029/2002JD002596, 2003.

Gamo, M., Yamamoto, S., and Yokoyama, O.: Airborne measurements of the free convective internal boundary layer during the sea breeze, *J. Meteor. Soc. Japan*, 60, 1284–1298, 1982.

Ganor, E., Levin, Z., and Van Grieken, R.: Composition of individual aerosol particles above the Israelian Mediterranean coast during the summer time, *Atmos. Environ.*, 32, 9, 1631-1642, doi:10.1016/S1352-2310(97)00397-X, 1998.

Ganor, E., Foner, H.A., Bingemer, H.G., Udisti, R., and Setter, I.: Biogenic sulphate generation in the Mediterranean Sea and its contribution to the sulphate anomaly in the aerosol over Israel and the Eastern Mediterranean, *Atmos. Environ.*, 34, 3453-3462, doi:10.1016/S1352-2310(00)00077-7, 2000.

Georgoulas, A. K., Kourtidis, K. A., Buchwitz, M., Schneising, O., and Burrows, J. P.: A case study on the application of SCIAMACHY satellite methane measurements for regional studies: the greater area of the Eastern Mediterranean, *Int. J. Remote Sens.*, 32, 787-813, doi:10.1080/01431161.2010.517791, 2011.

Gerasopoulos, E., Kouvarakis, G., Vrekoussis, M., Kanakidou, M., and Mihalopoulos, N.: Ozone variability in the marine boundary layer of the eastern Mediterranean based on 7-year observations, *J. Geophys. Res.*, 110, D15309, doi:10.1029/2005JD005991, 2005.

Gerasopoulos, E., Kouvarakis, G., Vrekoussis, M., Donoussis, C., Mihalopoulos, N., and Kanakidou, M.: Photochemical ozone production in the Eastern Mediterranean, *Atmos. Environ.*, 40, 3057-3069, doi:10.1016/j.atmosenv.2005.12.061, 2006.

Glaser, E., Dagan, N., Furer, O., Gamliel, M., Yogev, A., Fastig, S., Dayan, U., and Benayahu, Y.: A comparison of balloon soundings and lidar scans for measuring the height of the turbulent mixed-layer at a coastal site in Israel, *Water Sci. Technol.*, 27, 271-278, 1993.

Gryning, S. E.: The Oresund experiment—A Nordic mesoscale dispersion experiment over a land-water-land area, *Bull. Amer. Meteorol. Soc.*, 66, 1403-1407, doi:10.1175/1520-0477(1985)066<1403: TENMDE>2.0.CO;2, 1985.

Halevy, G., and Steinberger, E. H.: Inland penetration of the summer inversion from the Mediterranean coast in Israel, *Isr. J. Earth Sci.*, 23, 47-54, 1974.

Hansen, J., Lacis, A., and Prather, M.: Greenhouse effect of chlorofluorocarbons and other trace gases, *J. Geophys. Res.*, 94, 16417-16421, doi:10.1029/JD094iD13p16417, 1989.

- Harpaz, T., Ziv, B., Saaroni, H., and Beja, E.: Extreme summer temperatures in the East Mediterranean—dynamical analysis, *Int. J. Climatol.*, 34, 849–862. doi:10.1002/joc.3727, 2014.
- Harris, J. M.: The GMCC atmospheric trajectory program, NOAA Tech. Memo. ERL-ARL-116, 30 pp., 1982.
- Hein, R., Dameris, M., Schnadt, C., Land, C., Grewe, V., Kohler, I., Ponater, M., Sausen, R., Steil, B. B., Landgraf, J., and Bruhl, C.: Results of an interactively coupled atmospheric chemistry–general circulation model: Comparisons with observations, *Ann. Geophys.*, 19, 435–457, doi:10.5194/angeo-19-435-2001, 2001.
- Holt, T., and Raman, S.: Marine boundary layer structure and circulation in the region of offshore development of a cyclone during GALE, *Mon. Weather Rev.*, 118, 392–410, doi:10.1175/1520-0493(1990)118<0392:MBLSAC>2.0.CO;2, 1990.
- Holtzlag, A. A. M., and Van Ulden, A. P.: A simple scheme for daytime estimates of the surface fluxes from routine weather data, *J. Climate Appl. Meteorol.*, 22, 517–529, doi:10.1175/1520-0450(1983)022<0517: ASSFDE>2.0.CO;2, 1983.
- Hourdin, F., Musat, I., Bony, S., Braconnot, P., Codron, F., Dufresne, J. L., Fairhead, L., Filiberti, M. A., Friedlingstein, P., Grandpeix, J. Y., Krinner, G., LeVan, P., Li, Z. X., and Lott, F.: The LMDZ4 general circulation model: climate performance and sensitivity to parametrized physics with emphasis on tropical convection, *Clim. Dyn.*, 27, 787–813, doi:10.1007/s00382-006-0158-0, 2006.
- İm, U., Tayan, M., and Yenigün, O.: Interaction patterns of major photochemical pollutants in Istanbul, Turkey, *Atmos. Res.*, 89, 382–390, doi:10.1016/j.atmosres.2008.03.015, 2008.
- James, P., Stohl, A., Forster, C., Eckhardt, S., Seibert, P., and Frank, A.: A 15-year climatology of stratosphere–troposphere exchange with a Lagrangian particle dispersion model, 2, Mean climate and seasonal variability, *J. Geophys. Res.*, 108, 8522, doi:10.1029/2002JD002639, 2003.
- Kalnay, E., Kanamitsu, M., Kistler, R., Collins, W., Deaven, D., Gandin, L., Iredell, M., Saha, S., White, G., Woollen, J., Zhu, Y., Leetmaa, A., Reynolds, B.,

Chelliah, M., Ebisuzaki, W., Higgins, W., Janowiak, J., Mo, K. C., Ropelewski, C., Wang, J., Jenne, R., and Joseph, D.: The NCEP/NCAR 40-year reanalysis project, *Bull. Am. Meteorol. Soc.*, 77, 437–472, doi:10.1175/1520-0477(1996)077<0437:TNYRP>2.0.CO;2, 1996.

Kalthoff, N., Binder, H. J., Kossman, M., Vogtlin, R., Corsmeier, U., Fiedler, F., and Schlager, H.: Temporal evolution and spatial variation of the boundary layer over complex terrain, *Atmos. Environ.*, 32, 1179–1194, doi:10.1016/S1352-2310(97)00193-3, 1998.

Kanakidou, M., Mihalopoulos, N., Kindap, T., Im, U., Vrekoussis, M., Gerasopoulos, E., Dermitzaki, E., Unal, A., Koçak, M., Markakis, K., Melas, D., Kouvarakis, G., Youssef, A. F., Richter, A., Hatzianastassiou, N., Hilboll, A., Ebojje, F., Wittrock, F., von Savigny, C., Burrows, J. P., Ladstaetter-Weissenmayer, A., and Moubasher, H.: Megacities as hot spots of air pollution in the East Mediterranean, *Atmos. Environ.*, 45, 1223–1235 doi:10.1016/j.atmosenv.2010.11.048, 2011.

Karnieli, A., Derimian, Y., Indoitu, R., Panov, N., Levy, R. C., Remer L.A., Maenhaut, W., and Holben, B. N.: Temporal trend in anthropogenic sulfur aerosol transport from central and eastern Europe to Israel, *J. Geophys. Res.*, 114, D00D19, doi:10.1029/2009JD011870, 2009.

Kassomenos, P., Kotroni, V., and Kallos, G.: Analysis of climatological and air quality observations from greater Athens area, *Atmos. Environ.*, 29, 3671-3688, doi:10.1016/1352-2310(94)00358-R, 1995.

Katsoulis, B.D.: The potential for long-range transport of air-pollutants into Greece: a climatological analysis, *Sci. Total Environ.*, 231, 101-113, doi:10.1016/S0048-9697(99)00100-X, 1999.

Kistler, R., Kalnay, E., Collins, W., Saha, S., White, G., Woollen, J., Chelliah, M., Ebisuzaki, W., Kanamitsu, M., Kousky, V., van den Dool, H., Jenne, R., and Fiorino, M.: The NCEP/NCAR 50-year reanalysis: monthly means CD-ROM and documentation, *Bull. Am. Meteorol. Soc.*, 82, 247–267, doi:10.1175/1520-0477(2001)082<0247:TNNYRM>2.3.CO;2, 2001.

Kleanthous, S., Vrekoussis, M., Mihalopoulos, N., Kalabokas, P., and Lelieveld, J.: On the temporal and spatial variation of ozone in Cyprus, *Sci. Total Environ.*, 476-477, 677-687, doi:10.1016/j.scitotenv.2013.12.101, 2014.

Kley, D.: Tropospheric chemistry and transport, *Science*, 276, 1043–1045, doi:10.1126/science.276.5315.1043, 1997.

Koch, J., and Dayan, U.: A synoptic analysis of the meteorological conditions affecting dispersion of pollutants emitted from tall stacks in the coastal plain of Israel, *Atmos. Environ.*, 26, 2537–2543, doi:10.1016/0960-1686(92)90105-T, 1992.

Koulouri, E., Saarikoski, S., Theodosi, C., Markaki, Z., Gerasopoulos, E., Kouvarakis, G., Ma'kela, T., Hillamo, R., and Mihalopoulos, N.: Chemical composition and sources of fine and coarse aerosol particles in the Eastern Mediterranean, *Atmos. Environ.*, 42, 6542–6550, doi:10.1016/j.atmosenv.2008.04.010, 2008.

Kourtidis, K., Cerefos, C., Rapsomanikis, S., Simeonov, C., Balis, D., Perros, P. E., Thompson, A. M., Witte, J., Calpini, B., Sharobiem, W. M., Papayannis, A., Mihalopoulos, N., and Draku, R.: Regional levels of ozone in the troposphere over eastern Mediterranean, *J. Geophys. Res.*, 107, 8140, doi:10.1029/2000JD000140, 2002.

Kouvarakis, G., K. Tsigaridis, M. Kanakidou, and N. Mihalopoulos, Temporal variations of surface regional background ozone over Crete Island in southeast Mediterranean, *J. Geophys. Res.*, 105, 4399 – 4407, 2000.

Kouvarakis, G., Vrekoussis, M., Mihalopoulos, N., Kourtidis, K., Rappenglueck, B., Gerasopoulos, E., and Zerefos, C.: Spatial and temporal variability of tropospheric ozone (O₃) in the boundary layer above the Aegean Sea (eastern Mediterranean), *J. Geophys. Res.*, 107, 8137, doi:10.1029/2000JD000081, 2002.

Kubilay, N.: The composition of atmospheric aerosol over the Eastern Mediterranean; sources and temporal variability, Ph.D. Thesis, Middle East Technical University, Ankara, Turkey, 1996.

Kuwagata, T., Masuko, N., Sumioka, M., and Kondo, J.: The daytime PBL heating process over complex terrain in central Japan under fair and calm weather conditions. Part II: Regional heat budget, convective boundary layer and surface moisture availability, *J. Meteor. Soc. Japan*, 68, 639–650, doi:10.2151/jmsj1965.68.6_639, 1990.

Langenfelds, R.L., Francey, R.G., Pak, B.C., Steele, L.P., Lloyd, J., Trudinger, C.M., and Allison, C.E.: Interannual growth rate variations and atmospheric CO₂ and its δ¹³C, H₂, CH₄ and CO between 1992 and 1999 linked to biomass burning, *Global Biogeochemical Cycles*, 16, 1048, 21-1 – 21-22, doi:10.1029/2001GB001466, 2002.

Lammel, G., and Cape, J. N.: Nitrous acid and nitrite atmosphere, *Chemical Society Reviews Articles*, 25, 361–369, 1996.

Lashof, D. A., and Ahuja, D. R.: Relative contributions of greenhouse gas emissions to global warming, *Nature*, 344, 529-531; doi:10.1038/344529a0, 1990.

Lawrence, M. G., and Crutzen, P. J.: Influence of NO_x emissions from ships on tropospheric photochemistry and climate, *Nature*, 402, 167–170, doi:10.1038/46013, 1999.

Lelieveld, J., Crutzen, P. J., and Dentener, F. J.: Changing concentration, lifetime and climate forcing of atmospheric methane, *Tellus B*, 50, 128–150, doi:10.1034/j.1600-0889.1998.t01-1-00002.x, 1998.

Lelieveld, J., and Dentener, F. J.: What controls tropospheric ozone? *J. Geophys. Res.*, 105, 3531-3551, doi:10.1029/1999JD901011, 2000.

Lelieveld, J., Berresheim, H., Borrmann, S., Crutzen, P. J., Dentener, F. J., Fischer, H., Feichter, J., Flatau, P. J., Heland, J., Holzinger, R., Kormann, R., Lawrence, M. G., Levin, Z., Markowicz, K. M., Mihalopoulos, N., Minikin, A., Ramanathan, V., de Reus, M., Roelofs, G. J., Scheeren, H. A., Sciare, J., Schlager, H., Schultz, M., Siegmund, P., Steil, B., Stephanou, E. G., Stier, P., Traub, M., Warneke, C., Williams, J., and Ziereis, H.: Global air pollution crossroads over the Mediterranean, *Science*, 298, 794-799, doi:10.1126/science.1075457, 2002.

- Lensky, I. M., and Dayan, U.: Continuous detection and characterization of the Sea Breeze in clear sky conditions using Meteosat Second Generation, *Atmos. Chem. Phys.*, 12, 6505-6513, doi:10.5194/acp-12-6505-2012, 2012.
- Lensky, I. M., and Dayan, U.: Satellite observations of land surface temperature patterns induced by synoptic circulation, *Int. J. Climatol.*, 35, 189–195. doi:10.1002/joc.3971, 2015.
- Leventidou, E., Zanis, P., Balis, D., Giannakaki, E., Pytharoulis, I., and Amiridis, V.: Factors affecting the comparisons of planetary boundary layer height retrievals from CALIPSO, ECMWF and radiosondes over Thessaloniki, Greece, *Atmos. Environ.*, 74, 360-366, doi:10.1016/j.atmosenv.2013.04.007, 2013.
- Levy, I., Dayan, U., and Mahrer, I.: A 5-yr study of the coastal recirculation and its effect on air pollutants over the East Mediterranean region, *J. Geophys. Res.*, 113, doi:10.1029/07JD009529, 2008.
- Lieman, R., and Alpert, P.: Investigation of the planetary boundary layer height variations over complex terrain, *Boundary-Layer Meteorol.*, 62, 129-142, doi:10.1007/BF00705550, 1993.
- Liu, J. J., Jones, D. B. A., Worden, J. R., Noone, D., Parrington, M., and Kar, J.: Analysis of the summertime buildup of tropospheric ozone abundances over the Middle East and NorthAfrica as observed by the tropospheric emission spectrometer instrument, *J. Geophys. Res.*, 114, D05304, doi:10.1029/2008JD010993, 2009.
- Luria, M., Almog, H., and Peleg, M.: Transport and transformation of air pollutants from Israel's coastal area, *Atmos. Environ.*, 18, 2215-2221, doi:10.1016/0004-6981(84)90209-9, 1984.
- Luria, M., Peleg, M., Sharf, G., Siman Tov- Alper, D., Spitz, N., Ben Ami, Y., Gawii, Z., Lifschitz, B., Yitzchaki, A., and Seter, I.: Atmospheric sulfur over the east Mediterranean region, *J. Geophys. Res.*, 101, 25917-25930, doi:10.1029/96JD01579, 1996.
- Mallet, M., Dulac, F., Formenti, P., Nabat, P., Sciare, J., Roberts, G., Pelon, J., Ancellet, G., Tanré, D., Parol, F., Denjean, C., Brogniez, G., di Sarra, A.,

Alados-Arboledas, L., Arndt, J., Auriol, F., Blarel, L., Bourriane, T., Chazette, P., Chevaillier, S., Claeys, M., D'Anna, B., Derimian, Y., Desboeufs, K., Di Iorio, T., Doussin, J.-F., Durand, P., Féron, A., Freney, E., Gaimoz, C., Goloub, P., Gómez-Amo, J. L., Granados-Muñoz, M. J., Grand, N., Hamonou, E., Jankowiak, I., Jeannot, M., Léon, J.-F., Maillé, M., Mailler, S., Meloni, D., Menut, L., Momboisse, G., Nicolas, J., Podvin, T., Pont, V., Rea, G., Renard, J.-B., Roblou, L., Schepanski, K., Schwarzenboeck, A., Sellegri, K., Sicard, M., Solmon, F., Somot, S., Torres, B., Totems, J., Triquet, S., Verdier, N., Verwaerde, C., Waquet, F., Wenger, J., and Zapf, P.: Overview of the Chemistry-Aerosol Mediterranean Experiment/Aerosol Direct Radiative Forcing on the Mediterranean Climate (ChArMEx/ADRIMED) summer 2013 campaign, *Atmos. Chem. Phys.*, 16, 455-504, doi:10.5194/acp-16-455-2016, 2016.

Marmer, E., and Langmann, B.: Impact of ship emissions on the Mediterranean summertime pollution and climate: A regional model study, *Atmos. Environ.*, 39, 26, 4659–4669, doi:10.1016/j.atmosenv.2005.04.014, 2005.

Marmer, E., Dentener, F., Aardenne, J. V., Cavalli, F., Vignati, E., Velchev, K., Hjorth, J., Boersma, F., Vinken, G., Mihalopoulos, N., and Raes, F.: What can we learn about ship emission inventories from measurements of air pollutants over the Mediterranean Sea? *Atmos. Chem. Phys.*, 9, 6815–6831, doi:10.5194/acp-9-6815-2009, 2009.

Matvev, V., Dayan, U., Tass, I., and Peleg, M.: Atmospheric sulfur flux rates to and from Israel, *Sci. Total Environ.*, 291, 143-154, doi:10.1016/S0048-9697(01)01089-0, 2002.

McElroy, J. L., and Smith, T. B.: Lidar description of mixing-layer thickness characteristics in a complex terrain/coastal environment, *J. Appl. Meteor.*, 30, 585–597, doi:10.1175/1520-0450(1991)030<0585: LDOMLT>2.0.CO;2, 1991.

Meagher, J. F., Stockburger, L., Bonanno, R. J., Bailey, E. M., and Luria, M.: Atmospheric oxidation of flue-gases from coal-fired power-plants-A

comparison between conventional and scrubbed plumes, *Atmos. Environ.*, 15, 749–762, doi:10.1016/0004-6981(81)90279-1, 1981.

Michou, M., Saint-Martin, D., Teysse re, H., Alias, A., Karcher, F., Olivie , D., Voldoire, A., Peuch, V.-H., Clark, H., Lee, J.N. and Ch eroux, F.: A new version of the CNRM Chemistry-Climate Model, CNRM-CCM: description and improvements from the CCMVal-2 simulations, *Geosci. Model Dev.*, 4, 873-900, doi:10.5194/gmd-4-873-2011, 2011.

Mihalopoulos, N., Stephanou, E., Kanakidou, M., Pilitsidis, S., and Bousquet, Q.: Tropospheric aerosol ionic composition in the Eastern Mediterranean region, *Tellus*, 49B, 314-326, 1997.

Mihalopoulos, N., Kerminen, V. M., Kanakidou, M., Berresheim, H., and Sciare, J.: Formation of particulate sulfur species (sulfate and methanesulfonate) during summer over the Eastern Mediterranean: A modelling approach, *Atmos. Environ.*, 41, 6860–6871, doi:10.1016/j.atmosenv.2007.04.039, 2007.

Miller, S. T., Keim, B. D., Talbot, R. W., and Mao H.: Sea breeze: Structure, forecasting, and impacts, *Rev. Geophys.*, 41(3), 1011, doi:10.1029/2003RG000124, 2003.

Moulin C., Lambert, C. E., Dayan, U., Masson, V., Ramonet, M., Bousquet, P., Legrand, M., Balkanski, Y. J., Guelle, W., Marticorena, B., Bergametti, G., and Dulac, F.: Satellite climatology of African dust transport in the Mediterranean atmosphere, *J. Geophys. Res.*, 103, 13137-13144, doi:10.1029/98JD00171, 1998.

Myriokefalitakis, S., Daskalakis, N., Fanourgakis, G. S., Voulgarakis, A., Krol, M. C., Aan de Brugh, J. M. J., and Kanakidou, M.: Ozone and carbon monoxide budgets over the Eastern Mediterranean, *Sci. Total Environ.*, 563–564, 40–52, doi:10.1016/j.scitotenv.2016.04.061, 2016.

Nabat, P., Somot, S., Mallet, M., Chiapello, I., Morcrette, J. J., Solmon, F., Szopa, S., Dulac, F., Collins, W., Ghan, S., Horowitz, L. W., Lamarque, J. F., Lee, Y. H., Naik, V., Nagashima, T., Shindell, D., and Skeie, R.: A 4-D climatology (1979–2009) of the monthly tropospheric aerosol optical depth distribution

over the Mediterranean region from a comparative evaluation and blending of remote sensing and model products, *Atmos. Meas. Tech.*, 6, 1287-1314, doi:10.5194/amt-6-1287-2013, 2013.

Neumann, J.: Diurnal variation of the subsidence inversion and radio wave propagation phenomena over the coastal area of Israel, Israel Meteorological Service, Jerusalem, Series A, Meteorol. Notes, 16, 12 pp., 1952.

Nirel, R., and Dayan, U.: On the ratio of sulfur dioxide to nitrogen oxides as an indicator of air pollution sources, *J. Appl. Meteorol.*, 40, 1209-1222, doi:10.1175/1520-0450(2001)040<1209:OTROSD>2.0.CO;2, 2001.

Novelli, P. C., Steele, L. P., and Tans, P. P.: Mixing ratios of carbon-monoxide in the troposphere, *J. Geophys. Res.-Atmos.*, 97, 20731-20750, doi:10.1029/92JD02010, 1992.

Özden, O., Döğeroğlu, T., and Kara, S.: Assessment of ambient air quality in Eskişehir, Turkey, *Environ. Intern.*, 34, 678 – 687, doi:10.1016/j.envint.2007.12.016, 2008.

Peleg, M., Luria, M., Setter, I., Perner, D., and Russel, P.: Ozone levels in central Israel, *Isr. J. Chem.*, 34, 375–386, doi:10.1002/ijch.199400041, 1994.

Pielke, R.A. and Stocker, R.A.: A procedure to estimate worst-case air quality in complex terrain, *Envir. Int.* 17,6, 559-574, [https://doi.org/10.1016/0160-4120\(91\)90168-P](https://doi.org/10.1016/0160-4120(91)90168-P), 1991.

Ranmar, D. O., Matveev, V., Dayan, U., Peleg, M., Kaplan, J., Gertler, A. W., Luria, M., Kallos, G., Katsafados, P., and Mahrer, Y.: Impact of coastal transportation emissions on inland air pollution over Israel: Utilizing numerical simulations, airborne measurements and synoptic analyses, *J. Geophys. Res.*, 107, 4331, doi:10.1029/2001JD000808, 2002.

Ricaud, P., Sič, B., El Amraoui, L., Attié, J. -L., Zbinden, R., Huszar, P., Szopa, S., Parmentier, J., Jaidan, N., Michou, M., Abida, R., Carminati, F., Hauglustaine, D., August, T., Warner, J., Imasu, R., Saitoh, N., and Peuch, V. -H.: Impact of the Asian monsoon anticyclone on the variability of mid-to-

upper tropospheric methane above the Mediterranean Basin, *Atmos. Chem. Phys.*, 14, 11427-11446, doi:10.5194/acp-14-11427-2014, 2014.

[Ricaud, P., R. Zbinden, V. Catoire, V. Brocchi, F. Dulac, E. Hamonou, J.-C. Canonici, L. El Amraoui, S. Massart, B. Pignatelli, U. Dayan, P. Nabat, J. Sciare, M. Ramonet, M. Delmotte, A. di Sarra, D. Sferlazzo, T. Di Iorio, S. Piacentino, P. Cristofanelli, N. Mihalopoulos, G. Kouvarakis, M. Pikridas, C. Savvides, R. Mamouri, A. Nisantzi, D. Hadjimitsis, J.-L. Attié, H. Ferré, P. Theron, Y. Kangah, N. Jaidan, J. Guth, P. Jacquet, S. Chevrier, C. Robert, A. Bourdon, J.-F. Bourdinot, J.-C. Etienne, G. Krysztofiak, P. Theron, The GLAM Airborne Campaign over the Mediterranean Basin, Bulletin of the American Meteorological Society, in press, doi:10.1175/BAMS-D-16-0226.1, 2017.](#)

Riga-Karandinos, A., and Saitanis, C.: Comparative assessment of ambient air quality in two typical Mediterranean coastal cities in Greece. *Chemosphere* 59, 1125–1136, doi:10.1016/j.chemosphere.2004.11.059, 2005.

Rindsberger, M.: Analysis of mixing depth over Tel-Aviv, Israel, *J. Earth Sci.*, 23, 13-17, 1974.

Rindsberger, M.: Air pollution potential in greater Tel-Aviv area, Israel, *J. Earth Sci.*, 25, 127-132, 1976.

Rodwell, M. J., and Hoskins, B. J.: Monsoons and the dynamics of deserts, *Q.J.R. Meteorol. Soc.*, 122, 1385–1404, doi:10.1002/qj.49712253408, 1996.

Roelofs, G. J., Scheeren, H. A., Heland, J., Ziereis, H., and Lelieveld, J.: A model study of ozone in the Eastern Mediterranean free troposphere during MINOS (August 2001), *Atmos. Chem. Phys.*, 3, 1199–1210, doi:10.5194/acp-3-1199-2003, 2003.

Rudich, Y., Kaufman, J., Dayan, U., Hongbin Y., and Kleidman, R. G.: Estimation of transboundary transport of pollution aerosols by remote sensing in the eastern Mediterranean, *J. Geophys. Res. – Atmos.*, 113, D14S13, doi:10.1029/2007JD009601, 2008.

Safieddine, S., Boynard, A., Coheur, P. -F., Hurtmans, D., Pfister, G., Quennehen, B., Thomas, J. L., Raut, J. -C., Law, K. S., Klimont, Z., Hadji-Lazaro, J., George, M., and Clerbaux, C.: Summertime tropospheric ozone assessment over the Mediterranean region using the thermal infrared IASI/MetOp sounder and the WRF-Chem model, *Atmos. Chem. Phys.*, 14, 10119–10131, doi:10.5194/acp-14-10119-2014, 2014.

Saliba, N.A., Moussa, S., Salame, H., and El-Fadel, M.: Variation of selected air quality indicators over the city of Beirut, Lebanon: Assessment of emission sources, *Atmos. Environ.*, 40, 3263–3268, doi:10.1016/j.atmosenv.2006.01.054, 2006.

Sinclair, V.A., Belcher, S.E., and Gray, S.L.: Synoptic controls on boundary-layer characteristics, *Boundary-Layer Meteorol.*, 134, 387–409, doi:10.1007/s10546-009-9455-6, 2010.

Sciare, J., Bardouki, H., Moulin, C., and Mihalopoulos, N.: Aerosol sources and their contribution to the chemical composition of aerosols in the eastern Mediterranean Sea during summertime, *Atmos. Chem. Phys.*, 3, 291–302, doi:10.5194/acp-3-291-2003, 2003.

Sciare, J., Oikonomou, K., Cachier, H., Mihalopoulos, N., Andreae, M. O., Maenhaut, W., Sarda-Estève, M.: Aerosol mass closure and reconstruction of the light scattering coefficient over the eastern Mediterranean Sea during the MINOS campaign, *Atmos. Chem. Phys.*, 5, 2253–2265, doi:10.5194/acp-5-2253-2005, 2005.

Schneising, O., Buchwitz, M., Burrows, J. P., Bovensmann, H., Bergamaschi, P., and Peters, W.: Three years of greenhouse gas column-averaged dry air mole fractions retrieved from satellite. Part 2: Methane, *Atmos. Chem. Phys.*, 9, 443–465, doi:10.5194/acp-9-443-2009, 2009.

Seinfeld, J. H., Urban air pollution: state of the science, *Science*, 243, 745–752, doi:10.1126/science.243.4892.745, 1989.

Sič, B., El Amraoui, L., Piacentini, A., Marécal, V., Emili, E., Cariolle, D., Prather, M., and Attié, J.-L.: Aerosol data assimilation in the chemical transport model

MOCAGE during the TRAQA/ChArMEx campaign: aerosol optical depth, *Atmos. Meas. Tech.*, 9, 5535-5554, doi:10.5194/amt-9-5535-2016, 2016.

Sprenger, M., and Wernli, H.: A northern hemispheric climatology of cross-tropopause exchange for the ERA15 time period (1979–1993), *J. Geophys. Res.*, 108, 8521, doi:10.1029/2002JD002636, 2003.

Stohl, A., James, P., Forster, C., Spinthinger, N., Marenco, A., Thouret, V., and Smit, H. G. J.: An extension of MOZAIC ozone climatologies using trajectory statistics, *J. Geophys. Res.*, 106, 27757–27768, doi:10.1029/2001JD000749, 2001.

Stunder, M., and Sethuraman, S.: A comparative evaluation of the coastal internal boundary layer height, *Bound. -Layer Meteorol.*, 32, 177–204, doi:10.1007/BF00120934, 1985.

Svensson, G.: A numerical model for chemical and meteorological processes in the atmospheric boundary layer. Part II: A case study of the air quality situation in Athens, Greece, *J. Appl. Meteor.*, 35, 955– 973, doi:10.1175/1520-0450(1996)035<0955:ANMFCA>2.0.CO;2, 1996.

Teyssèdre, H., Michou, M., Clark, H. L., Josse, B., Karcher, F., Olivie, D., Peuch, V. -H., Saint-Martin, D., Cariolle, D., Attie, J. -L., Nedelec, P., Ricaud, P., Thouret, V., Van Der A, R. J., Volz-Thomas, A., and Cheroux, F., A new tropospheric and stratospheric Chemistry and Transport Model MOCAGE-Climat for multi-year studies: evaluation of the present-day climatology and sensitivity to surface processes. *Atmos. Chem. Phys.*, 7, 5815-5860, <hal-00328553>

Tombrou, M., Bossioli, E., Kalogiros, J., Allan, J.D., Bacak, A., Biskos, G., Coe, H., Dandou, A., Kouvarakis, G., Mihalopoulos, N., Percival, C.J., Protonotariou, A.P., and Szabó-Takács, B.: Physical and chemical processes of air masses in the Aegean Sea during Etesians: Aegean-GAME airborne campaign, *Sci. Total Environ.*, 506–507, 201–216, <http://dx.doi.org/10.1016/j.scitotenv.2014.10.098>, 2015.

- Traub, M., Fischer, H., de Reus, M., Kormann, R., Heland, J., Ziereis, H., Schlager, H., Holzinger, R., Williams, J., Warneke, C., de Gouw, J., and Lelieveld, J.: Chemical characteristics assigned to trajectory clusters during the MINOS campaign, *Atmos. Chem. Phys.*, 3, 459–468, www.atmos-chem-phys.org/acp/3/459/, 2003.
- Tsitouridou, R., and Samara, C.: First results of acidic and alkaline constituents determination in air particulates of Thessaloniki, Greece, *Atmos. Environ.*, 27, 313–319, 1993.
- Tyrlis, E., and Lelieveld, J.: Climatology and dynamics of the summer Etesian winds over the Eastern Mediterranean, *J. Atmos. Sci.*, 70, 3374–3396, doi:10.1175/JAS-D-13-035, 2013.
- Tyrlis, E., Lelieveld, J., Steil, B.: The summer circulation over the eastern Mediterranean, and the Middle East: influence of the South Asian monsoon, *Clim. Dyn.*, 40, 1103–1123, doi:10.1007/s00382-012-1528-4, 2013.
- Tyrlis, E., Škerlak, B., Sprenger, M., Wernli, H., Zittis, G., and Lelieveld, J.: On the linkage between the Asian summer monsoon and tropopause fold activity over the eastern Mediterranean and the Middle East, *J. Geophys. Res.*, 119, 6, 3202–3221, doi:10.1002/2013JD021113, 2014.
- Večeřa, Z., Mikuška, P., Smolík, J., Eleftheriadis, K., Bryant, C., Colbeck, I., and Lazaridis, M.: Shipboard measurements of nitrogen dioxide, nitrous acid, nitric acid and ozone in the eastern Mediterranean Sea, *Water Air Soil Poll., Focus* 8, 117–125, doi:10.1007/s11267-007-9133-y, 2008.
- Vinken, G. C. M., Boersma, K. F., van Donkelaar, A., and Zhang, L.: Constraints on ship NO_x emissions in Europe using GEOS-Chem and OMI satellite NO₂ observations, *Atmos. Chem. Phys.*, 14, 1353–1369, doi:10.5194/acp-14-1353-2014, 2014.
- Voulgarakis, A., Savage, N. H., Braesicke, P., Wild, O., Carver, G. D., and Pyle, J. A.: Interannual variability of tropospheric composition: The influence of changes in emission, meteorology and clouds, *Atmos. Chem. Phys.*, 10, 2491–2506, doi:10.5194/acp-10-2491-2010, 2010.

Wanger, A., Peleg, M., Sharf, G., Mahrer, Y., Dayan, U., Kallos, G., Kotroni, V., Lagouvardos, K., Varinou, M., Papadopoulos, A., and Luria, M.: Some observational and modelling evidence of long-range transport of air pollutants from Europe towards the Israeli coast, *J. Geophys. Res.*, 105, D6, 7177-7186, doi:10.1029/1999JD901060, 2000.

Webster, P.J.: The role of hydrological processes in ocean atmosphere interactions. *Rev. Geophys.* 32, (4), 427–476, 1994.

Yarnal, B.: *Synoptic Climatology in Environmental Analysis*, Belhaven Press, London, 1993.

Yuval, Dubowski, Y., and Broday, D.M.: Allocation of routinely monitored mixing ratios of Nitrogen Oxides to their sources, *Environ. Sci. Technol.*, 41, 7215-7221, 10.1021/es0702317, 2007.

Zanis, P., Hadjinicolaou, P., Pozzer, A., Tyrllis, E., Dafka, S., Mihalopoulos, N., and Lelieveld, J.: Summertime free-tropospheric ozone pool over the eastern Mediterranean/Middle East, *Atmos. Chem. Phys.*, 14, 115–132, doi:10.5194/acp-14-115-2014, 2014.

Zbinden, R. M., Thouret, V., Ricaud, P., Carminati, F., Cammas, J. -P., and Nédélec, P.: Climatology of pure tropospheric profiles and column contents of ozone and carbon monoxide using MOZAIC in the mid-northern latitudes (24° N to 50° N) from 1994 to 2009, *Atmos. Chem. Phys.*, 13, 12363-12388, doi:10.5194/acp-13-12363-2013, 2013.

Zbinden R. M., Ricaud, P., Catoire, V., Brocchi, V., Massart, S., El Amraoui, L., Attie, J. L., Nabat, P., Dulac, F., Hamonou, E., Dayan, U., Piguet, B., and the SAFIRE team: Processes affecting the tropospheric chemical variability over the Mediterranean Basin: results from the summer GLAM campaign, *Atmospheric Processes in the Mediterranean (APM 2016): A joint ACTRIS - BACCHUS – CHArMEx Int. Workshop*, 17-21 Oct. 2016, <http://www.cyi.ac.cy/index.php/apm-workshop-2016-home.html>, 2016.

Zhang, J. S., and Rao, S. T.: The role of vertical mixing in the temporal evolution of ground-level ozone concentrations, *J. Appl. Meteor.*, 38, 1674–1691, doi:10.1175/1520-0450(1999)038<1674: TROVMI>2.0.CO;2, 1999.

Ziemke, J. R., Chandra, S., Labow, G. J., Bhartia, P. K., Froidevaux, L., and Witte, J. C.: A global climatology of tropospheric and stratospheric ozone derived from Aura OMI and MLS measurements, *Atmos. Chem. Phys.*, 11, 9237–9251, doi:10.5194/acp-11-9237-2011, 2011.

Ziv, B., Saaroni, H., and Alpert, P.: The factors governing the summer regime of the eastern Mediterranean, *Int. J. Climatol.*, 24, 1859-1871, doi:10.1002/joc.1113, 2004.

Table 1. Monthly long-term means (LTM) and standard deviation (S.D.) of the mixing layer depth (MLD), wind speed and range of ventilation rates over Beit-Dagan in the central coast of the EM. LTM and S.D. values for MLD include the years 1955-1968 (Rindsberger, 1974), 1981-1984 (Dayan et al., 1988), and 1987-1989 (Dayan and Rodniski, 1999). LTM and S.D. values for wind speeds are from the NCEP/NCAR Reanalysis Project (NOAA- CIRES Climate Diagnostic Center) for a 51-year data record over 1948-1999 from <http://www.esrl.noaa.gov/psd/> (adapted from Matvev et al., 2002).

Month	MLD (m)		Wind Speed (m s ⁻¹)		Ventilation Rates (m ² s ⁻¹)
	LTM	S.D.	LTM	S.D.	Range of LTM
June	810	470	5.5	2.25	1105 – 9920
July	870	450	5.0	1.65	1365 – 8780
August	820	395	4.5	1.50	1275 – 7290

Table 2. Compilation by Rudich et al. (2008) of sulfate particulate concentrations and yearly fluxes from [a] Luria et al. (1996), [b] Wanger et al. (2000) and [c] Matvev et al. (2002).

Regions	Measurement Periods	Conc. Avg (nmole m ⁻³)	Yearly Flux (Tg y ⁻¹) (*)	Authors
Judean mountains	July-Aug. 1984,1986	86	0.08	[a]
	May-June 1989	70	0.06	
	July-Aug. 1987,1988	103	0.09	
	July-Aug. 1990	128	0.12	
	May, July 1990, 1991	85	0.08	
Sea of Galilee	Aug.-Sept. 1993	87	0.03	
	Dec. 1993	71	0.07	
North coastal plain	June 1993	106	0.12	
	Sept. 1993	38	0.08	
	June 1994 (**)	108	0.22	
Eastern Mediterranean coast	June 1998	105	0.16	[b]
	Sept. 1996	26	0.04	
	Nov. 1995	21	0.03	

(*) following Matvev et al. (2002) conversion from nmole m⁻³ to yearly fluxes takes into account the vector component of onshore wind speed, length of flight leg, and the MLD.

(**) the June 1994 flight has been performed during a highly-polluted month over Israel.

Table 3. Locations and elevations of NOAA Earth System Research Laboratory Global Monitoring Division (ESRL/GMD) background sites for CO measurements plotted in [figure Figure 19](#).

Code	Name	Latitude	Longitude	Elevation (m)	Country
WIS	WIS Station Negev Desert	31.13	34.88	400.0	Israel
HUN	Hegyhatsal	46.95	16.65	248.0	Hungary
LMP	Lampedusa	35.52	12.62	45.0	Italy
BSC	Black Sea Constanta	44.17	28.68	3.0	Romania
OXK	Ochsenkopf	50.03	11.80	1022.0	Germany
BAL	Baltic Sea	55.35	17.22	3.0	Poland
MHD	Mace Head County Galway	53.33	-9.90	5.0	Ireland

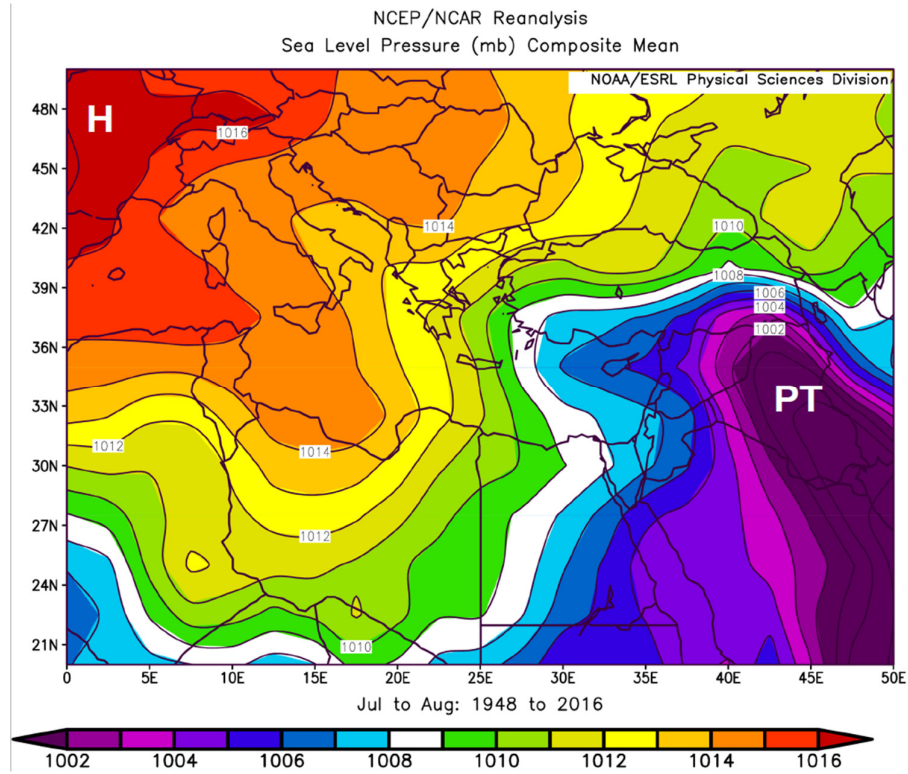


Figure 1. Composite long-term mean Sea Level Pressure (hPa) for July-August over 1948-2016. “PT” indicates the Persian Trough position. “H” indicates the Anticyclone position. Source: NCEP reanalysis data provided by the NOAA/OAR/ESRL PSD, Boulder, Colorado, USA, <http://www.esrl.noaa.gov/psd/>.

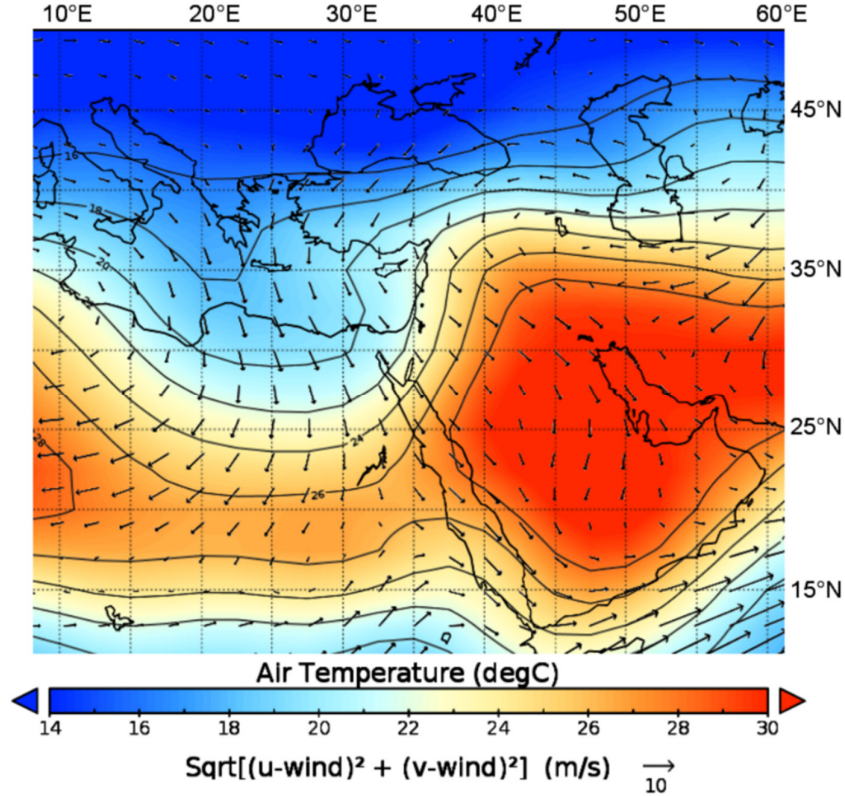


Figure 2. NCEP/NCAR reanalysis composite long-term mean temperature at 850 hPa (~1500 m, above sea level or a.s.l.) with wind vectors, averaged over 1948-2016 for July-August. Note the southward penetration of the European cold air over the Mediterranean Basin. This cold air mass is transported at shallow tropospheric layers towards the Eastern Mediterranean by the Etesian northwesterlies characterizing the Persian trough. Source: NCEP reanalysis data provided by the NOAA/OAR/ESRL PSD, Boulder, Colorado, USA, <http://www.esrl.noaa.gov/psd/>.

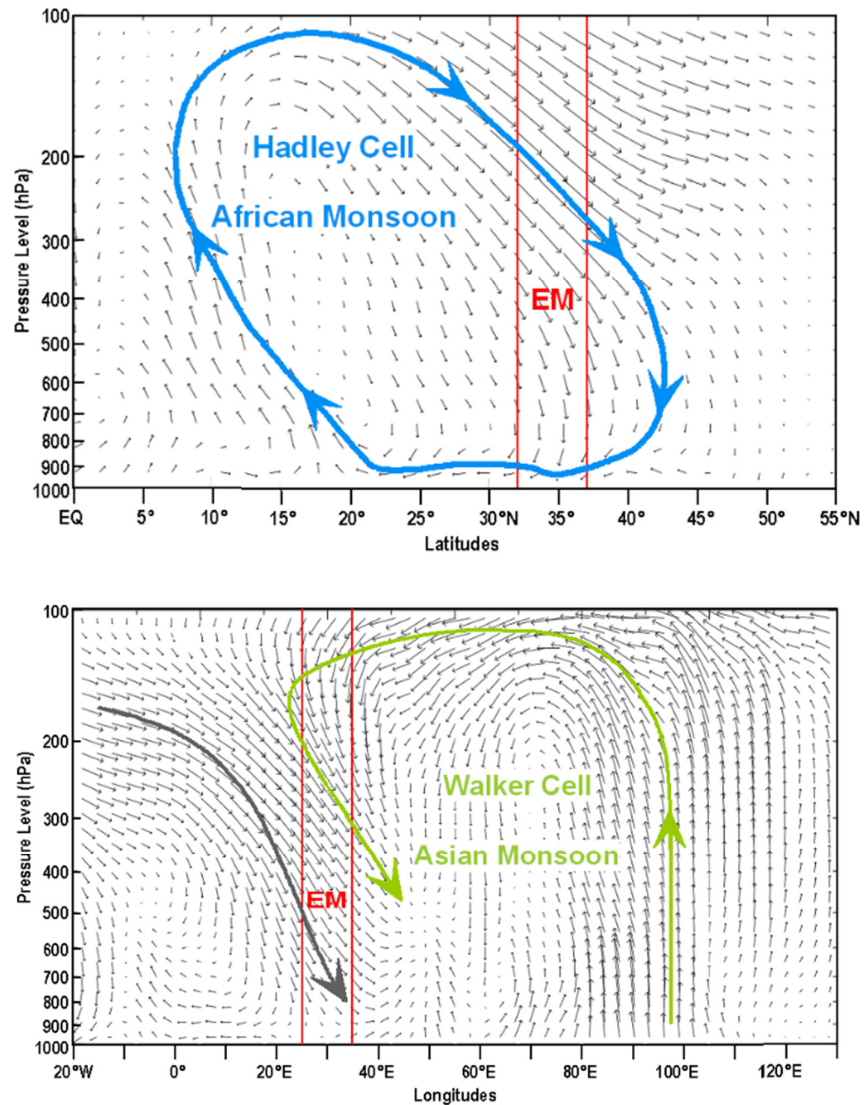


Figure 3. (TopLeft) Closed Hadley cell circulation of the African Monsoon-monsoon depicted by the vertical cross section of wind vectors for July-August averaged over the 30-40°E longitudinal band. (BottomRight) Closed Walker cell circulation of the Asian mMonsoon depicted by the vertical cross section of wind vectors for July-August averaged over the 20-35°N latitudinal band. The two figures are based on the NCEP/NCAR long-term averages (1948-2016) with the position of the eastern Mediterranean (EM) in red. Source: NCEP reanalysis data provided by the NOAA/OAR/ESRL PSD, Boulder, Colorado, USA, <http://www.esrl.noaa.gov/psd/>.

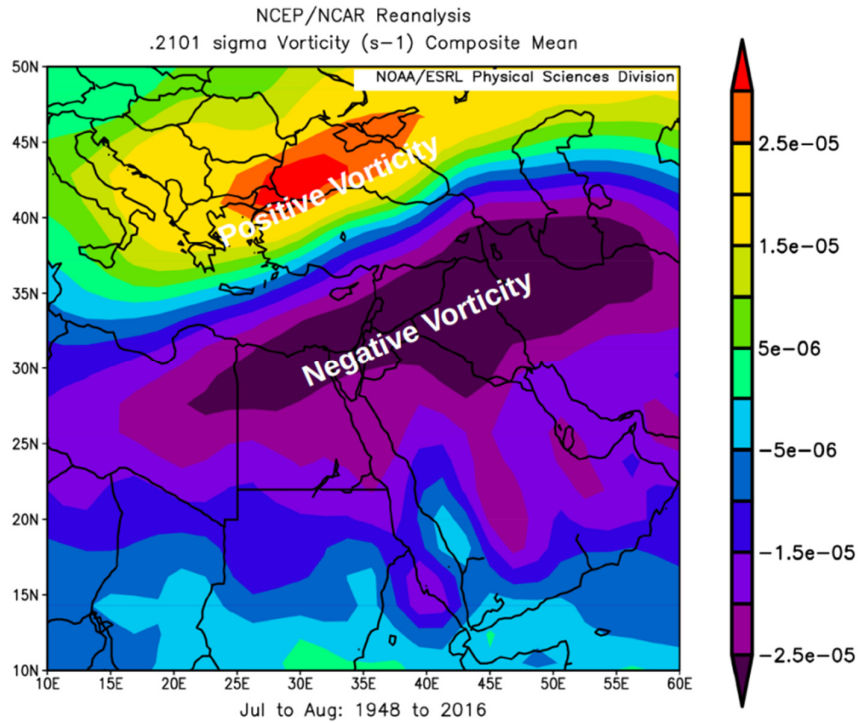


Figure 4. NCEP/NCAR Reanalysis long-term averages (1948-2016) of the relative vorticity at 200 hPa (~12 km a.s.l.) for July-August. The relative vorticity vector is generally perpendicular to the ground, positive when the vector points upward, negative when it points downward. Note the negative relative vorticity region located over the southeastern Mediterranean as a result from both shear and curvature negative relative vorticity. Relative vorticity units are 10^{-5} s^{-1} . Source: NCEP reanalysis data provided by the NOAA/OAR/ESRL PSD, Boulder, Colorado, USA, <http://www.esrl.noaa.gov/psd/>.

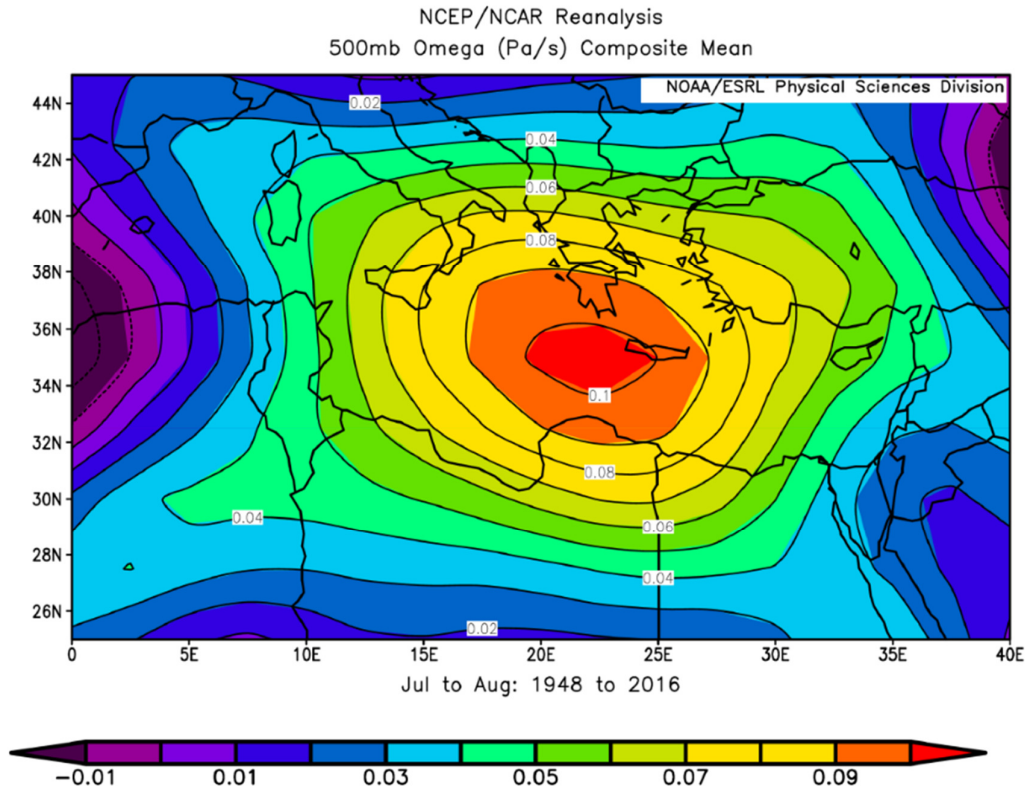


Figure 5. NCEP/NCAR reanalysis long-term averages of Omega (Pa s^{-1}) at 500 hPa (~ 5.5 km a.s.l.) designating vertical motion for July to August 1948-2016. The maximum subsidence of 0.1 Pa s^{-1} is equivalent to a downward air motion of $\sim 1.5 \text{ cm s}^{-1}$. Source: NCEP reanalysis data provided by the NOAA/OAR/ESRL PSD, Boulder, Colorado, USA, <http://www.esrl.noaa.gov/psd/>.

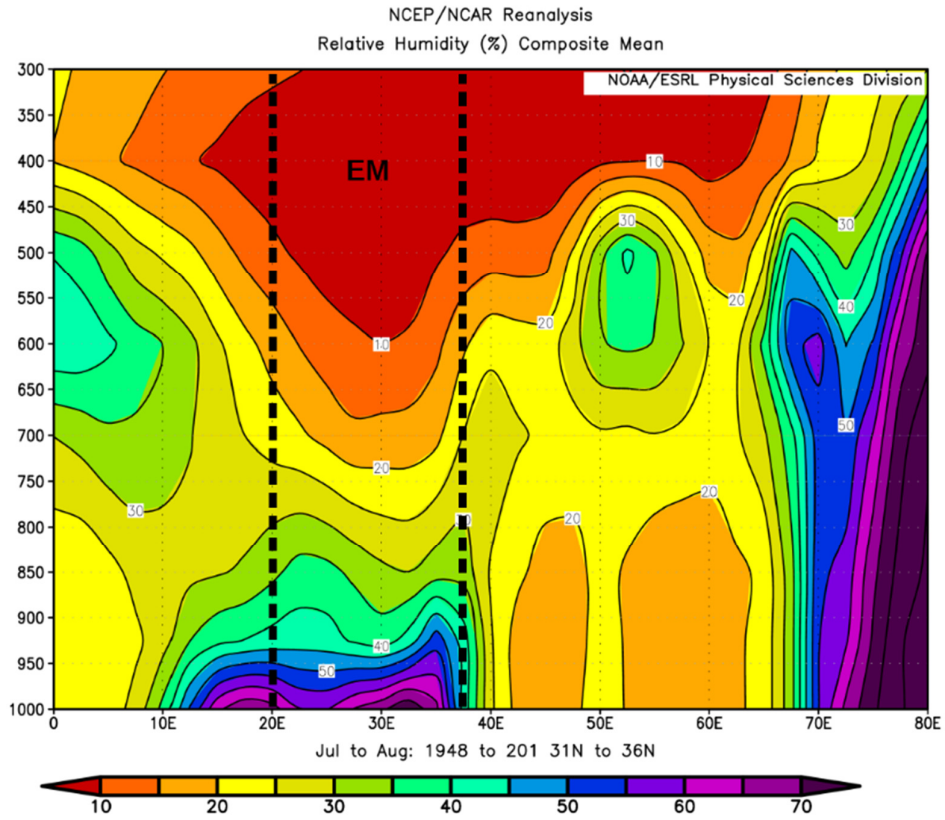


Figure 6. Long-term mean vertical cross section of relative humidity, averaged over the 31-36° N latitudinal band for July-August 1948-2016 with the eastern Mediterranean position (EM), in dashed black lines. Source: NCEP reanalysis data provided by the NOAA/OAR/ESRL PSD, Boulder, Colorado, USA, <http://www.esrl.noaa.gov/psd/>.

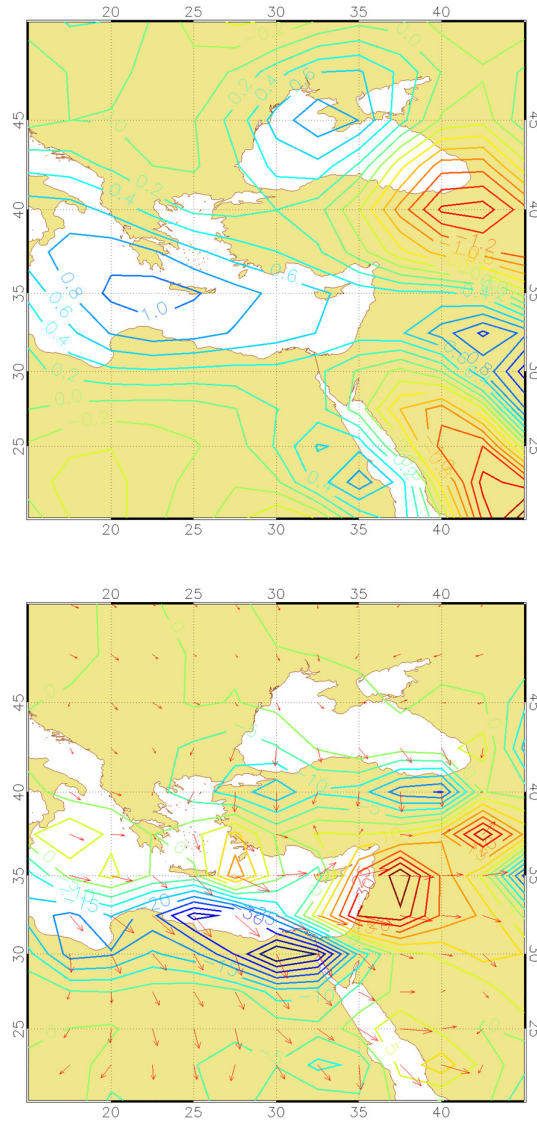


Figure 7. (Top) Blue contours display positive Omega values (cm s^{-1}) representing the vertical descending air motion at a mid-tropospheric level (700 hPa) (~ 3 km a.s.l.) pointing at a core of 1 cm s^{-1} located over Crete. Red contours are negative Omega values. (Bottom) Blue contours display cold advection calculated as multiplication of the horizontal thermal gradient by the wind vector. Red contours indicate warm advection, both at 995 hPa level, equivalent to about 140 m a.s.l at 12:00 UTC during Persian trough summer synoptic conditions. Source: NCEP reanalysis data for 2000-2012, provided by the NOAA/OAR/ESRL PSD, Boulder, Colorado, USA, <http://www.esrl.noaa.gov/psd/>.

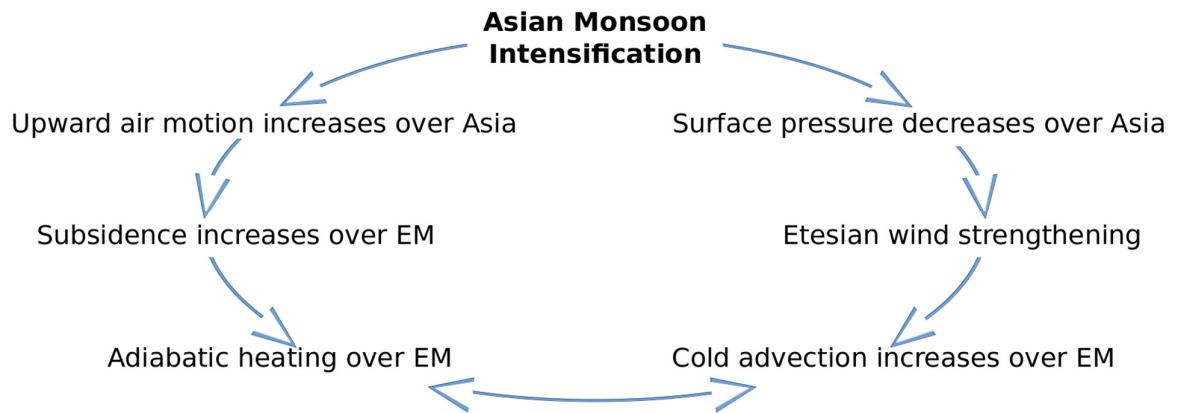


Figure 8. Schematic of the proposed mechanism during intensification of the Asian Monsoon (reproduced ~~adapted~~ from Ziv et al., (2004)).

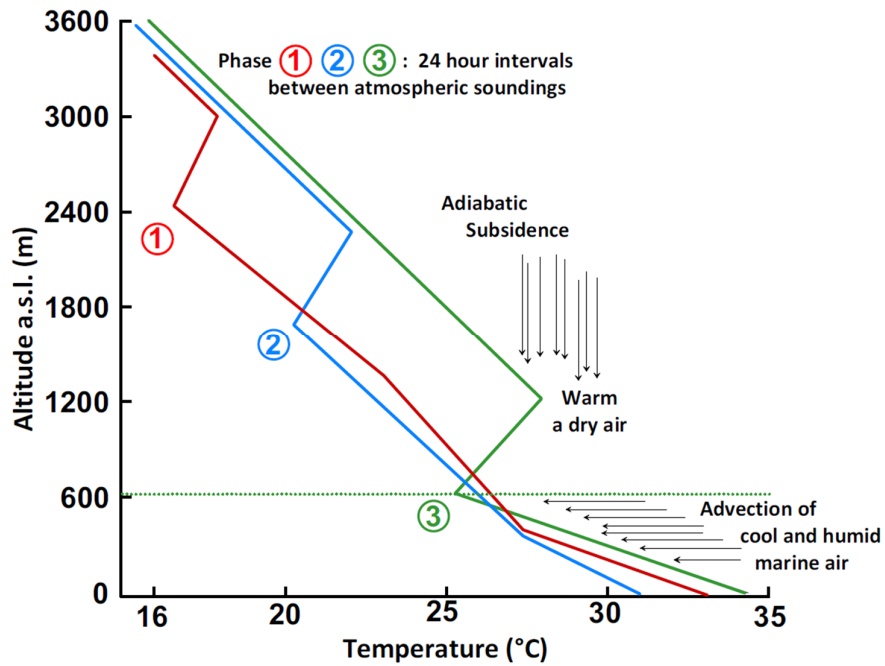


Figure 9. Successive schematic sounding thermal profiles indicating the downward motion of adiabatic subsidence accompanied by a weakening of the Persian Trough, which restricts the mixing layer depthMLD to shallow layer of the atmosphere (phases 1-3 are 24 h intervals between each sounding at Beit-Dagan, Israel); (from Dayan et al. (1988); ©American Meteorological Society; used with permission).

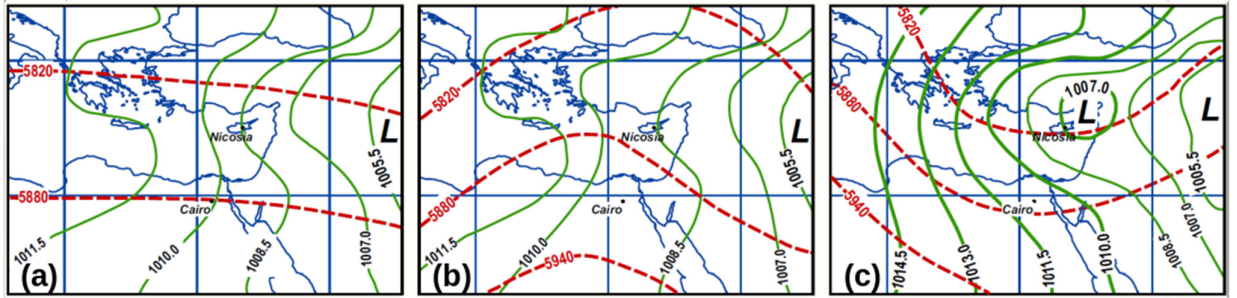


Figure 10. Typical synoptic charts showing the three modes: (a) moderate, (b) shallow, and (c) deep mode of the Persian Trough as defined by the surface-pressure differences between Nicosia (Cyprus) and Cairo (Egypt), and their associated upper level conditions. Solid lines are isobars of sea level pressure with 1.5-hPa intervals. Dashed lines are contours at 500-hPa level with 60-m intervals (from Dayan et al. (2002)); ©American Meteorological Society; used with permission).

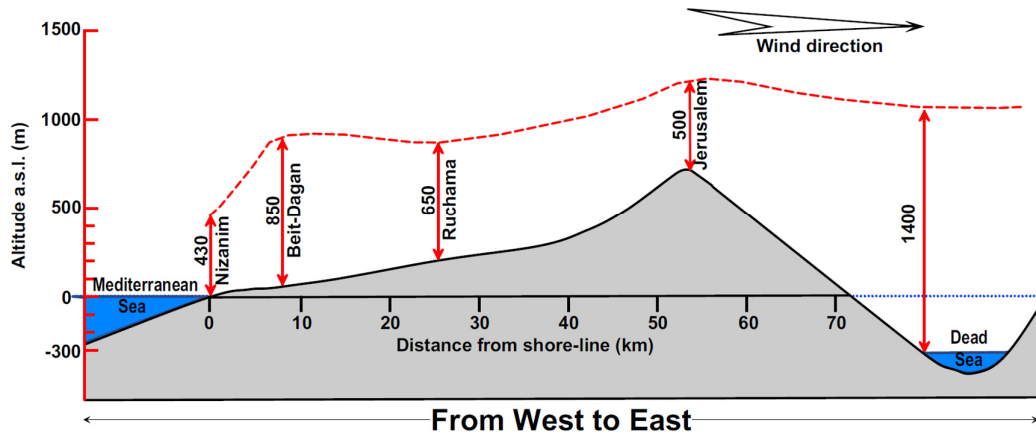


Figure 11. Schematic description of the lateral variation of the mixing layer depth (m, a.s.l.) from the Mediterranean Sea to the Dead Sea (from Dayan et al. (1988)); ©American Meteorological Society; used with permission).

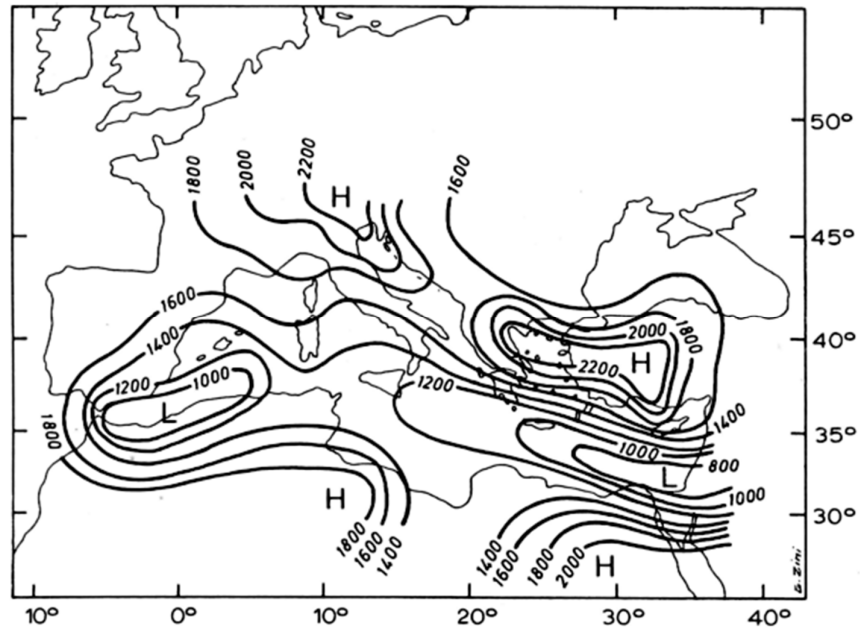


Figure 12. Seasonal map of the mixing layer depth (MLD, in-m) for summer (June, July, August) 1987 over the Mediterranean region at 12:00 UTC (from Dayan et al. (1996), with permission requested from Kluwer Academic Publishers).

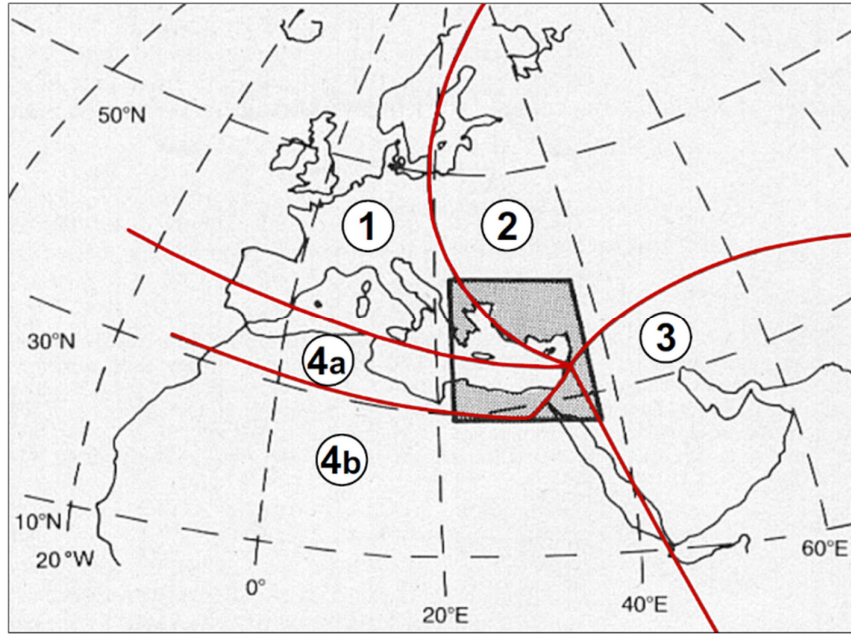


Figure 13. Trajectory typing method used to categorize 5-day back-trajectories from the EM—Eastern Mediterranean region at 850 hPa using the Air Resources Laboratory’s trajectory model GAMBIT over the 1978-1982 period (from Dayan (1986), ©American Meteorological Society; used with permission).

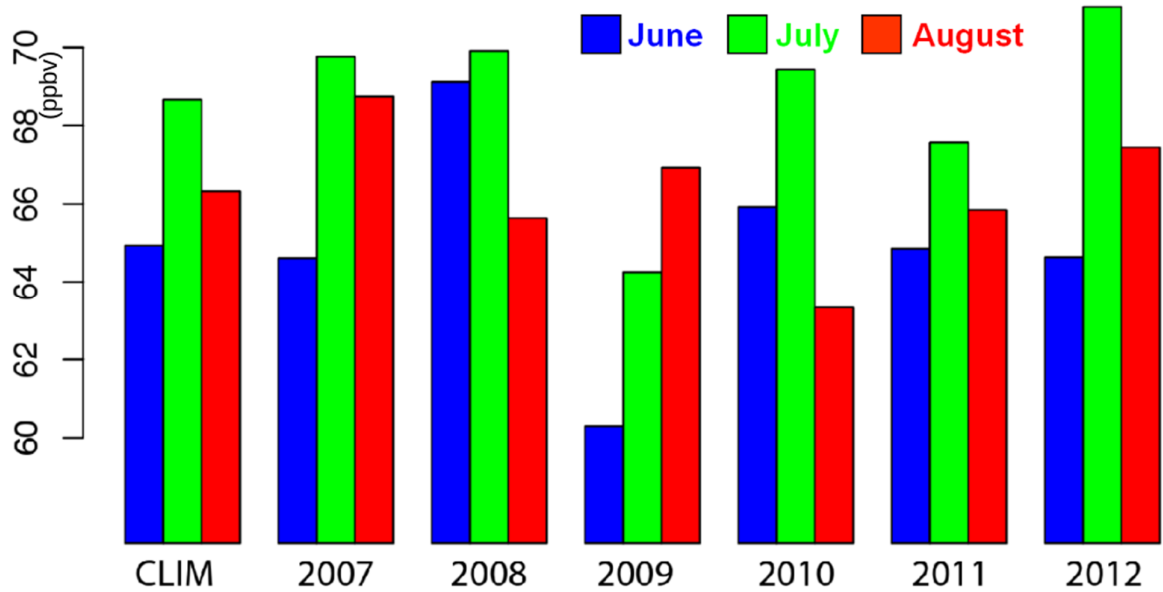


Figure 14. June, July and August monthly means of O₃ concentrations (ppbv) at 3 km partial column measured by IASI in summer (JJA) (June, July, August) within the 2007-2012 period over the Mediterranean (IASI morning overpasses). Only the observations over the sea are considered in the averages. The monthly means referred to as “CLIM” represent the averages over the whole period (~~reproduced~~-adapted from Doche et al., 2014).

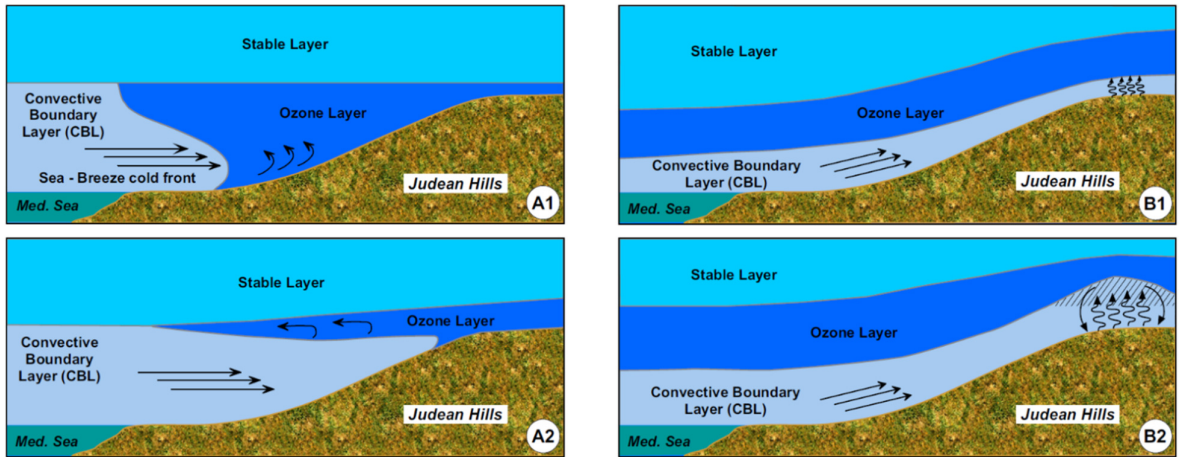


Figure 15. Scheme of the mechanism causing fumigation of a rich O₃ cloud toward the ground as moving inland over the Eastern Mediterranean coast during the weakening of a deep mode of the Persian Trough (from Dayan and Koch (1996); ©American Meteorological Society; used with permission).

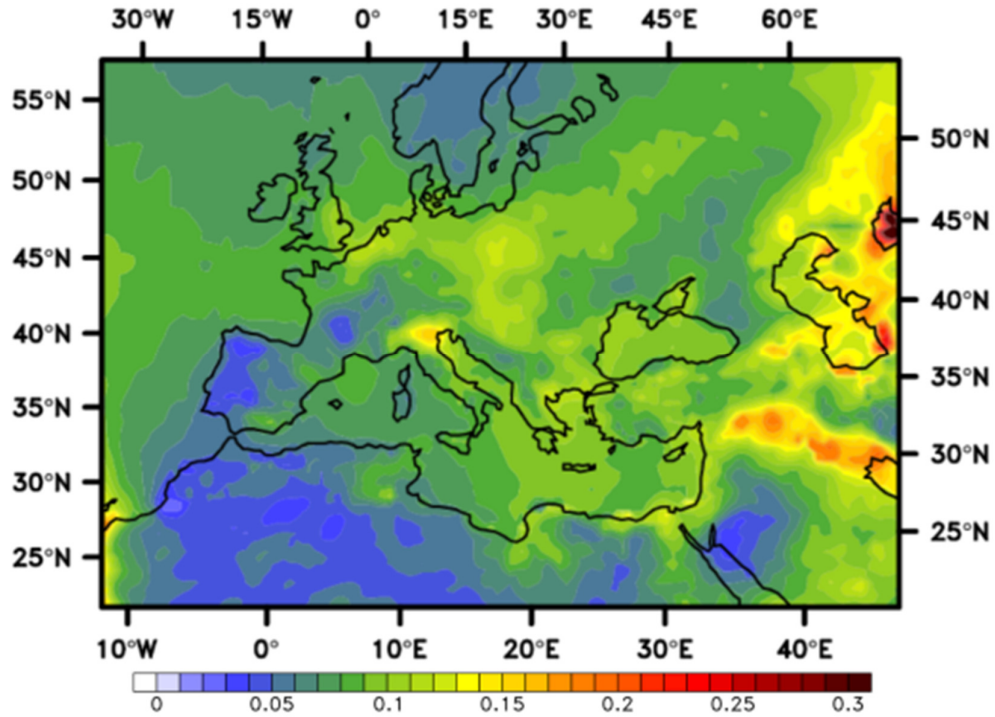


Figure 16: Average aerosol optical depth (AOD) contributed by particulate sulfate validated against AERONET AOD observations over the period 2003–2009. As mentioned by <http://www.esrl.noaa.gov/gmd/grad/surfrad/aod/>, a value of 0.01 corresponds to an extremely clean atmosphere, and a value of 0.4 to a very hazy condition (the 2003-2010 average AOD over the Mediterranean Basin is ~0.20) (adapted from Nabat et al., 2013).

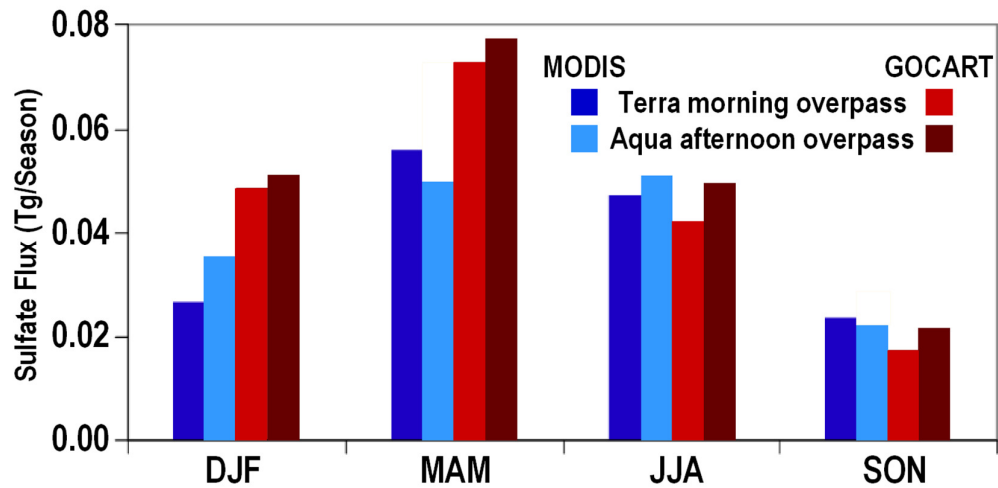


Figure 17. Seasonal flux (Tg season⁻¹) of dry sulfate as derived from MODIS/Terra and MODIS/Aqua space-borne observations compared to GOCART model-derived results, along the 150-km Israeli coastline of the Eastern Mediterranean Sea. Seasons on Xaxis are: winter (DJF), spring (MAM), summer (JJA), autumn (SON). (adapted from Rudich et al., 2008).

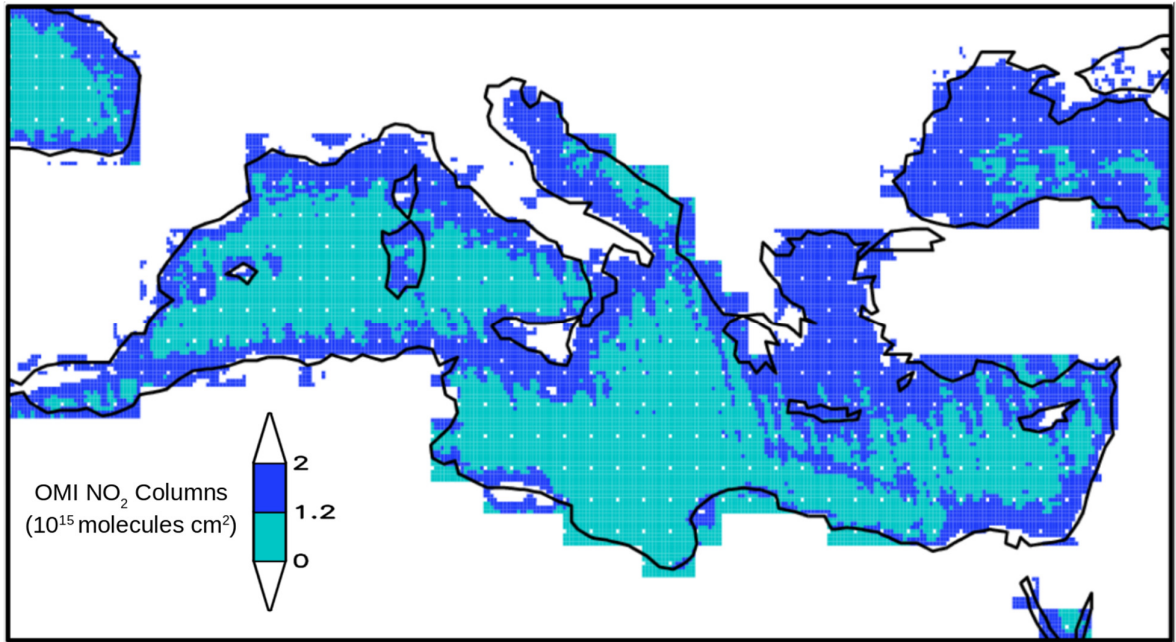


Figure 18. Seasonal average over June-August 2006 of OMI NO₂ columns over the Mediterranean Sea (10¹⁵ molecules cm⁻²), retrieved from the OMI satellite and considering only maritime pixels (reproduced from Marmar et al., 2009).

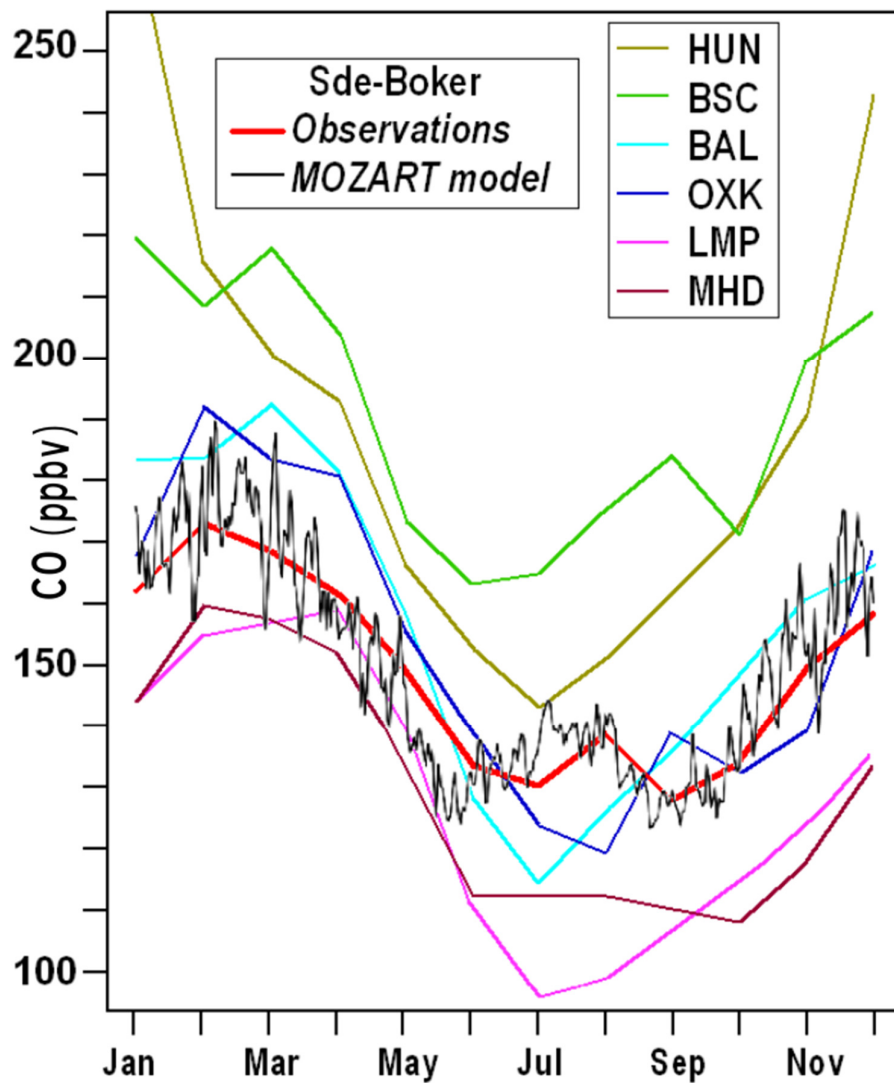


Figure 19. Monthly mean CO concentrations over 1996-2009 at Sde-Boker (red) and at seven European ESRL/GMD background stations (listed in Table 3, multiple colors), compared to the five-year averaged CO surface concentrations at Sde-Boker (black) over 2003-2007 from the MOZART-4 chemistry-transport model (adapted from Drori et al., 2012).

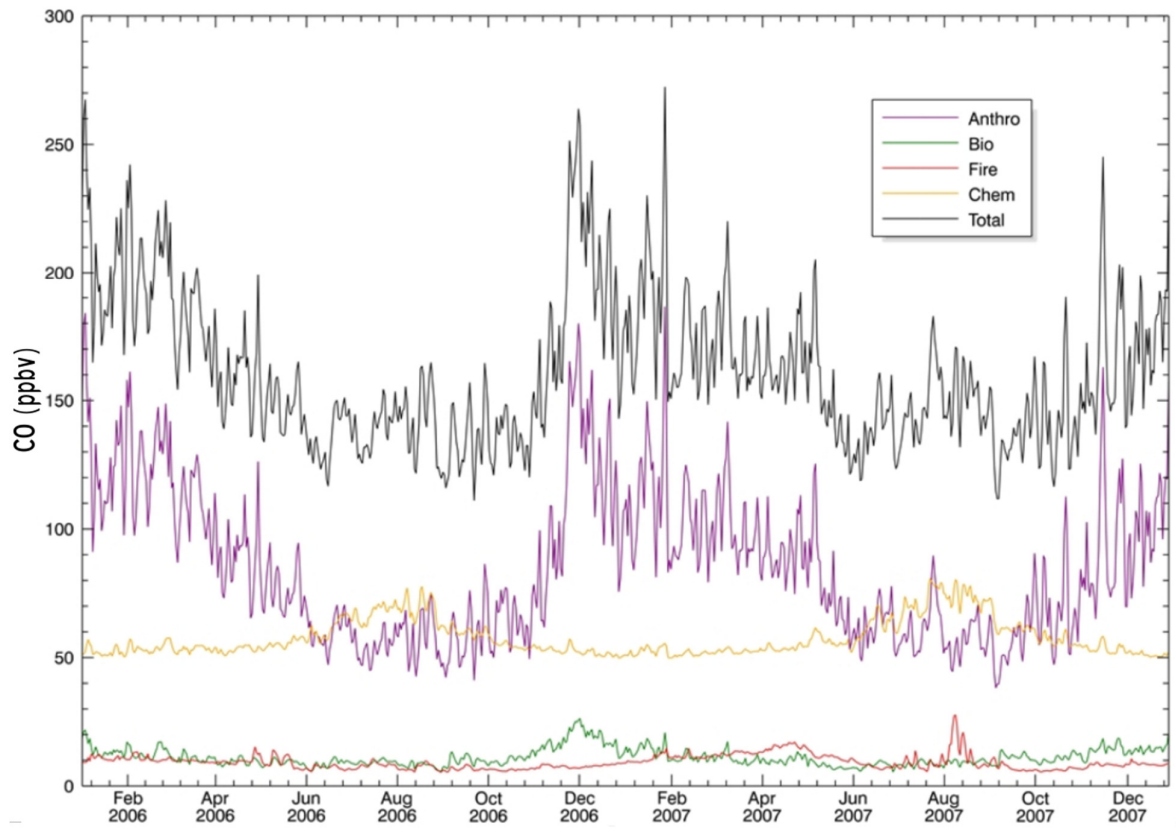


Figure 20. Monthly timeseries of total surface CO (black) at Sde-Boker, Israel, and contributions from specific sources (anthropogenic in purple, chemical production in orange, biogenic in green, and fires in red; ocean is negligible and not shown) as simulated by MOZART for 2006–2007 (adapted from Drori et al., 2012).

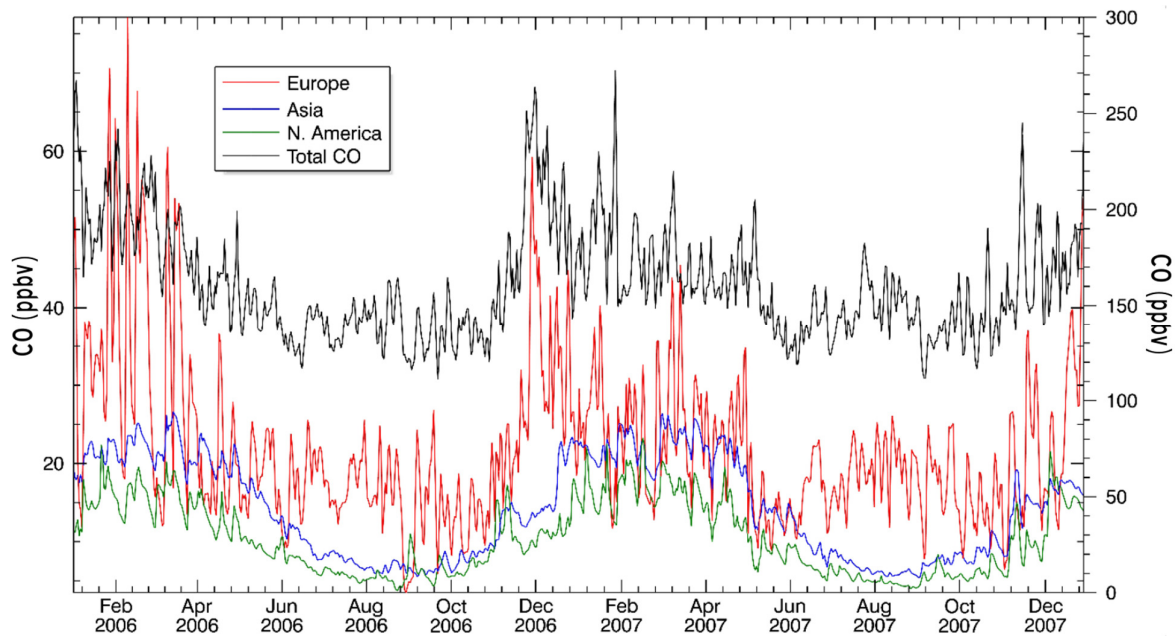


Figure 21. Monthly timeseries of the European (red), Asian (blue) and North American (green) anthropogenic contribution to the total surface CO (black) at Sde-Boker as simulated by MOZART over 2006-2007. Distinct continents are scaled on the left vertical axis and total CO on the right vertical axis (adapted from Drori et al., 2012).

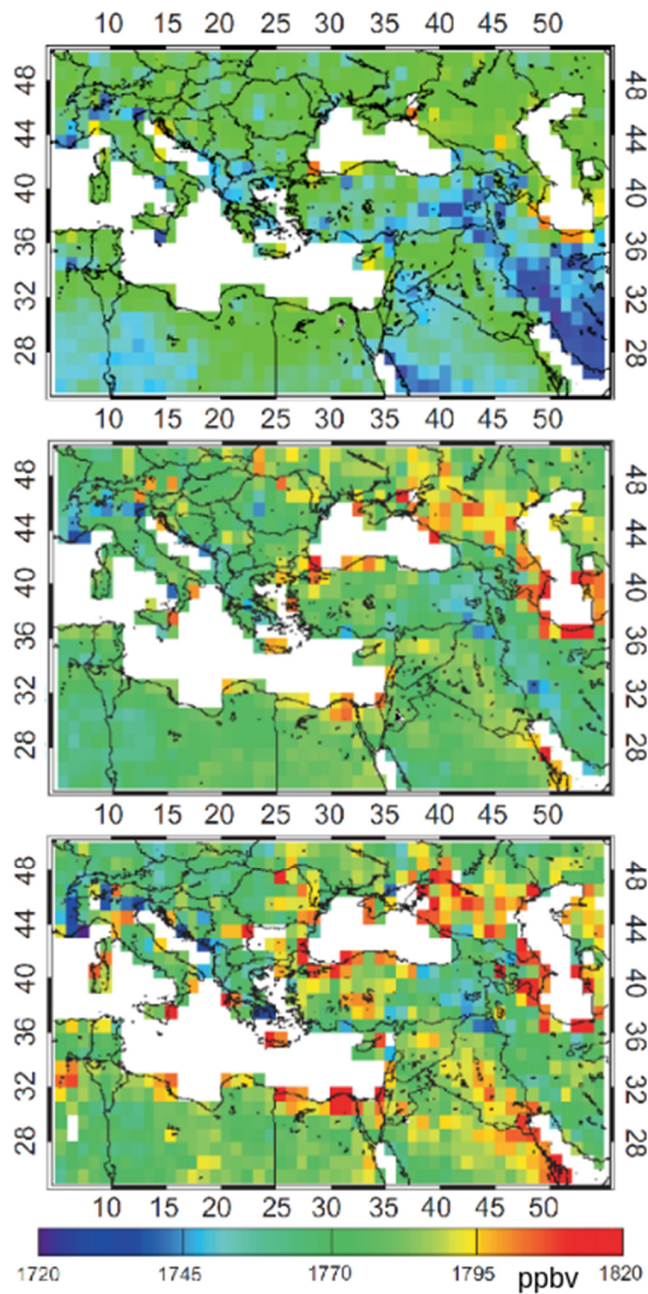


Figure 22. Maps by $1^\circ \times 1^\circ$ resolution of dry air column-averaged mole fractions, denoted as SCIAMACHY WFM-DOAS XCH₄ levels in 2003 including a yearly average (top panel), a summer average (mid-panel) and an August average (bottom panel), in ppbv (from Georgoulias et al. (2011), permission requested from Taylor and Francis).

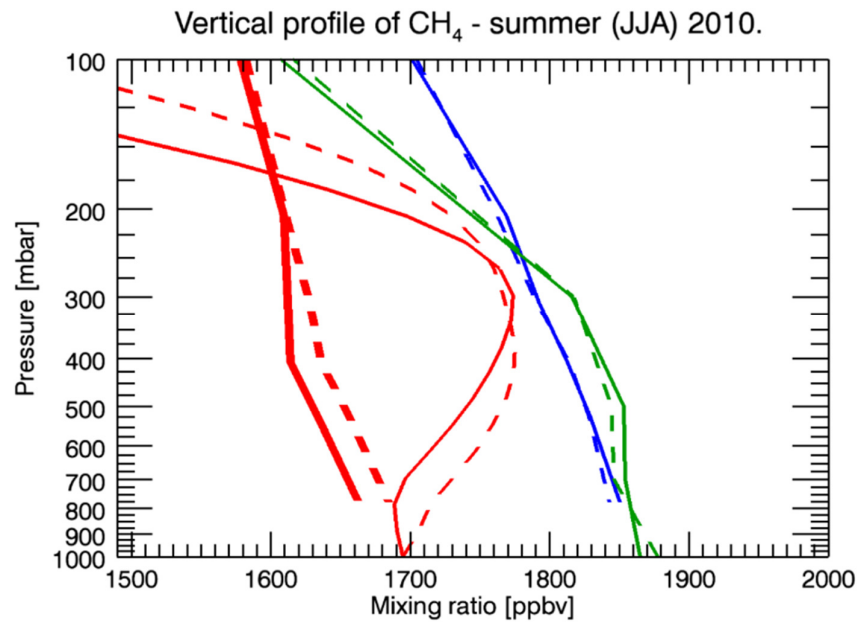


Figure 23. Summer averaged vertical profiles of CH₄ as measured by AIRS (blue lines) and GOSAT (green lines), and as calculated by MOCAGE (thin red lines) over the eastern (dashed lines) and western (solid lines) Mediterranean Basins in summer 2010. Also shown are the seasonally-averaged MOCAGE profiles convolved with the AIRS averaging kernels (thick red lines) for the summer over the eastern (dashed lines) and western (solid lines) Mediterranean Basins (adapted from Ricaud et al., 2014).

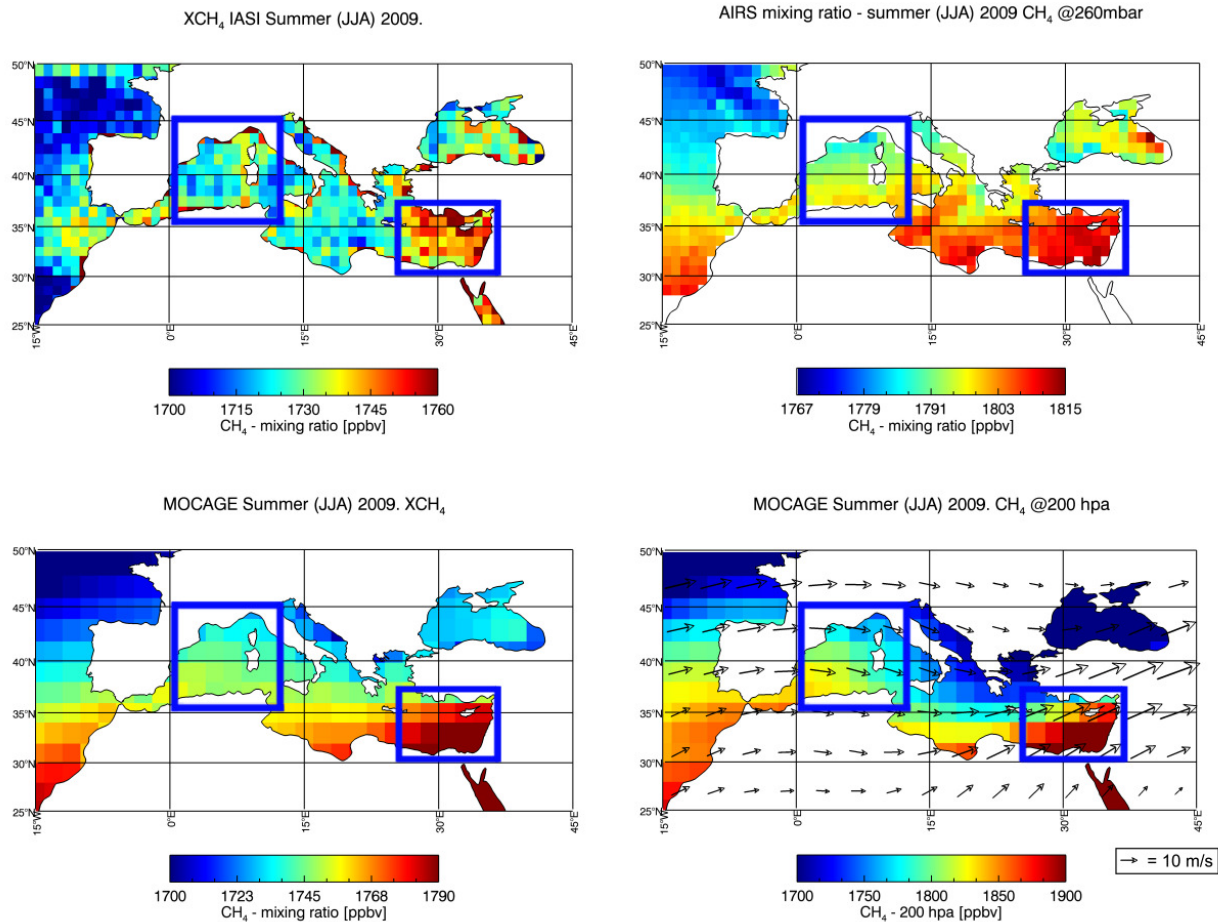


Figure 24. Fields of CH₄ as calculated by MOCAGE (bottom) and as measured by IASI (top left) in total column and AIRS (top right) at 260 hPa averaged for summer JJA (July, July, August) 2009. Horizontal winds are from ARPEGE averaged over the same period. The two blue squares represent the West and East Mediterranean Basins (adapted from Ricaud et al., 2014).

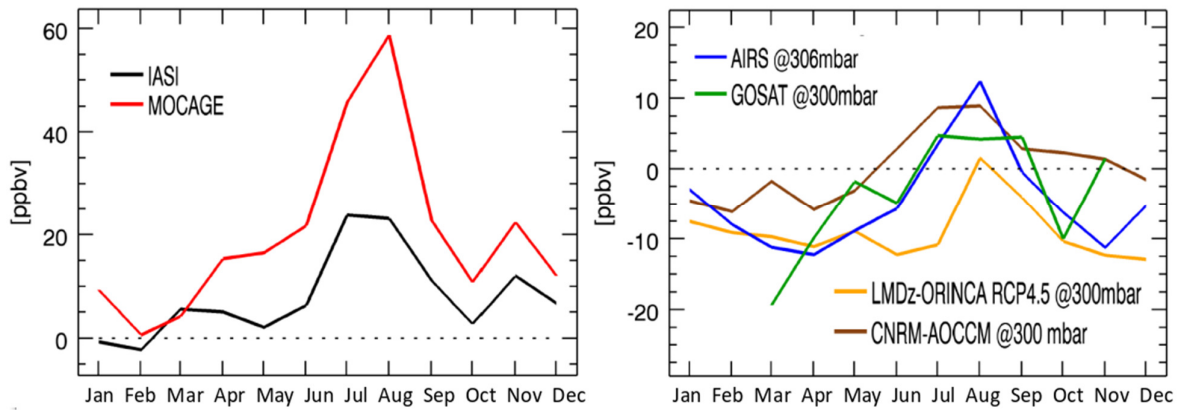


Figure 25. Seasonal evolution of the difference in CH₄ fields between the eastern and western Mediterranean Basin: (right) around 300 hPa as measured by AIRS (blue) and GOSAT (green) and as calculated by LMDz-OR-INCA (yellow) and CNRM-AOCCM (brown), and (left) in total column as measured by IASI and calculated by MOCAGE (adapted from Ricaud et al. 2014).

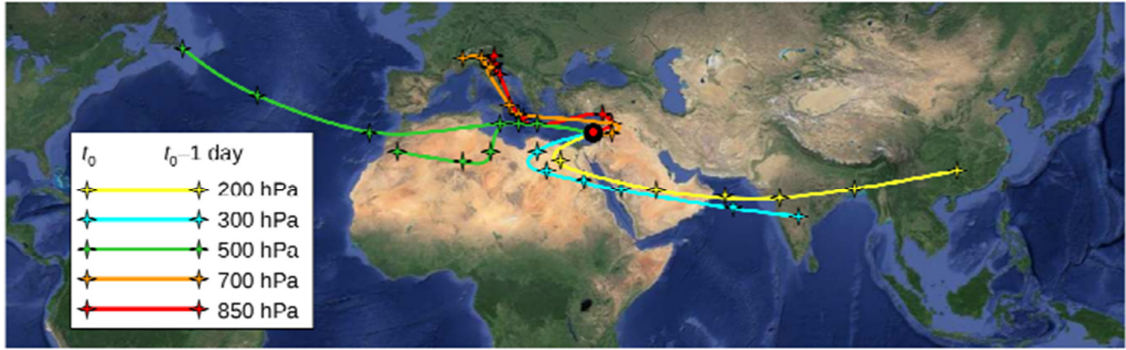


Figure 26. Six-day back-trajectories climatology from the point at 33°N and 35°E located off Israel in the eastern Mediterranean Basin (red filled circle) derived for July-August over 2001-2010 every 12 hours. The position of the gravity center of each distribution (i.e. the maximum in the probability density function) at each level is represented every 24 h by a star (adapted from Ricaud et al., 2014).

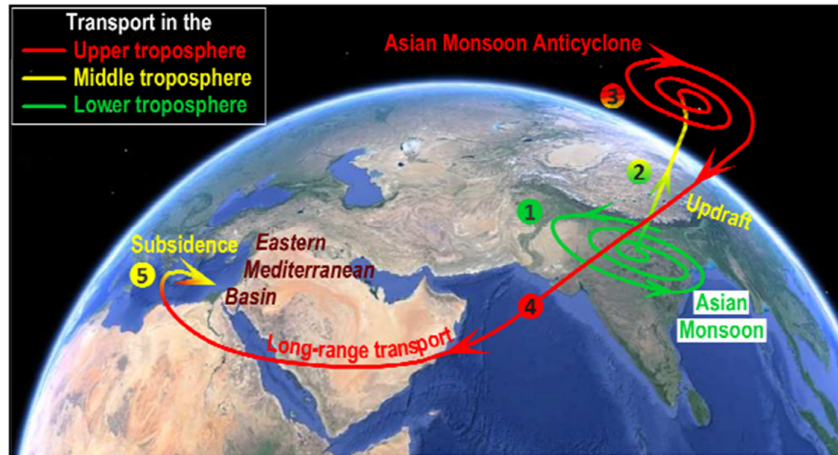


Figure 27. Schematic representation of the processes impacting the mid-to-upper tropospheric pollutants, including CH₄ above the Eastern Mediterranean Basin in summer (July-August) (adapted from Ricaud et al., 2014).